OCRWM	DESIGN CALCULATION OR ANALYSIS COVER SHEET	1. QA: QA 2. Page 1

3. System	4. Document Identifier
Uncanistered Spent Nuclear Fuel	CAL-DSU-NU-000006 REV 00C

5. Title

21-PWR Waste Package with Absorber Plates Loading Curve Evaluation

6. Group

Licensing/Criticality

7. Document Status Designation

☒ Preliminary ☐ Final ☐ Cancelled

8. Notes/Comments

Attachments	Total Number of Pages
Attachment I: Sensitivity Studies	12
Attachment II: PWR Assembly Lattice Design Sensitivity	6
Attachment III: Attachment CD Listing	2
Attachment IV: Compact Disc Attachment	N/A

RECORD OF REVISIONS

9. No.	10. Reason For Revision	11. Total # of Pgs.	12. Last Pg. #	13. Originator (Print/Sign/Date)	14. Checker (Print/Sign/Date)	15. QER (Print/Sign/Date)	16. Approved/Accepted (Print/Sign)	17. Date
00A	Initial Issue							
00B	Complete revision because changes are extensive to update study to use a new neutron absorber material (Ni-Gd Alloy) and modify configuration sensitivity evalautions	82	III-2	J.M. Scaglione	L. Montierth	W.N. Dockery	D.A. Thomas	
00C	Revised to correct editorial errors in Table of Contents, Table of Tables, and page 16. Changed lines are indicated by a black vertical line in the margin and only affect pages 1, 3, 7, and 16. Attachment IV was copied over from previous revision (00B) but had no modifications.	82	III-2	J.M. Scaglione SIGNATURE ON FILE 12/15/04	A.A. Alsaed SIGNATURE ON FILE 12/16/04	W.N. Dockery SIGNATURE ON FILE 16 DEC '04	W.E. Hutchins SIGNATURE ON FILE	12/17/04

INTENTIONALLY LEFT BLANK

CONTENTS

Page

CONTENTS (Continued)

Page

FIGURES

Page

FIGURES (Continued)

Page

TABLES

Page

TABLES (Continued)

Page

1. PURPOSE

The objective of this calculation is to evaluate the required minimum burnup as a function of initial pressurized water reactor (PWR) assembly enrichment that would permit loading of spent nuclear fuel into the 21 PWR waste package with absorber plates design as provided in Attachment IV. This calculation is an example of the application of the methodology presented in the *Disposal Criticality Analysis Methodology Topical Report* (YMP 2003). The scope of this calculation covers a range of enrichments from 0 through 5.0 weight percent U-235, and a burnup range of 0 through 45 GWd/MTU. Higher burnups were not necessary because 45 GWd/MTU was high enough for the loading curve determination.

This activity supports the validation of the use of burnup credit for commercial spent nuclear fuel applications. The intended use of these results will be in establishing PWR waste package configuration loading specifications.

Limitations of this evaluation are as follows:

- The results are based on burnup credit for actinides and selected fission products as proposed in YMP (2003, Table 3-1) and referred to as the *Principal Isotopes*. Any change to the isotope listing will have a direct impact on the results of this report.

- The results are based on 1.5 wt% Gd in the Ni-Gd Alloy material and having no tuff inside the waste package. If the Gd loading is reduced or a process to introduce tuff inside the waste package is defined, then this report would need to be reevaluated based on the alternative materials.

This calculation is subject to the *Quality Assurance Requirements and Description* (QARD) (DOE 2004) because it concerns engineered barriers that are included in the *Q-List* (BSC 2004k, Appendix A) as items important to safety and waste isolation.

2. METHOD

The method used to perform the reactivity calculations involves the simulation of the burnup and decay of fuel assemblies, for various initial enrichments and spent nuclear fuel (SNF) burnups, and the calculation of k_{eff} (effective neutron multiplication factor) for the loaded waste package configuration. The isotopic compositions for SNF were calculated in *Isotopic Generation and Confirmation of the PWR Application Model* (BSC 2003b) and used as input to *Software Code: MCNP* (CRWMS M&O 1998e) to calculate k_{eff} for the waste package loaded with various burnup/enrichment pairs. The k_{eff} calculations are based on taking credit for burnup with a subset of the total isotopes present in commercial SNF known as the *Principal Isotopes* (YMP 2003, Table 3-1).

The k_{eff} calculations were performed using continuous-energy neutron cross-section libraries as selected in *Selection of MCNP Cross Section Libraries* report (CRWMS M&O 1998b, pp. 61-68). The SNF from the various burnup/enrichment pairs were simulated, and the results reported from the MCNP calculations were the combined average values of k_{eff} from three estimates (collision, absorption, and track length) listed in the final generation summary in the MCNP output. Each of the waste package configurations was represented in detail using specifications for the Babcock & Wilcox (B&W) 15x15 assembly design (*Summary Report of Commercial Reactor Criticality Data for Crystal River Unit 3* [Punatar 2001, Section 2]), and waste package dimensions provided in Attachment IV from the following references: *Design and Engineering, 21 PWR A, B, D & E Fuel Plates* (BSC 2004a), *Design and Engineering, 21 PWR C Fuel Plate* (BSC 2004b), *Design and Engineering, 21 PWR Corner Guide* (BSC 2004c), *Design and Engineering, 21 PWR End Side Guide* (BSC 2004d), *Design and Engineering, 21 PWR Side Guide* (BSC 2004e), *Design and Engineering, 21-PWR Waste Package Configuration* (BSC 2004f), *Design and Engineering, 21-PWR Waste Package Configuration* (BSC 2004g), and *Design and Engineering, Fuel Tube* (BSC 2004h).

3. ASSUMPTIONS

3.1 ASSEMBLY DESIGN

Assumption: It is assumed that the B&W 15x15 assembly design is the most limiting PWR fuel assembly design.

Rationale: The basis for this assumption is that a previous analysis for the BR-100 transportation cask established the B&W 15x15 fuel assembly as one of the most reactive fuel assembly designs (B&W Fuel Company 1991, p. II 6-6). In addition, several assembly designs were evaluated in Attachment II and the results show the B&W 15x15 design to be the most reactive.

Confirmation Status: This assumption requires no further confirmation based on the stated rationale.

Use in the Calculation: This assumption was used in Section 5.

3.2 MATERIAL DEGRADATION PRODUCTS

Assumption: It was assumed that all of the iron within the waste package internal components turns into hematite (Fe_2O_3) or goethite (FeOOH) as it oxidizes and hydrates, and all of the aluminum turns into gibbsite ($Al[OH]_3$).

Rationale: The basis for this assumption is that these are considered the primary minerals that iron and aluminum will form, and are substantiated by *Geochemistry Model Abstraction and Sensitivity Studies for the 21 PWR CSNF Waste Packages* (BSC 2004i, Sections 6.3.2 and 6.4.2).

Confirmation Status: This assumption requires no further confirmation based on the stated rationale.

Use in the Calculation: This assumption is used in the sensitivity studies in Attachment I and the postclosure bounding configuration cases in Section 5.

3.3 RANGE OF APPLICABILITY VERSUS RANGE OF PARAMETERS

Assumption: It is assumed that range of parameters (ROP) for the configurations evaluated in this report match the range of applicability (ROA) of the benchmarks used to establish the lower bound tolerance limits provided by Framatome ANP (2003).

Rationale: The basis for this assumption is that the ROP concerning materials, geometry, and neutron spectrum for the given configurations are considered sufficiently similar to the benchmark experiment parameters.

Confirmation Status: This assumption requires no further confirmation based on the stated rationale.

Use in the Calculation: This assumption is used in Section 6 and Attachment I.

3.4 CROSS SECTION SUBSTITUTION

Assumption: Since the zinc cross section libraries are unavailable, it was assumed that representing the zinc material composition in SB-209 A96061 T4 as aluminum would maintain the same neutronic characteristics.

Rationale: The rationale for this assumption is that the nuclear cross-sections for these two elements are sufficiently similar (Parrington et al. 1996, pp. 20 and 24).

Confirmation Status: This assumption requires no further confirmation based on the stated rationale.

Use in the Calculation: This assumption was used in Section 5.2.1.

3.5 RADIAL PROFILE EFFECTS

Assumption: It was assumed that the radial variation in burnup within the spent fuel assemblies is accounted for during the depletion calculations for BSC (2003b).

Rationale: The basis for this assumption is that BSC (2003b) uses inserted burnable absorbers and other parameters during the depletion to harden the neutron spectrum and represent heterogeneous effects, which increases the buildup of plutonium and thus increases the fuel assembly's reactivity worth. This method of depletion is confirmed in BSC (2003b) to provide conservative results with comparisons against measured values.

Confirmation Status: This assumption requires no further confirmation based on the stated rationale.

Use in the Calculation: This assumption is used in Section 5.

3.6 DUST MASS COLLECTED ON WASTE PACKAGE OUTER BARRIER

Assumption: It is assumed that up to 20 kg of dust per waste package will collect on the outer barrier following closure of the repository.

Rationale: During the ventilation period prior to sealing the primary entrances to the repository, dust will accumulate on the waste package outer barrier surfaces (*Total Dust Settling on Naval Long Waste Packages in 100 Years* [BSC 2004l, Section 1]). The source of a majority of this dust is expected to be from the outside air being used for the ventilation. Rock dust from construction activities is expected to be removed prior to waste package emplacement. Preliminary results BSC (2004l, Table 4) indicate that the maximum mass of dust per waste package accumulated in 100 years is approximately 18.2 kg. Thus, the assumption is conservative.

Confirmation Status: This assumption requires no further confirmation based on the stated rationale.

Use in the Calculation: This assumption is used in Attachment I.

3.7 HYDRAULIC FLUID COMPOSITION

Assumption: It was assumed that the hydraulic fluid used as an alternative moderator material was a conventional silicone fluid (polysiloxane fluid) with a viscosity of 10cSt with a degree of polymerization of four (which is necessary for a viscosity of 10 cSt at 25°C (Gelest Inc. 2004, p.11).

Rationale: The basis for this assumption is that this material is a common hydraulic fluid (Gelest Inc. 2004, p. 7).

Confirmation Status: This assumption requires no further confirmation based on the stated rationale.

Use in the Calculation: This assumption is used in Attachment I.

3.8 IRON AND ALUMINUM OXIDE VOLUME EXPANSION

Assumption: It was assumed that the volume expansion from the oxidation and hydration of the iron in carbon steel and aluminum in SB-209 A96061 T4 components followed the ratio of theoretical densities.

Rationale: The basis for this assumption is that the internal components can degrade over time and the amount present and volume will vary as the exposed region oxidizes and hydrides before flaking off. This assumption is used in representations to capture these effects on system reactivity for various degrees of degradation with retention of various amounts of corrosion products.

Confirmation Status: This assumption requires no further confirmation since an adequate range for various amounts of degradation and volume occupied have been evaluated in Attachment I.

Use in the Calculation: This assumption is used in Attachment IV.

3.9 DIMENSIONAL SCALING FACTORS

Assumption: The following scaling factors were assumed for purposes of scaling dimensions from the drawings in *Characteristics of Spent Fuel, High-Level Waste, and Other Radioactive Wastes Which May Require Long-Term Isolation* (DOE 1987):

1) 5 mm is equal to 0.937 in. for the Combustion Engineering (CE) 14x14 assembly design.

2) 12.5 mm is equal to 1.8125 in. for the CE 15x15 assembly design.

3) 5 mm is equal to 0.891 in. for the CE 16x16 assembly design.

Rationale: The basis for this assumption is that the dimensions were scaled from DOE (1987, Figures 1-4, 1-1, and 1-9, respectively).

Confirmation Status: This assumption requires no further confirmation since minor variations in the scaled dimensions will have a negligible effect on system reactivity. The effect is considered negligible as long as the materials for the scaled regions are represented in some capacity.

Use in the Calculation: This assumption is used in Attachment II.

3.10 CE 15X15 ASSEMBLY DESIGN INSTRUMENT TUBE

Assumption: It was assumed that the instrument tube outer diameter and cladding thickness in the CE 15x15 assembly design was the same as that listed for the CE 16x16 assembly design.

Rationale: The basis for this assumption is that the designs are similar and manufactured by the same vendor.

Confirmation Status: This assumption requires no further confirmation since minor variations in the dimensions will have a negligible effect on system reactivity. The effect is considered negligible as long as the instrument tube is represented.

Use in the Calculation: This assumption is used in Attachment II.

3.11 CE NICKEL ALLOY

Assumption: It was assumed that CE nickel alloy is similar to Inconel 718.

Rationale: The basis for this assumption is that fuel assembly design information for Babcock & Wilcox and Westinghouse assemblies typically use Inconel 718 in the end-fittings.

Confirmation Status: This assumption requires no further confirmation since axial reflection from the end-fitting region has a negligible effect on system reactivity. The effect is considered negligible as long as a similar type of material is represented in this region.

Use in the Calculation: This assumption is used in Attachment II.

4. USE OF COMPUTER SOFTWARE AND MODELS

4.1 MCNP

The baselined MCNP code (CRWMS M&O 1998e) was used to calculate the neutron multiplication factor for the various spent fuel compositions. The software specifications are as follows:

- Software Title: MCNP
- Version/Revision Number: Version 4B2LV
- Status/Operating System: Qualified/HP-UX B.10.20
- Software Tracking Number: 30033 V4B2LV (Computer Software Configuration Item Number)
- Computer Type: Hewlett Packard 9000 Series Workstations
- Computer Processing Unit number: 700887

The input and output files for the MCNP calculations are contained on a compact disc attachment to this calculation report (Attachment IV) as described in Sections 5 and 8, such that an independent repetition of the software use may be performed. The MCNP software used was (1) appropriate for the application of multiplication factor calculations, (2) used only within the range of validation as documented throughout Briesmeister (1997) and *Software Qualification Report for MCNP Version 4B2, A General Monte Carlo N-Particle Transport Code* (CRWMS M&O 1998a), and (3) obtained from Software Configuration Management in accordance with appropriate procedures.

4.2 EXCEL

- Software Title: Excel
- Version/Revision number: Microsoft® Excel 97 SR-2
- Computer Environment: Software is installed on a DELL OptiPlex GX240 personal computer, Civilian Radioactive Waste Management System (CRWMS) Management and Operating Contractor (M&O) tag number 150527, running Microsoft Windows 2000, Service Pack 4.

Microsoft Excel for Windows, Version 1997 SR-2, is used in calculations and analysis to manipulate the inputs using standard mathematical expressions and operations. It is also used to tabulate and chart results. The user-defined formulas, inputs, and results are documented in sufficient detail to allow an independent repetition of computations. Thus, Microsoft Excel is used only as a worksheet and not as a software routine. Microsoft Excel 1997 SR-2 is an exempt software product in accordance with *Software Management* (LP-SI.11Q-BSC, Subsection 2).

The spreadsheet files for the Excel calculations are documented in Attachment IV.

5. CALCULATION

This report evaluates the minimum required burnup of an assembly, for a specific initial enrichment, at which the calculated k_{eff} is equal to the critical limit (CL). The CL is the value of k_{eff} at which the configuration is potentially critical, and accounts for the criticality analysis methodology bias and uncertainty. In equation notation the CL is represented as shown in Equation 1.

$$CL(x) = f(x) - \Delta k_{EROA} - \Delta k_{ISO} - \Delta k_m \quad \text{(Eq. 1)}$$

where

- x = a neutronic parameter used for trending
- $f(x)$ = the lower bound tolerance limit function accounting for biases and uncertainties that cause the calculation results to deviate from the true value of k_{eff} for a critical experiment, as reflected over an appropriate set of critical experiments
- Δk_{EROA} = penalty for extending the range of applicability
- Δk_{ISO} = penalty for isotopic composition bias and uncertainty
- Δk_m = an arbitrary margin to ensure subcriticality for preclosure and turns the CL function into an upper subcritical limit (USL) function (it is not applicable for use in postclosure analyses because there is no risk associated with a subcritical event)

A more detailed discussion of the CL calculation is provided in YMP (2003, Section 3.5.3). A series of computer calculations were performed in order to develop a set of curves which show k_{eff} versus burnup for different initial enrichments, and the minimum burnup required to reach the CL or USL.

A burnup credit loading curve depicts the relationship between the initial enrichment of a fuel assembly and the required minimum burnup needed to suppress the reactivity of that fuel assembly sufficiently to allow it to be safely loaded into the waste package. Any assembly whose burnup exceeds the required minimum burnup, given the initial enrichment of the fuel assembly, may be loaded into the waste package.

There are two time periods to consider for applicability of a loading curve - preclosure and postclosure. The preclosure time-period is the period before permanent closure of the repository and includes the operations involving handling, loading, and sealing of the waste packages. During the preclosure time period it is currently required that the system be designed such that the calculated k_{eff} be sufficiently below unity to show at least a five percent margin after allowance for the bias in the method of calculation, and the uncertainty in the experiments used to validate the method of calculation (*Project Design Criteria Document* [Doraswamy 2004, Section 4.9.2.2]). The postclosure time-period is the period after permanent closure of the repository throughout the

10,000-year regulatory period (10 CFR 63.2). During the postclosure time-period a variety of conditions may affect the waste package internal configurations. A process to identify configuration classes that have the potential for criticality is provided in YMP (2003, Section 3.6). YMP (2003) is the source for the postclosure methodology (*Project Requirements Document* [Canori and Leitner 2003, PRD-013/T-016 and PRD-013/T-038]). This report provides a limited search for potential configurations that provide the highest k_{eff} values.

5.1 PARAMETER DESCRIPTION

5.1.1 Burnup Profiles

A bounding profile is defined as one that would maximize fuel assembly reactivity. Thus, a truly bounding profile would be where the fuel has not been irradiated, which is referred to as the "fresh fuel" assumption. This "fresh fuel" assumption is very conservative in calculations of criticality potential. As fuel is burned in a reactor, the burnup of the fuel becomes distributed axially and the reactivity of the fuel decreases. The profile of this axial distribution attains a flattened cosine shape with time, although the exact profile will vary significantly with operating history and other effects unique to the individual reactor. An axial profile database has been composed for various PWR fuel assembly designs, which included variations in enrichment, burnup, and burnable absorbers (Cacciapouti and Van Volkinburg, 1997). To develop a waste package loading curve, which would encompass the isotopic axial variations caused by different assembly irradiation histories, requires the development of a limiting axial profile that takes credit for fuel burnup.

The axial profiles used in this calculation were developed from an axial profile database (Cacciapouti and Van Volkinburg 1997). Limiting axial profiles were developed for a set of eight burnup groups in *PWR Axial Burnup Profile Analysis* (BSC 2003a, Table 32) as listed in Table 1. Radial profiles are accounted for during the fuel depletion calculations (see Assumption 3.5).

Table 1. Seven-Node Limiting Axial Burnup Profiles by Group

Axial Pos.[a]	Group 1[b] 10 ≤ x < 15	Group 2[b] 15 ≤ x < 20	Group 3[b] 20 ≤ x < 25	Group 4[b] 25 ≤ x < 30	Group 5[b] 30 ≤ x < 35	Group 6[b] 35 ≤ x < 40	Group 7[b] 40 ≤ x < 45	Group 8[b] 45 ≤ x
0.028	0.497	0.554	0.525	0.587	0.599	0.619	0.635	0.640
0.083	0.837	0.882	0.882	0.903	0.907	0.914	0.923	0.926
0.139	1.009	1.021	0.986	1.016	1.028	1.027	1.024	1.023
0.194 – 0.806	1.150	1.126	1.122	1.113	1.104	1.094	1.094	1.086
0.861	0.859	0.920	0.934	0.950	0.971	0.988	0.991	0.998
0.917	0.664	0.694	0.766	0.738	0.778	0.822	0.800	0.841
0.972	0.333	0.416	0.440	0.454	0.471	0.506	0.502	0.541

NOTES: [a] Axial Pos. is percent of core height from bottom to top
[b] Burnup ranges are in units of GWd/MTU

5.2 INPUT PARAMETER DESCRIPTION

Sensitivity studies provided in Attachment I were used as the basis for the selection of parameters that maximize the resultant k_{eff} values.

5.3 MATERIALS

This section provides an overview of the materials that were selected for use in the MCNP inputs.

5.3.1 Tuff Material Description

Waste package configurations were represented with a tuff reflector since this is the composition of the drift material. The base components of the tuff composition used for the loading curve determinations is presented in Table 2 with the derived material specifications for the input files presented in Attachment IV (workbook *Tuff composition.xls*, sheet *Latest_Tuff*).

Table 2. Tuff Material Composition

Compound	Wt%
SiO_2	76.29
Al_2O_3	12.55
FeO	0.14
Fe_2O_3	0.97
MgO	0.13
CaO	0.5
Na_2O	3.52
K_2O	4.83
TiO_2	0.11
P_2O_5	0.05
MnO	0.07

Source: DTN:GS000308313211.001, mean values from file zz_sep_249138.txt

NOTE: Derived elemental/isotopic number densities for MCNP inputs are provided in Attachment IV, spreadsheet *Tuff composition.xls*, sheet *Latest_Tuff*

5.3.2 Waste Package MCNP Material Descriptions

The waste package representation for the MCNP calculations follows the description as that shown in Attachment IV. The outer barrier of the waste package was represented as SB-575 N06022, which is a specific type of nickel-based alloy as described in Table 3. The inner barrier was represented as SA-240 S31600, which is nuclear grade 316 stainless steel (SS) with tightened control on carbon and nitrogen content (ASM International 1987, p. 931; and ASME 2001, Section II, SA-240, Table 1) as described in Table 4. The fuel basket plates were represented as Ni-Gd Alloy (Unified Numbering System [UNS] designation is UNS N06464) with 1.5 wt% Gd as described in Table 5, and the thermal shunts were represented as SB-209 A96061 T4 (aluminum 6061) as described in Table 6. The basket side and corner guides, and the basket stiffeners were represented as Grade 70 A 516 carbon steel as described in Table 7. Stiffeners were placed

equidistant along the length of the basket in eight axial locations. Waste package basket material thicknesses were taken from the PWR drawings in Attachment IV.

The chromium, nickel, and iron elemental weight percents obtained from the references were expanded into their constituent natural isotopic weight percents for use in MCNP. This expansion was performed by: (1) calculating a natural weight fraction of each isotope in the elemental state, and (2) multiplying the elemental weight percent in the material of interest by the natural weight fraction of the isotope in the elemental state to obtain the weight percent of the isotope in the material of interest. This process is described mathematically in Equations 2 and 3. The atomic mass values and atom percent of natural element values for these calculations are from Parrington et al. (1996).

$$WF_i = \frac{A_i(At\%_i)}{\sum_{i=1}^{I} A_i(At\%_i)} \qquad \text{(Eq. 2)}$$

where

WF_i = the weight fraction of isotope$_i$ in the natural element
A_i = the atomic mass of isotope$_i$
$At\%i$ = the atom percent of isotope$_i$ in the natural element
I = the total number of isotopes in the natural element

$$Wt\%_i = WF_i(E_{wt\%}) \qquad \text{(Eq. 3)}$$

where

$Wt\%_i$ = the weight percent of isotope$_i$ in the material composition
WF_i = the weight fraction of isotope$_i$ from Equation 2
$E_{wt\%}$ = the referenced weight percent of the element in the material composition

Table 3. SB-575 N06022 Material Composition

Element/ Isotope	ZAID[a]	Wt%	Element/ Isotope	ZAID	Wt%
C-nat	6000.50c	0.0150	Co-59	27059.50c	2.5000
Mn-55	25055.50c	0.5000	W-182[b]	74182.55c	0.7877
Si-nat	14000.50c	0.0800	W-183[b]	74183.55c	0.4278
Cr-50	24050.60c	0.8879	W-184[b]	74184.55c	0.9209
Cr-52	24052.60c	17.7863	W-186[b]	74186.55c	0.8636
Cr-53	24053.60c	2.0554	V	23000.50c	0.3500
Cr-54	24054.60c	0.5202	Fe-54	26054.60c	0.2260
Ni-58	28058.60c	36.8024	Fe-56	26056.60c	3.6759
Ni-60	28060.60c	14.6621	Fe-57	26057.60c	0.0865
Ni-61	28061.60c	0.6481	Fe-58	26058.60c	0.0116
Ni-62	28062.60c	2.0975	S-32	16032.50c	0.0200
Ni-64	28064.60c	0.5547	P-31	15031.50c	0.0200
Mo-nat	42000.50c	13.5000	Density = 8.69 g/cm^3		

Source: DTN: MO0003RIB00071.000

NOTES: [a] ZAID = MCNP material identifier
[b] W-180 cross section libraries are not available so the atom percents of the remaining isotopes were used to renormalize the elemental weight and derive isotopic weight percents excluding the negligible 0.120 atom percent in nature contribution from W-180.

Table 4. Material Specifications for SA-240 S31600

Element/Isotope	ZAID[a]	Wt%	Element/Isotope	ZAID	Wt%
C-nat[b]	6000.50c	0.0200	Fe-54	26054.60c	3.6911
N-14[b]	7014.50c	0.0800	Fe-56	26056.60c	60.0322
Si-nat	14000.50c	1.0000	Fe-57	26057.60c	1.4119
P-31	15031.50c	0.0450	Fe-58	26058.60c	0.1897
S-32	16032.50c	0.0300	Ni-58	28058.60c	8.0641
Cr-50	24050.60c	0.7103	Ni-60	28060.60c	3.2127
Cr-52	24052.60c	14.2291	Ni-61	28061.60c	0.1420
Cr-53	24053.60c	1.6443	Ni-62	28062.60c	0.4596
Cr-54	24054.60c	0.4162	Ni-64	28064.60c	0.1216
Mn-55	25055.50c	2.0000	Mo-nat	42000.50c	2.5000
Density[c] = 7.98 g/cm^3					

NOTES: [a] ZAID = MCNP material identifier
[b] Carbon and nitrogen specifications are from ASM International (1987, p. 931) and remaining material compositions are from ASM International (1990b p. 843)
[c] Density is for stainless steel 316 from ASTM (G 1-90, p. 7, Table X1)

Table 5. Material Specifications for Ni-Gd Alloy (UNS N06464) with 1.5 wt% Gd[b]

Element/Isotope	ZAID[a]	Wt%	Element/Isotope	ZAID	Wt%
C-nat	6000.50c	0.0100	Gd-152	64152.50c	0.0029
Mn-55	25055.50c	0.5000	Gd-154	64154.50c	0.0320
Si-nat	14000.50c	0.0800	Gd-155	64155.50c	0.2187
Cr-50	24050.60c	0.6602	Gd-156	64156.50c	0.3045
Cr-52	24052.60c	13.2247	Gd-157	64157.50c	0.2343
Cr-53	24053.60c	1.5283	Gd-158	64158.50c	0.3742
Cr-54	24054.60c	0.3868	Gd-160	64160.50c	0.3335
Ni-58	28058.60c	43.3679	Fe-54	26054.60c	0.0565
Ni-60	28060.60c	17.2778	Fe-56	26056.60c	0.9190
Ni-61	28061.60c	0.7637	Fe-57	26057.60c	0.0216
Ni-62	28062.60c	2.4717	Fe-58	26058.60c	0.0029
Ni-64	28064.60c	0.6537	S-32	16032.50c	0.0050
Mo-nat	42000.50c	14.5500	P-31	15031.50c	0.0050
Co-59	27059.50c	2.0000	O-16	8016.50c	0.0050
Density = 8.76 g/cm^3					

Source: ASTM B 932-04, Table 1 and Section 8

NOTE: [a] ZAID = MCNP material identifier
[b] 1.5wt% Gd is based on typical value of 75% credit (NRC 2000, p. 8-4) allowed for fixed neutron absorbers and a nominal Gd loading of 2.0 wt% for Ni-Gd Alloy

Table 6. Material Specifications for SB-209 A96061 T4

Element/Isotope	ZAID[a]	Wt%	Element/Isotope	ZAID	Wt%
Si-nat	14000.50c	0.6000	Mg-nat	12000.50c	1.0000
Fe-54	26054.60c	0.0396	Cr-50	24050.60c	0.0081
Fe-56	26056.60c	0.6433	Cr-52	24052.60c	0.1632
Fe-57	26057.60c	0.0151	Cr-53	24053.60c	0.0189
Fe-58	26058.60c	0.0020	Cr-54	24054.60c	0.0048
Cu-63	29063.60c	0.1884	Ti-nat	22000.50c	0.1500
Cu-65	29065.60c	0.0866	Al-27[b]	13027.50c	96.9300
Mn-55	25055.50c	0.1500	Density[c] = 2.7065 g/cm^3		

Source: ASM International 1990a, p. 102

NOTES: [a] ZAID = MCNP material identifier.
[b] Zn cross-section data unavailable; therefore, it was substituted as Al-27 (See Assumption 3.4).
[c] ASTM G 1-90 1999, p. 7, Table X1 indicates 2.7 g/cm^3; ASME 2001, Section II, Table NF-2 indicates a converted value from 0.098 lb/in^3 of 2.713 g/cm^3; therefore the midpoint was used.

Table 7. Grade 70 A516 Carbon Steel Composition

Element/Isotope	ZAID[a]	Wt%	Element/Isotope	ZAID	Wt%
C-nat	6000.50c	0.2700	Fe-54	26054.60c	5.5558
Mn-55	25055.50c	1.0450	Fe-56	26056.60c	90.3584
P-31	15031.50c	0.0350	Fe-57	26057.60c	2.1252
S-32	16032.50c	0.0350	Fe-58	26058.60c	0.2856
Si-nat	14000.50c	0.2900	Density = 7.850 g/cm^3		

Source: ASTM A 516/A 516M-90 1991, p. 2, Table 1; density from ASME 2001, Sec II, Part A, SA-20, Section 14.1

NOTE: [a] ZAID = MCNP material identifier

5.3.3 Fuel Assembly MCNP Material Descriptions

The fuel assembly materials listed in this section refer to the upper and lower end-fitting materials, the cladding, and fuel plenum materials. In order to simplify the geometry the spacer grids were omitted from the MCNP representations. This is considered conservative with respect to criticality calculations for under-moderated lattices because there is less moderator displacement thereby increasing the moderator effectiveness where the spacer grids would normally be.

The cladding composition was Zircaloy-4 as presented in Table 8.

Table 8. Zircaloy-4 Material Composition

Element/Isotope	ZAID[a]	Wt%	Element/Isotope	ZAID	Wt%
Cr-50	24050.60c	0.0042	Fe-57	26057.60c	0.0045
Cr-52	24052.60c	0.0837	Fe-58	26058.60c	0.0006
Cr-53	24053.60c	0.0097	O-16	8016.50c	0.1250
Cr-54	24054.60c	0.0024	Zr-nat	40000.60c	98.1150
Fe-54	26054.60c	0.0119	Sn-nat	50000.35c	1.4500
Fe-56	26056.60c	0.1930	Density[b] = 6.56 g/cm^3		

Source: ASTM B 811-97 2000, p. 2, Table 2

NOTES: [a] ZAID = MCNP material identifier.
[b] From ASM International 1990a, p. 666, Table 6.

The primary material components in the upper and lower end-fitting regions are SS304 (Table 9), Inconel (represented as Inconel-718 as shown in Table 10), Zircaloy-4 as represented in Table 8, and moderator (represented as water at 1.0 g/cm^3 density). Both the upper and lower end-fitting regions are represented with material compositions that represent the homogenization of all of the components in the regions for the B&W 15x15 assembly design. The homogenization of the base components into single homogenized material compositions is performed using Equations 4 through 6. Table 11 presents the component material volume fractions for the upper and lower end-fitting regions and Table 12 presents the base case upper and lower end-fitting homogenized material compositions. Table 13 presents the upper and lower fuel rod plenum material volume fractions and Table 14 presents the base case upper and lower fuel rod plenum homogenized material compositions.

$$Homogenized\ Material\ Density = \sum_{m}^{M}\left[(\rho)_m\left(Volume\ Fraction\ in\ Homogenized\ Material\right)_m\right]$$

(Eq. 4)

where

m = a single component material of the homogenized material
M = the total number of component materials in the homogenized material
ρ = the mass density of the component material.

$$\begin{pmatrix} Mass\ Fraction\ of\ Component \\ Material\ in\ Homogenized\ Material \end{pmatrix} = \left[\frac{(\rho)_m\left(Volume\ Fraction\ in\ Homogenized\ Material\right)_m}{Homogenized\ Material\ Density}\right]$$

(Eq. 5)

$$\begin{pmatrix} Weight\ Percent\ of \\ Component\ Material \\ Constituent\ in \\ Homogenized\ Material \end{pmatrix} = \begin{pmatrix} Mass\ Fraction\ of \\ Component\ Material\ in \\ Homogenized\ Material \end{pmatrix}\begin{pmatrix} Weight\ Percent\ of\ Component \\ Material\ Constituent \\ in\ Component\ Material \end{pmatrix}$$

(Eq. 6)

Table 9. SS304 Material Composition

Element	Wt%	Element	Wt%
Carbon	0.080 (0.030[a])	Chromium	19.000
Nitrogen	0.100	Manganese	2.000
Silicon	0.750	Iron	Balance 68.745 (68.045[a])
Phosphorous	0.045	Nickel	9.250 (10.000[a])
Sulfur	0.030	Density = 7.94 g/cm^3	

Source: ASME (2001, Section II, SA-240, Table 1); Density from ASTM (1999, G 1-90, p. 7, Table X1)

NOTE: [a] Carbon and Nickel composition corresponds to SS304L which yields a different iron balance

Table 10. Inconel 718 Material Composition

Element	Wt%	Element	Wt%	Element	Wt%
Nickel	52.500	Molybdenum	3.050	Silicon	0.180
Chromium	19.000	Titanium	0.900	Carbon	0.040
Iron	18.500	Aluminum	0.500	Sulfur	0.008
Niobium[a]	5.130	Manganese	0.180	Density = 8.19 g/cm^3	

Source: Lynch 1989, p. 496

NOTE: [a] Reference identifies this material as “columbium,” which is actually the element niobium.

Table 11. End-Fitting Component Material Volume Fractions

Assembly Design	Stainless Steel Type 304	Inconel	Zircaloy-4	Moderator
Upper End-Fitting	0.2756	0.0441	0.0081	0.6722
Lower End-Fitting	0.1656	0.0306	0.0125	0.7913

Source: Punatar 2001, Table 2-3

Table 12. End-Fitting Homogenized Material Compositions

Element/ Isotope	ZAID[a]	Upper End-Fitting Wt%[b]	Lower End-Fitting Wt%[b]
C-nat	6000.50c	0.0245	0.0203
N-14	7014.50c	0.0668	0.0539
Si-nat	14000.50c	0.5210	0.4229
P-31	15031.50c	0.0301	0.0243
S-32	16032.50c	0.0209	0.0170
Cr-50	24050.60c	0.6181	0.5098
Cr-52	24052.60c	12.3822	10.2114
Cr-53	24053.60c	1.4309	1.1800
Cr-54	24054.60c	0.3622	0.2987
Mn-55	25055.50c	1.3563	1.0968
Fe-54	26054.60c	2.6847	2.1808
Fe-56	26056.60c	43.6633	35.4677
Fe-57	26057.60c	1.0269	0.8342
Fe-58	26058.60c	0.1380	0.1121
Ni-58	28058.60c	8.3820	7.2490
Ni-60	28060.60c	3.3394	2.8880
Ni-61	28061.60c	0.1476	0.1277
Ni-62	28062.60c	0.4777	0.4132
Ni-64	28064.60c	0.1263	0.1093
H-1	1001.50c	2.2972	3.6312
O-16	8016.50c	18.2314	28.8196
Al-27	13027.50c	0.0552	0.0514
Ti-nat	22000.50c	0.0993	0.0925
Nb-93	41093.50c	0.5659	0.5272
Mo-nat	42000.50c	0.3364	0.3135
Zr-nat	40000.60c	1.5920	3.2990
Sn-nat	50000.35c	0.0235	0.0488
Density (g/cm^3)		3.2748	2.4388

NOTES: [a] ZAID = MCNP material identifier.
[b] Homogenization used stainless steel 304L values for carbon, nickel, and iron

Table 13. Fuel Rod Plenum Material Volume Fractions

Assembly Design	Plenum Location	Type 304 Stainless Steel	Gas (modeled as void)	Zircaloy-4
Babcock & Wilcox 15×15	Upper	0.0811	0.7793	0.1396
	Lower	0.1569	0.5973	0.2458

Source: Punatar 2001, Table 2-9 and Figures 2-3 and 2-7

NOTE: Volume fractions are renormalized to exclude the cladding, which is modeled explicitly in the input.

Table 14. Fuel Rod Plenum Homogenized Material Compositions

Element/Isotope	ZAID[a]	Wt% of Element/Isotope in Material Composition	
		Upper Fuel Rod Plenum[b]	Lower Fuel Rod Plenum[b]
C-nat	6000.50c	0.0124	0.0131
N-14	7014.50c	0.0413	0.0436
Si-nat	14000.50c	0.3096	0.3270
P-31	15031.50c	0.0186	0.0196
S-32	16032.50c	0.0124	0.0131
Cr-50	24050.60c	0.3302	0.3485
Cr-52	24052.60c	6.6148	6.9806
Cr-53	24053.60c	0.7644	0.8067
Cr-54	24054.60c	0.1935	0.2042
Mn-55	25055.50c	0.8257	0.8720
Fe-54	26054.60c	1.5943	1.6829
Fe-56	26056.60c	25.9299	27.3712
Fe-57	26057.60c	0.6099	0.6438
Fe-58	26058.60c	0.0820	0.0865
Ni-58	28058.60c	2.7744	2.9298
Ni-60	28060.60c	1.1053	1.1672
Ni-61	28061.60c	0.0489	0.0516
Ni-62	28062.60c	0.1581	0.1670
Ni-64	28064.60c	0.0418	0.0442
O-16	8016.50c	0.0734	0.0705
Zr-nat	40000.60c	57.6077	55.3392
Sn-nat	50000.35c	0.8514	0.8178
Density (g/cm^3)		1.5597	2.8583

NOTES: [a] ZAID = MCNP material identifier.
[b] Homogenization used stainless steel 304L values for carbon and nickel

5.3.4 Fuel Material

The following information provides the details needed to duplicate the input file specifications. The uranium dioxide fresh fuel compositions for each U-235 enrichment used in this evaluation are specified in Table 15, and were calculated using Equation 7 (Bowman et al. 1995, p. 20) for each isotope based on the U-235 wt%.

Table 15. Fresh Fuel Compositions

Enrichment (wt% U-235)	Wt% U-234	Wt% U-235	Wt% U-236	Wt% U-238	Wt% Oxygen
1.5	0.0106	1.3222	0.0061	86.8098	11.8513
2.0	0.0144	1.7630	0.0081	86.3625	11.8519
2.5	0.0184	2.2037	0.0101	85.9152	11.8526
3.0	0.0224	2.6444	0.0122	85.4677	11.8533
3.5	0.0265	3.0851	0.0142	85.0202	11.8540
4.0	0.0306	3.5258	0.0162	84.5727	11.8547
4.5	0.0348	3.9665	0.0182	84.1251	11.8553
5.0	0.0390	4.4072	0.0203	83.6775	11.8560

$$U^{234}\ wt\% = (0.007731) * (U^{235}\ wt\%)^{1.0837}$$

$$U^{236}\ wt\% = (0.0046) * (U^{235}\ wt\%) \qquad \text{(Eq. 7)}$$

$$U^{238}\ wt\% = 100 - U^{234}\ wt\% - U^{235}\ wt\% - U^{236}\ wt\%$$

The initial oxygen mass is calculated using Equations 8 through 10. In Equations 8 and 9 the atomic mass values (M) come from Audi and Wapstra (1995).

$$\frac{U\ Mass}{mol\ UO_2} = \left(\sum_i \frac{\frac{wt\%_i}{100}}{M_i} \right)^{-1} \qquad \text{(Eq. 8)}$$

where the weight percentages ($wt\%_i$) of the uranium isotopes (U^{234}, U^{236}, and U^{238}) in uranium for a given initial enrichment were calculated using Equation 7.

$$\frac{O\ Mass}{mol\ UO_2} = (2)(M\ \ for\ oxygen) \qquad \text{(Eq. 9)}$$

$$O\ Mass\ in\ UO_2 = \left(\frac{O\ Mass / mol\ UO_2}{U\ Mass / mol\ UO_2} \right) (U\ Mass\ in\ UO_2) \qquad \text{(Eq. 10)}$$

where

U Mass in UO_2 is the fresh fuel uranium mass

The spent fuel isotopes used in the MCNP cases correspond to those of the Principal Isotope Set (YMP 2003, Table 3-1). The irradiated fuel material compositions were taken from BSC (2003b, Section 6). Each nodal-depleted fuel composition is contained in the MCNP input files provided

in Attachment IV. The nodal fuel isotopic compositions are listed in the input files in terms of ZAIDs and atoms/b-cm. The spreadsheet used for deriving interpolated values and the axial profile isotopics is contained in Attachment IV (spreadsheet *IDBinputs.xls*).

5.4 MCNP GEOMETRIC DESCRIPTIONS

The drawing for the 21-PWR waste package with absorber plates dimensions is contained electronically in Attachment IV. The MCNP representation of the 21-PWR waste package follows the same description as that shown in Attachment IV for the initial (at time of loading) configuration.

When developing a loading curve, a configuration that results in the highest k_{eff} should be used in order to set an upper bounding limit that encompasses all other configurations. Therefore, the selection of a bounding configuration follows a linear progression based upon the results of other cases. Several potential configurations that could occur in the repository over a 10,000 year regulatory period were evaluated to determine which result in the highest k_{eff} values. The configurations are intended to investigate the effects on system reactivity as the waste package internal components degrade and the geometry changes. A series of configurations were evaluated with the descriptions and results provided in Attachment I. Based on the results, a combination of parameters was selected which will produce the most reactive representation for the generation of the loading curve.

Based on the results of configurations presented in Attachment I, the preclosure bounding configuration is the as loaded representation with dry tuff surrounding the waste package. Dry tuff is used over saturated tuff due to the thermal load within the repository for the first 300 years precluding water from the surrounding drift area. The postclosure bounding configuration is represented by the intact fuel rods with saturated tuff surrounding the waste package and waste package internal hardware represented as in case3, from Attachment I, Section I.6. These configurations are the representative configurations for the loading curve evaluations.

5.4.1 Fuel Assembly

The physical dimensions for the fuel assembly design represented in the MCNP inputs were obtained from Punatar (2001), and are presented in Table 16, and illustrated in Figures 1 and 2.

Table 16. B&W 15x15 Fuel Assembly Specifications

Assembly Component	Specification
Fuel Pellet Outer Diameter	0.93980 cm
Fuel Rod Cladding Inner Diameter	0.95758 cm
Fuel Rod Cladding Outer Diameter	1.09220 cm
Guide Tube Inner Diameter	1.26492 cm
Guide Tube Outer Diameter	1.34620 cm
Instrument Tube Inner Diameter	1.12014 cm
Instrument Tube Outer Diameter	1.38193 cm

Source: Punatar 2001, p. 2-5

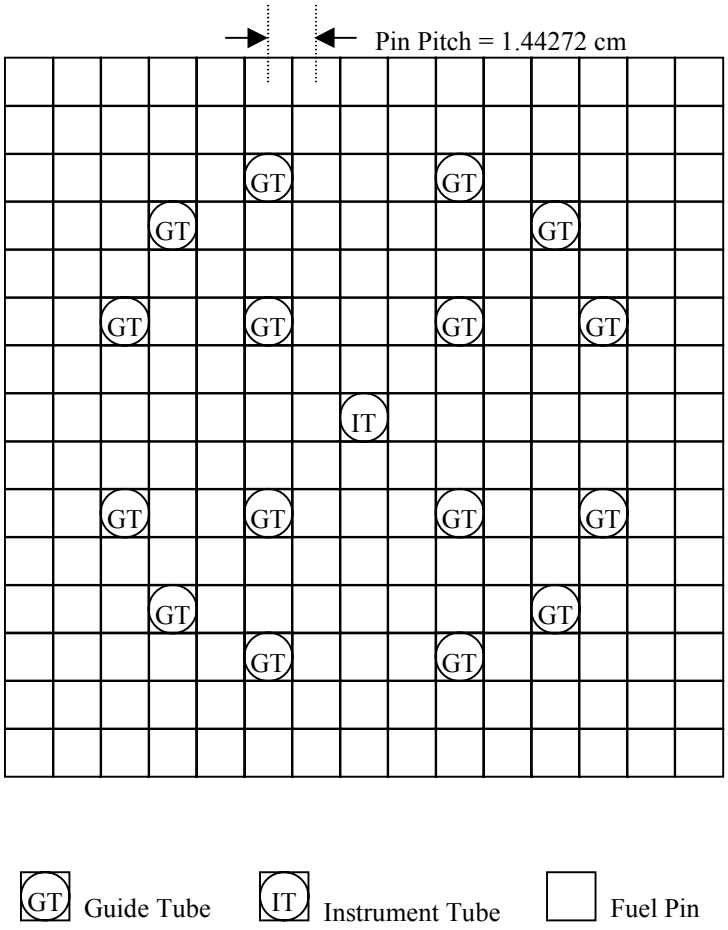

This sketch is not to scale.

Source: (Punatar 2001, p. 2-3)

Figure 1. Fuel Pin, Guide Tube, and Instrument Tube Locations in Fuel Assembly

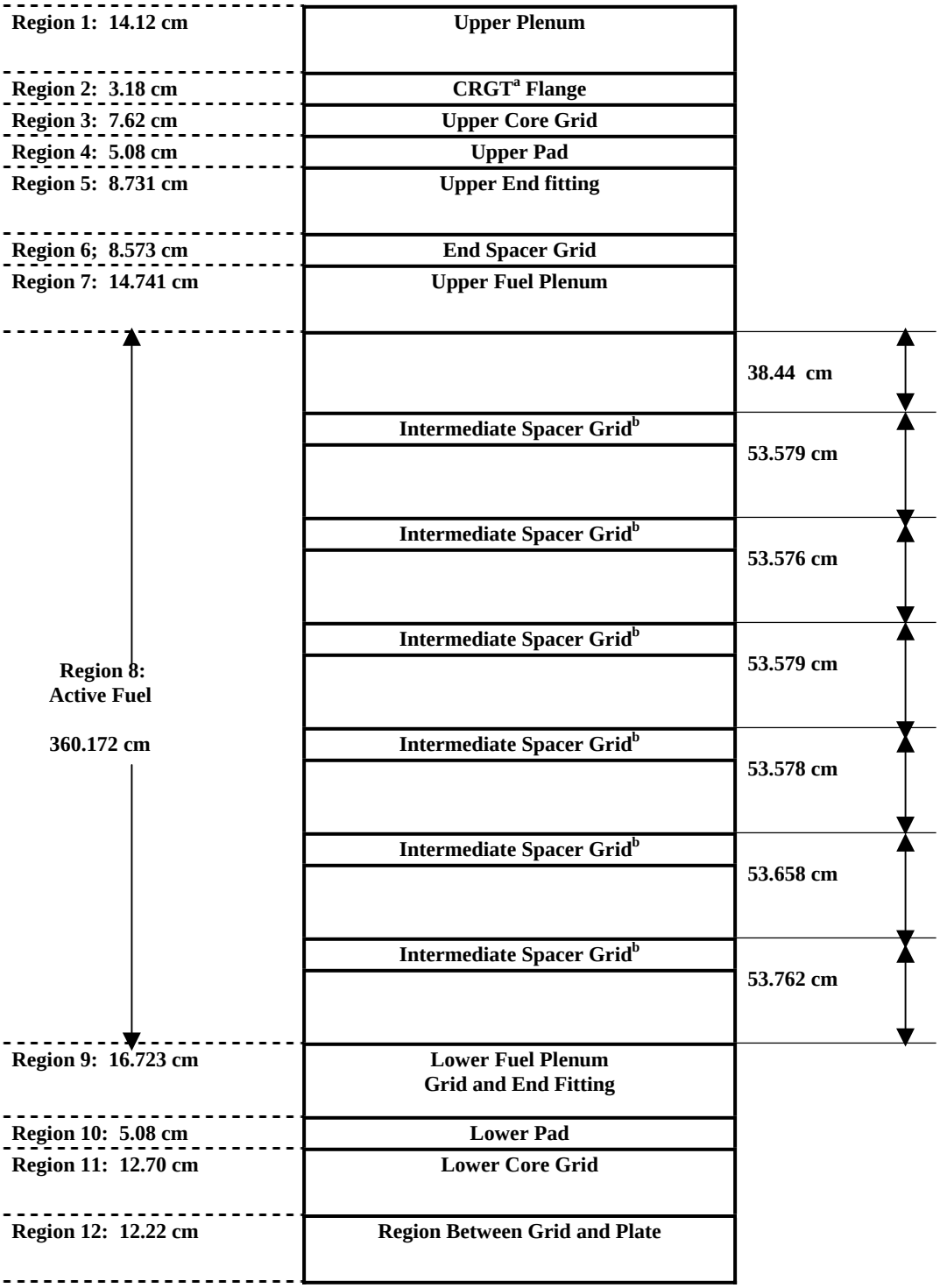

Source: Punatar 2001, p. 2-11

NOTES: [a] Control Rod Guide Tube (CRGT)
[b] Intermediate spacer grid height 3.81 cm

Figure 2. Mark-B4 Fuel Assembly Axial Dimensions by Region

5.5 INPUT PARAMETER SUMMARY

Based on the sensitivity studies presented in Attachment I, the following parameters listed in Table 17 were selected for use in the loading curve generation:

Table 17. Loading Curve Parameters

Parameter	Value	Selection Basis	Applicability
Fuel Material	UO_2	Typical commercial PWR fuel	Preclosure and Postclosure
Absorber	1.5 wt% Gd at nominal thickness	Based on typical value of 75% credit (NRC 2000, p. 8-4) allowed for fixed neutron absorbers and a nominal Gd loading of 2.0 wt% for Ni-Gd Alloy. Thickness based on results from Attachment I, Section I.6	Preclosure and Postclosure
Moderator	Water at density of 1.0 g/cm^3	Attachment I, Section I.3	Preclosure and Postclosure
Fuel Density	10.741 g/cm^3 [a]	Attachment I, Section I.1	Preclosure and Postclosure
Reflector	Dry Tuff	Attachment I, Section I.5	Preclosure
	100% Saturated Tuff	Attachment I, Section I.5	Postclosure
Geometry	Lattice array in Standard Vertical configuration (See Attachment I, Figure 36)	Attachment I, Section I.3	Preclosure
	Lattice array in Standard Vertical configuration (See Attachment I, Figure 36) with aluminum and iron in plates oxidized	Attachment I, Section I.6 (case3) and Section I.8	Postclosure

NOTE: [a] Calculated based on 98% theoretical density value of 10.96 g/cm^3 for UO_2 (Todreas and Kazimi 1990, p. 296)

6. RESULTS

The loading curves for the 21 PWR waste package are presented in this section. The k_{eff} results represent the average combined collision, absorption, and track-length estimator from the MCNP calculations. The standard deviation (σ) represents the standard deviation of k_{eff} about the average combined collision, absorption, and track-length estimate due to the Monte Carlo calculation statistics. It should be noted that in the following sections, any reference to enrichment refers to assembly average initial enrichment, and burnup refers to assembly average burnup.

The corresponding MCNP input and output files for the cases used in this evaluation are provided electronically in Attachment IV.

6.1 MAXIMUM FRESH FUEL ENRICHMENT

This section presents the results of the maximum fresh fuel enrichments that can be loaded into the waste package with no burnup required. The determination of the maximum fresh fuel enrichment limit for the 21-PWR waste package with Ni-Gd Alloy absorber plates is determined by calculating k_{eff} for a range of initial enrichments and plotting them against the initial enrichments. The k_{eff} values plotted include a two-σ allowance for computational uncertainty. The intersection of this curve and a line representing the critical limit (or USL) shows where the waste package has a potential for criticality. The results of the fresh fuel calculations are presented in Table 18 for the preclosure and postclosure bounding configurations, and are illustrated in Figure 3.

Table 18. Fresh Fuel k_{eff} Results

Configuration	Preclosure Configuration			Postclosure Configuration		
Enrichment (Wt % U-235)	k_{eff}	σ	$k_{eff} + 2\sigma$	k_{eff}	σ	$k_{eff} + 2\sigma$
1.5	0.85742	0.00049	0.85840	0.85504	0.00047	0.85598
2	0.94279	0.00051	0.94381	0.93989	0.0005	0.94089
2.5	1.00382	0.00048	1.00478	1.00146	0.00054	1.00254
3	1.04892	0.00051	1.04994	1.04666	0.00055	1.04776
3.5	1.08529	0.00053	1.08635	1.08269	0.00049	1.08367
4	1.11396	0.00055	1.11506	1.11283	0.00052	1.11387
4.5	1.13984	0.00046	1.14076	1.13819	0.00061	1.13941
5	1.16027	0.00055	1.16137	1.15837	0.00059	1.15955

Figure 3 shows that the maximum fresh fuel enrichment that would meet the loading curve criteria are 2.393 wt% U-235 for the postclosure bounding configuration, and 1.974 wt% U-235 for the preclosure bounding configuration. A CL = 0.9894 was taken from Framatome ANP (2003, Table 11) based on laboratory critical experiments. This CL was chosen because the fresh fuel configuration range of parameters (i.e., materials, geometry, spectrum) is subsumed by the laboratory critical experiment parameters, and since no burned fuel is present in these configurations, the commercial reactor critical benchmarks are not directly applicable. Using this CL with the five percent margin as described in Section 5 yields a preclosure USL = 0.9894.

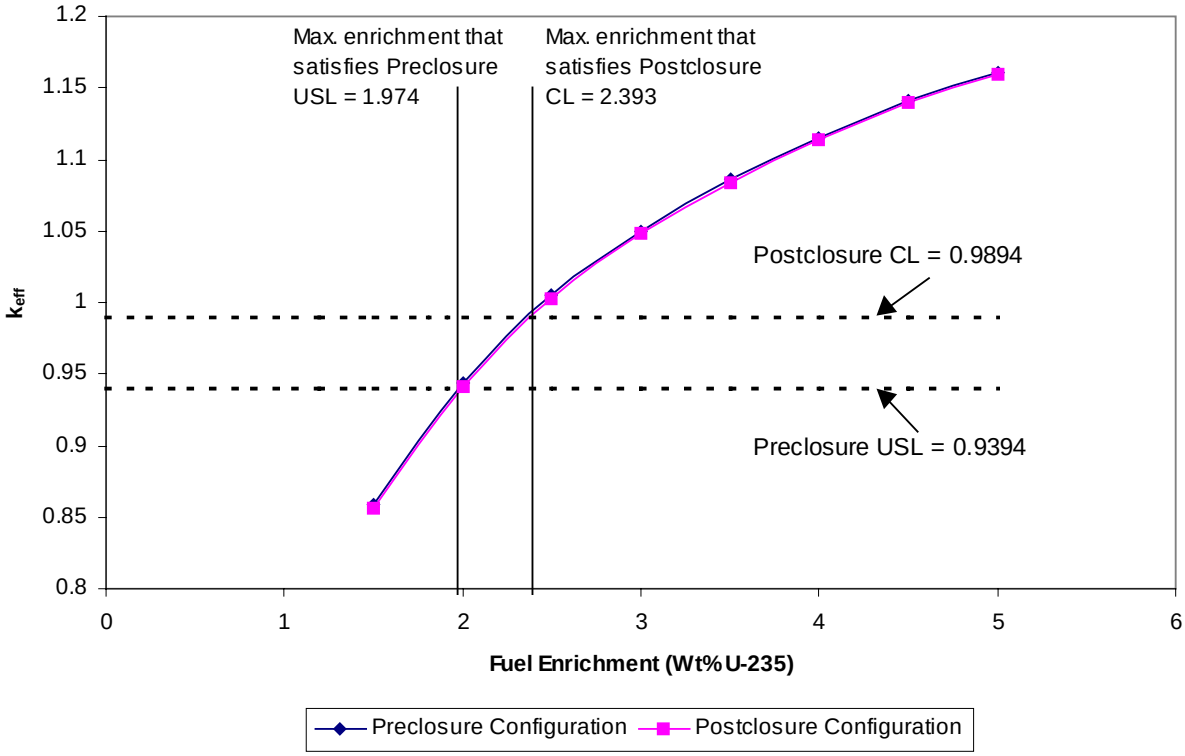

Figure 3. Fresh Fuel k_{eff} Results

6.2 BURNED FUEL

6.2.1 Preclosure

The results for spent fuel with five-year decay time (the five-year decay time is based on the minimum cooling time required for the fuel assemblies to be classified as standard fuel [10 CFR 961.11]) isotopic compositions are presented in Table 20. During the preclosure time period, each waste package is to remain at or below the USL. The minimum burnup required for each initial enrichment is determined by plotting the calculated k_{eff} versus the burnup. The burnup value of the intersection of the plotted curve with the USL is the required minimum burnup and are illustrated in Figures 4 through 17 and summarized in Table 21 and Figure 18. The k_{eff} values plotted include a two-σ allowance for computational uncertainty. Any burnup value greater than this will result in a k_{eff} less than the USL, and is acceptable to be loaded into the waste package. In Figures 4 through 17, the USL is presented as a function of average energy of a neutron causing fission (AENCF). The reported USL intercept values correspond to those for the USL as a function of the most conservative trend parameter as prescribed by YMP 2003 (Section 3.5.3.2.6). The USL equation is provided in Table 19.

Table 19. Spent Nuclear Fuel Upper Subcritical Limit Function

Trend Parameter	USL Equation
AENCF	USL (AENCF) = -0.06262*AENCF + 0.9920 - 0.05

NOTE: Framatome ANP (2003, Table 11) provides the CL function which is transformed into an USL function using $\Delta k_m = 0.05$ (see Section 5 for details of USL transformation)

Table 20. Preclosure Spent Nuclear Fuel k_{eff} Results

Initial Enrichment (Wt% U-235)	Burnup (GWd/ MTU)	7 Node Fuel Zone			1 Node Fuel Zone			$\Delta(k_{eff} + 2\sigma)$[a]
		k_{eff}	σ	AENCF (MeV)	k_{eff}	σ	AENCF (MeV)	
2.0	10	0.88508	0.0005	0.2096	0.8917	0.00049	0.2082	-0.0066
	15	0.85593	0.00053	0.2204	0.86227	0.00051	0.2208	-0.0063
	20	0.8308	0.00051	0.2304	0.83471	0.00049	0.2325	-0.0039
	25	0.80964	0.00047	0.2388	0.81034	0.00045	0.2435	-0.0007
2.5	10	0.93053	0.0005	0.1967	0.93733	0.00053	0.1961	-0.0069
	15	0.90045	0.00055	0.2068	0.90731	0.00047	0.2071	-0.0067
	20	0.8717	0.00053	0.2170	0.87521	0.00047	0.2187	-0.0034
	25	0.84898	0.0005	0.2248	0.84775	0.00052	0.2289	0.0012
	30	0.82512	0.00046	0.2334	0.82298	0.0005	0.2390	0.0021
3.0	10	0.97102	0.00054	0.1874	0.97732	0.00053	0.1867	-0.0063
	15	0.93966	0.00053	0.1969	0.94458	0.00053	0.1970	-0.0049
	20	0.91068	0.00054	0.2050	0.91454	0.00049	0.2074	-0.0038
	25	0.8859	0.00053	0.2131	0.88489	0.00057	0.2167	0.0009
	30	0.86123	0.0005	0.2212	0.85886	0.00045	0.2270	0.0025
	35	0.83547	0.00048	0.2300	0.83313	0.00043	0.2363	0.0024
	40	0.81789	0.00051	0.2362	0.81343	0.00045	0.2451	0.0046
3.5	10	1.00571	0.00051	0.1802	1.01182	0.00055	0.1804	-0.0062
	15	0.9743	0.00053	0.1898	0.97925	0.00053	0.1888	-0.0049
	20	0.94354	0.0005	0.1973	0.94982	0.00051	0.1979	-0.0063
	25	0.91901	0.00056	0.2035	0.92021	0.00049	0.2075	-0.0011
	30	0.89495	0.00055	0.2097	0.89216	0.00054	0.2177	0.0028
	35	0.86804	0.0005	0.2206	0.86561	0.00049	0.2259	0.0025
	40	0.84834	0.00056	0.2253	0.84127	0.00051	0.2344	0.0072
	45	0.82412	0.00053	0.2353	0.81916	0.00048	0.2439	0.0051
4.0	10	1.03478	0.00058	0.1758	1.0404	0.00055	0.1754	-0.0056
	15	1.00411	0.00056	0.1832	1.00895	0.00048	0.1832	-0.0047
	20	0.97336	0.00057	0.1904	0.97971	0.00051	0.1917	-0.0062
	25	0.95	0.00058	0.1966	0.95062	0.00053	0.1999	-0.0005
	30	0.92288	0.0006	0.2035	0.92289	0.0005	0.2073	0.0002
	35	0.8966	0.00057	0.2117	0.89614	0.0005	0.2170	0.0006
	40	0.87871	0.00053	0.2171	0.87118	0.00048	0.2247	0.0076
	45	0.85171	0.00058	0.2251	0.84819	0.00048	0.2332	0.0037

Table 20. Preclosure Spent Nuclear Fuel k_{eff} Results

Initial Enrichment (Wt% U-235)	Burnup (GWd/MTU)	7 Node Fuel Zone			1 Node Fuel Zone			$\Delta(k_{eff} + 2\sigma)$[a]
		k_{eff}	σ	AENCF (MeV)	k_{eff}	σ	AENCF (MeV)	
4.5	10	1.05854	0.00055	0.1720	1.06668	0.00055	0.1713	-0.0081
	15	1.0289	0.0006	0.1786	1.03462	0.00059	0.1780	-0.0057
	20	1.00001	0.00056	0.1855	1.00663	0.0005	0.1855	-0.0065
	25	0.97449	0.00061	0.1918	0.97767	0.00053	0.1940	-0.0030
	30	0.94911	0.00061	0.1977	0.95165	0.00053	0.2004	-0.0024
	35	0.92334	0.00053	0.2044	0.92505	0.00058	0.2092	-0.0018
	40	0.90304	0.00054	0.2104	0.89899	0.00049	0.2167	0.0041
	45	0.87742	0.00065	0.2188	0.8739	0.00052	0.2249	0.0038
5.0	10	1.08132	0.00055	0.1689	1.08738	0.00058	0.1681	-0.0061
	15	1.05225	0.00056	0.1741	1.05803	0.00052	0.1751	-0.0057
	20	1.02368	0.00055	0.1812	1.02929	0.00053	0.1810	-0.0056
	25	1.00005	0.00052	0.1864	1.00312	0.00054	0.1884	-0.0031
	30	0.9739	0.00056	0.1928	0.97666	0.00052	0.1954	-0.0027
	35	0.94695	0.00055	0.1994	0.94965	0.00052	0.2026	-0.0026
	40	0.9273	0.00046	0.2036	0.92413	0.00054	0.2105	0.0030
	45	0.90526	0.00057	0.2101	0.89889	0.00046	0.2179	0.0066

NOTE: [a] $\Delta(k_{eff} + 2\sigma) = (k_{eff} + 2\sigma)_{7\ Node} - (k_{eff} + 2\sigma)_{1\ Node}$

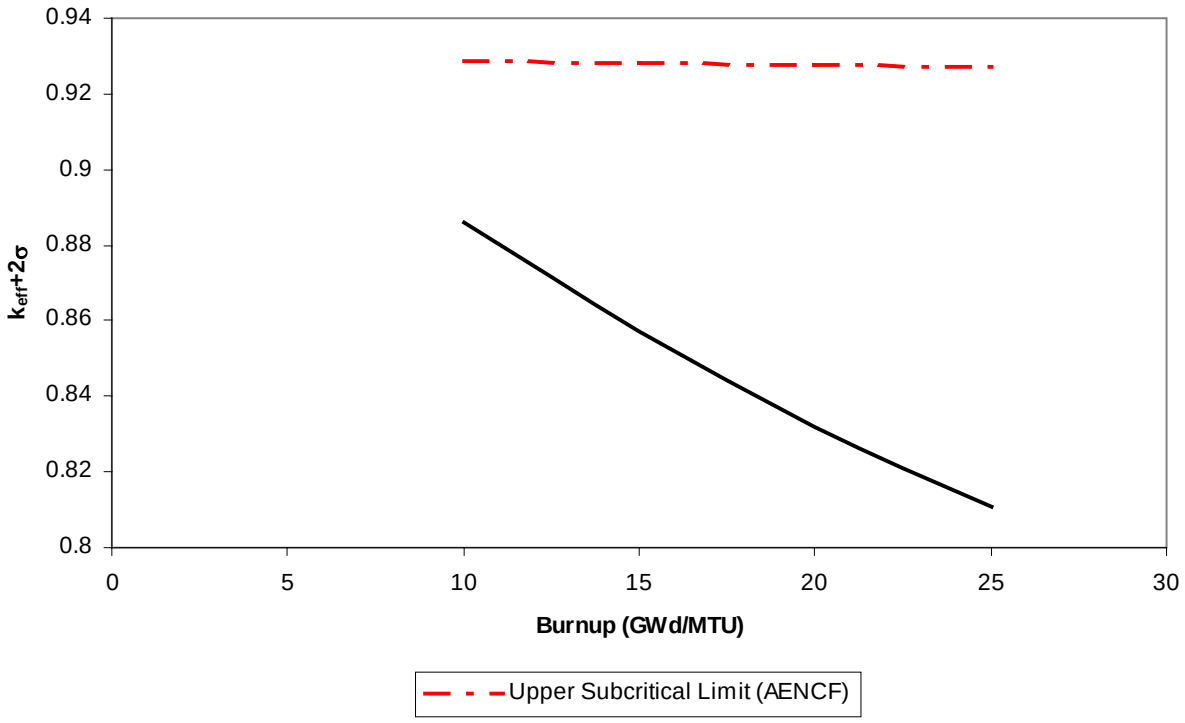

Figure 4. Preclosure 7 Node Spent Nuclear Fuel k_{eff} Results for 2.0 Wt% U-235 Initial Enrichment

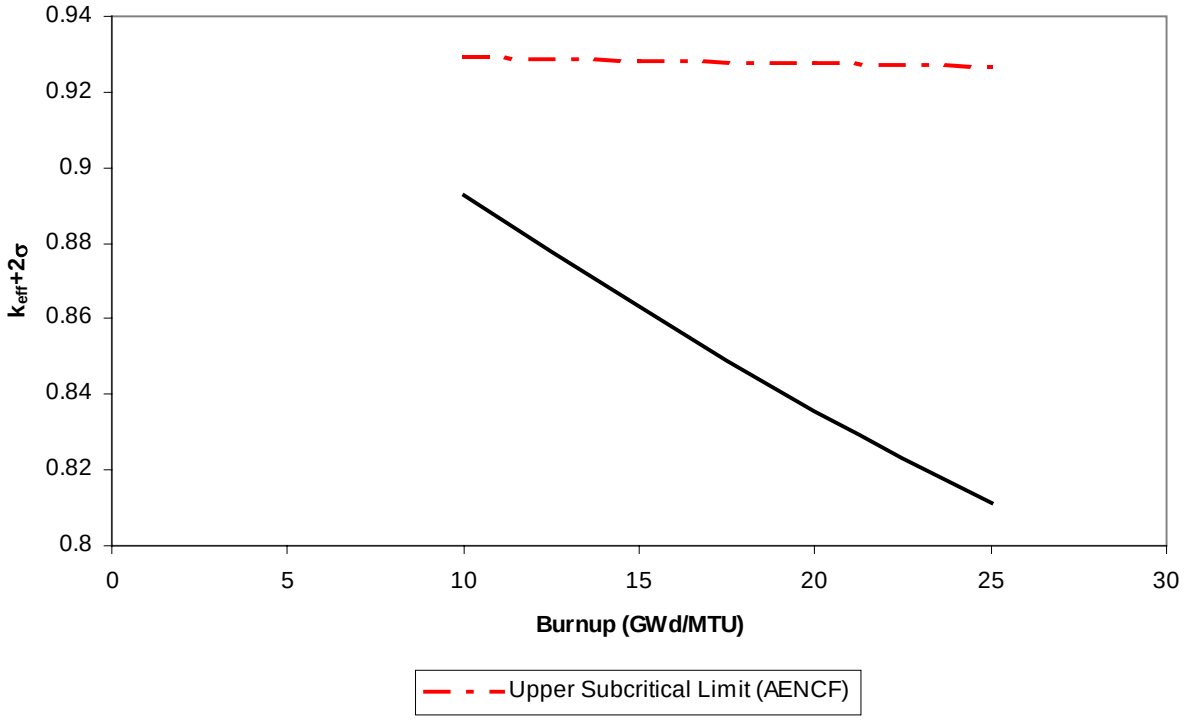

Figure 5. Preclosure 1 Node Spent Nuclear Fuel k_{eff} Results for 2.0 Wt% U-235 Initial Enrichment

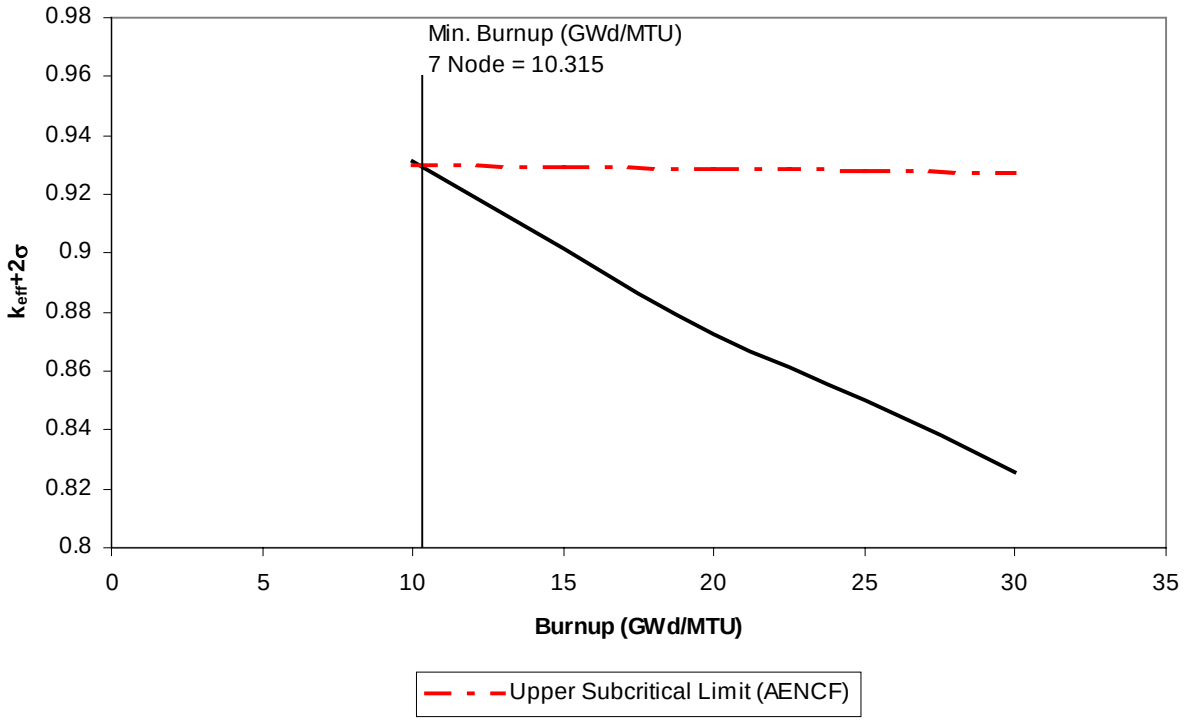

Figure 6. Preclosure 7 Node Spent Nuclear Fuel k_{eff} Results for 2.5 Wt% U-235 Initial Enrichment

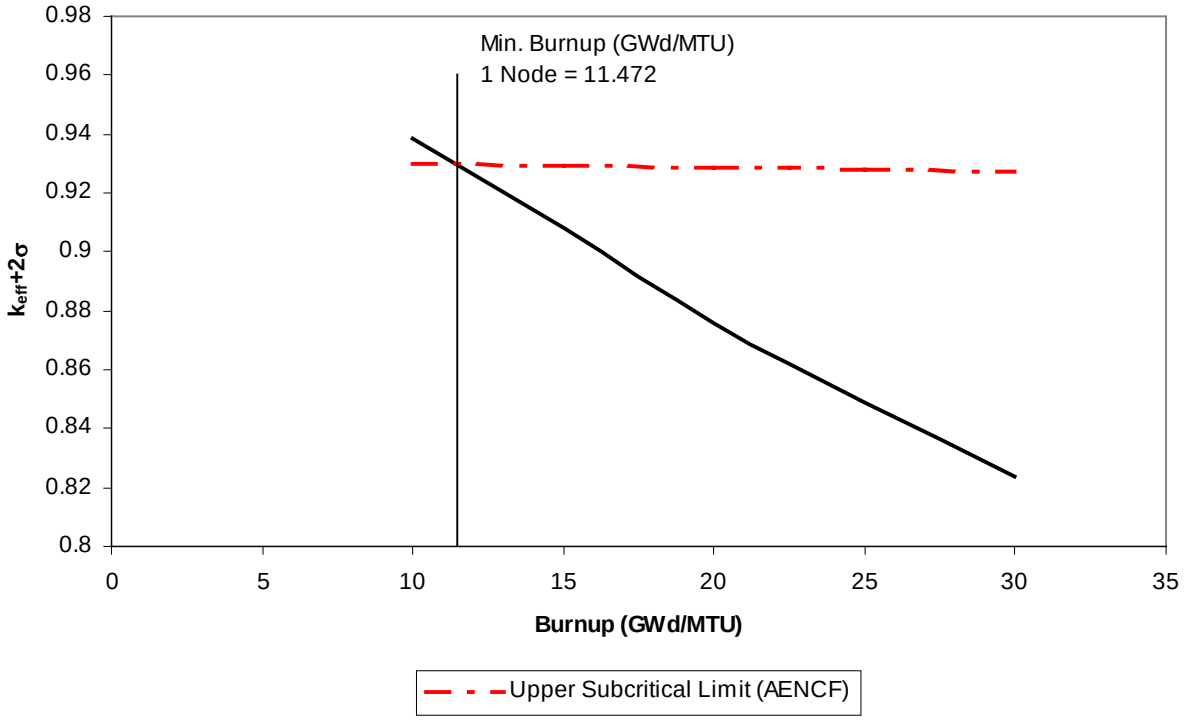

Figure 7. Preclosure 1 Node Spent Nuclear Fuel k_{eff} Results for 2.5 Wt% U-235 Initial Enrichment

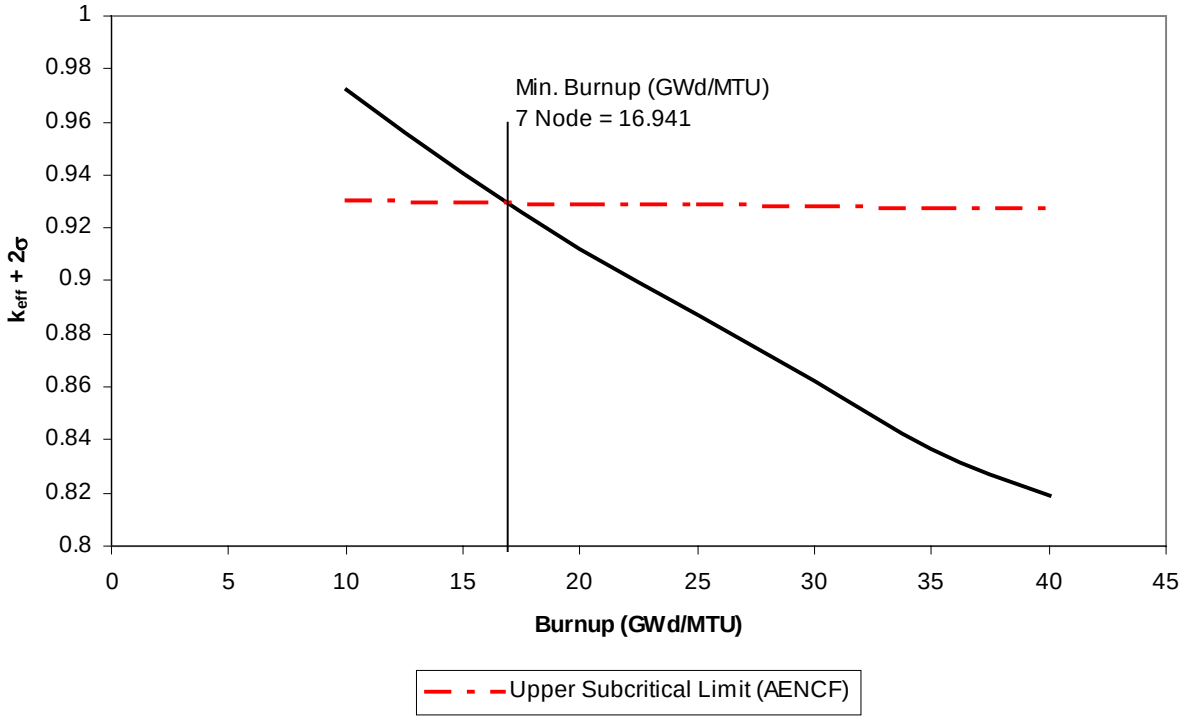

Figure 8. Preclosure 7 Node Spent Nuclear Fuel k_{eff} Results for 3.0 Wt% U-235 Initial Enrichment

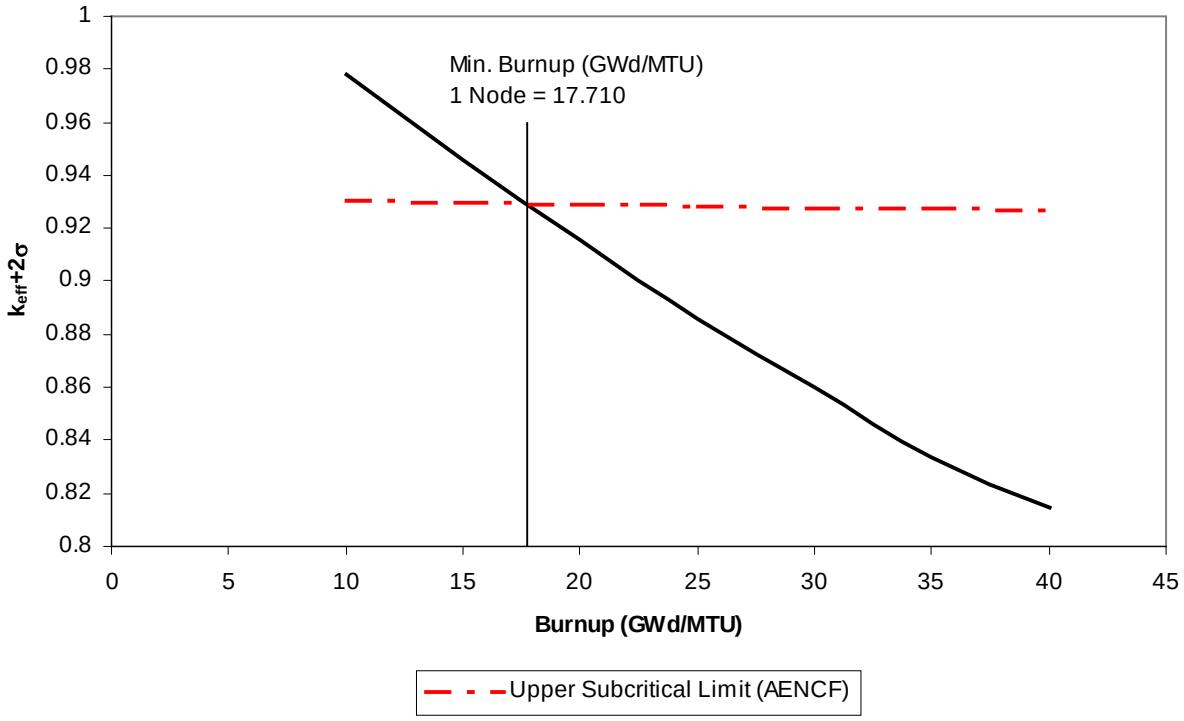

Figure 9. Preclosure 1 Node Spent Nuclear Fuel k_{eff} Results for 3.0 Wt% U-235 Initial Enrichment

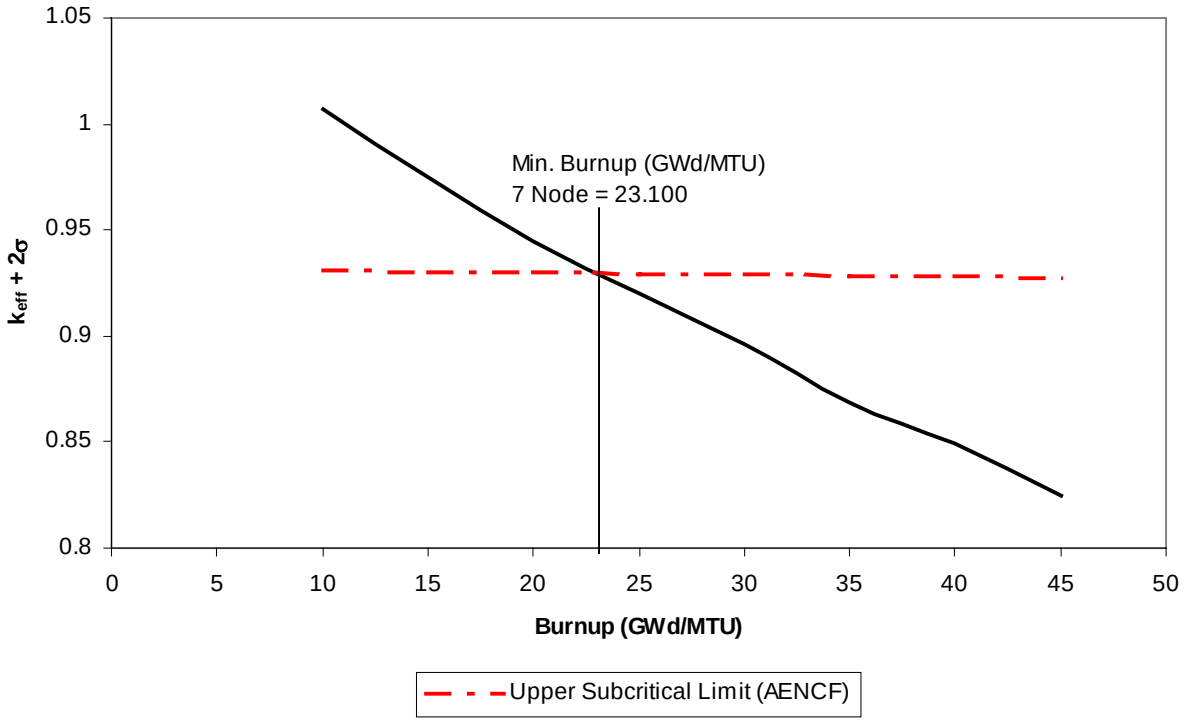

Figure 10. Preclosure 7 Node Spent Nuclear Fuel k_{eff} Results for 3.5 Wt% U-235 Initial Enrichment

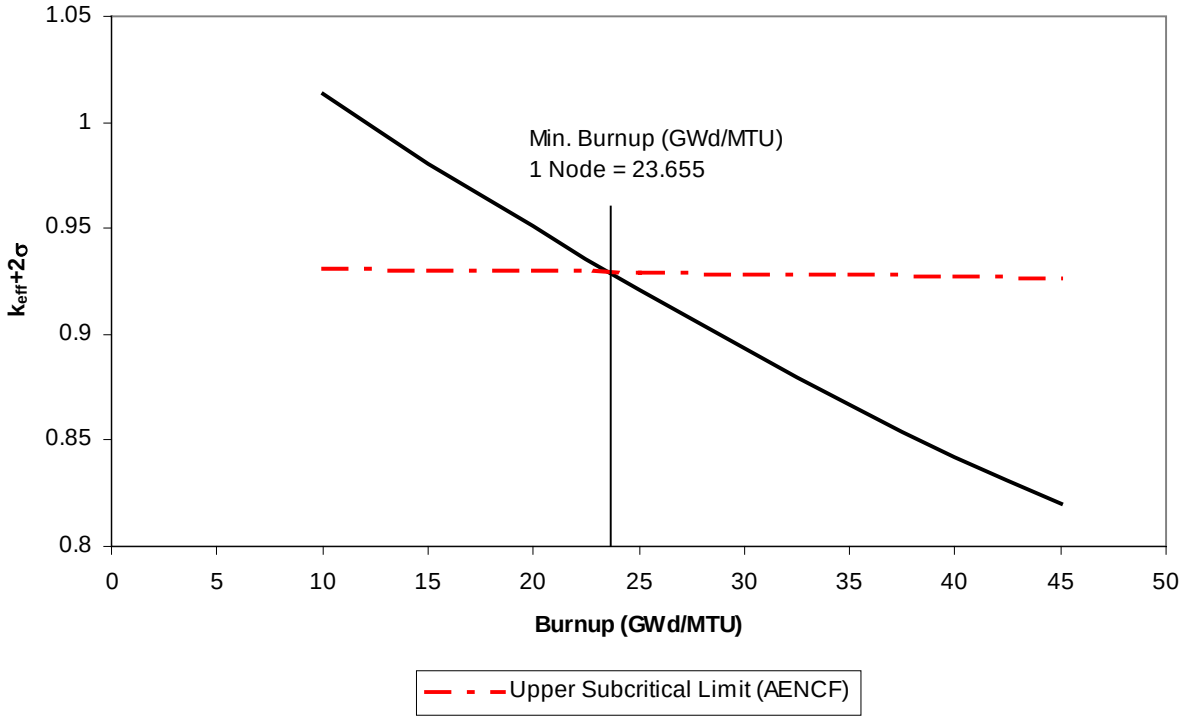

Figure 11. Preclosure 1 Node Spent Nuclear Fuel k_{eff} Results for 3.5 Wt% U-235 Initial Enrichment

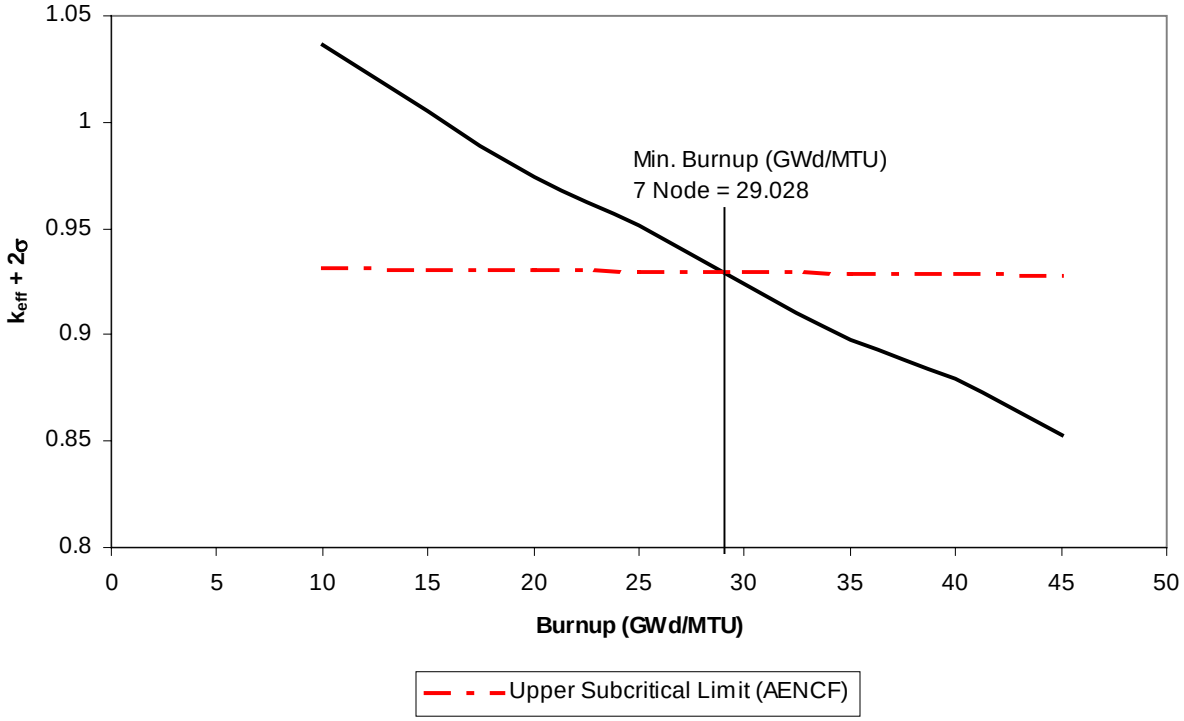

Figure 12. Preclosure 7 Node Spent Nuclear Fuel k_{eff} Results for 4.0 Wt% U-235 Initial Enrichment

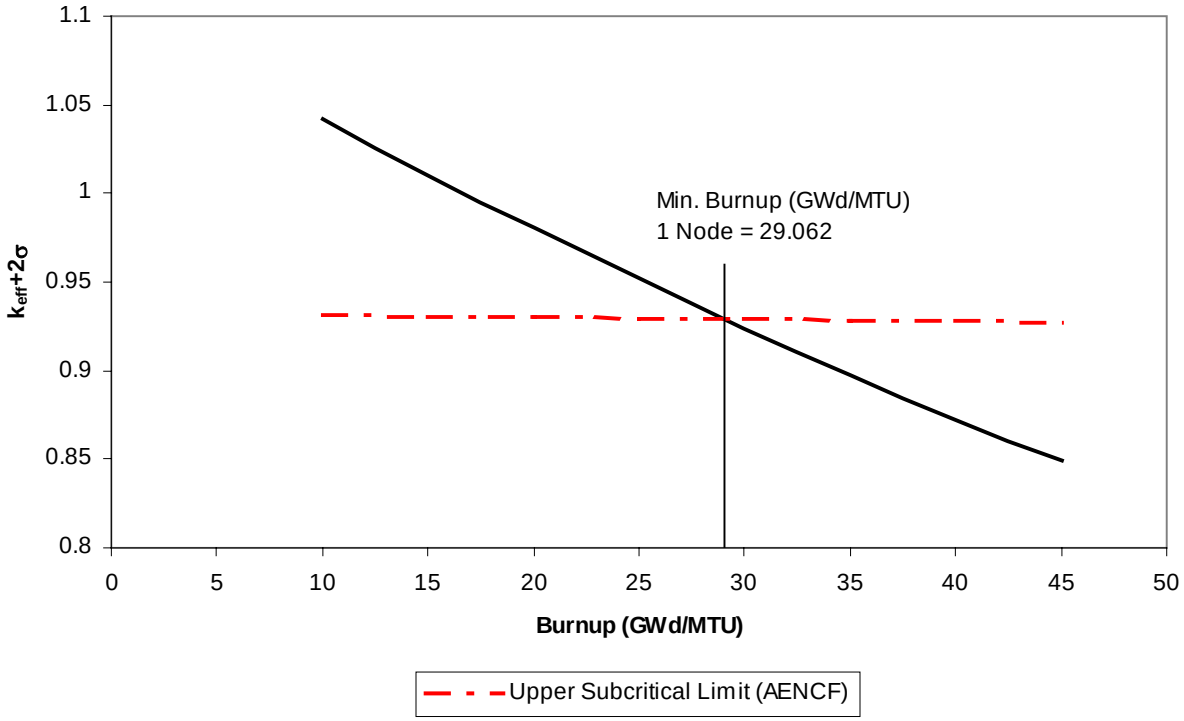

Figure 13. Preclosure 1 Node Spent Nuclear Fuel k_{eff} Results for 4.0 Wt% U-235 Initial Enrichment

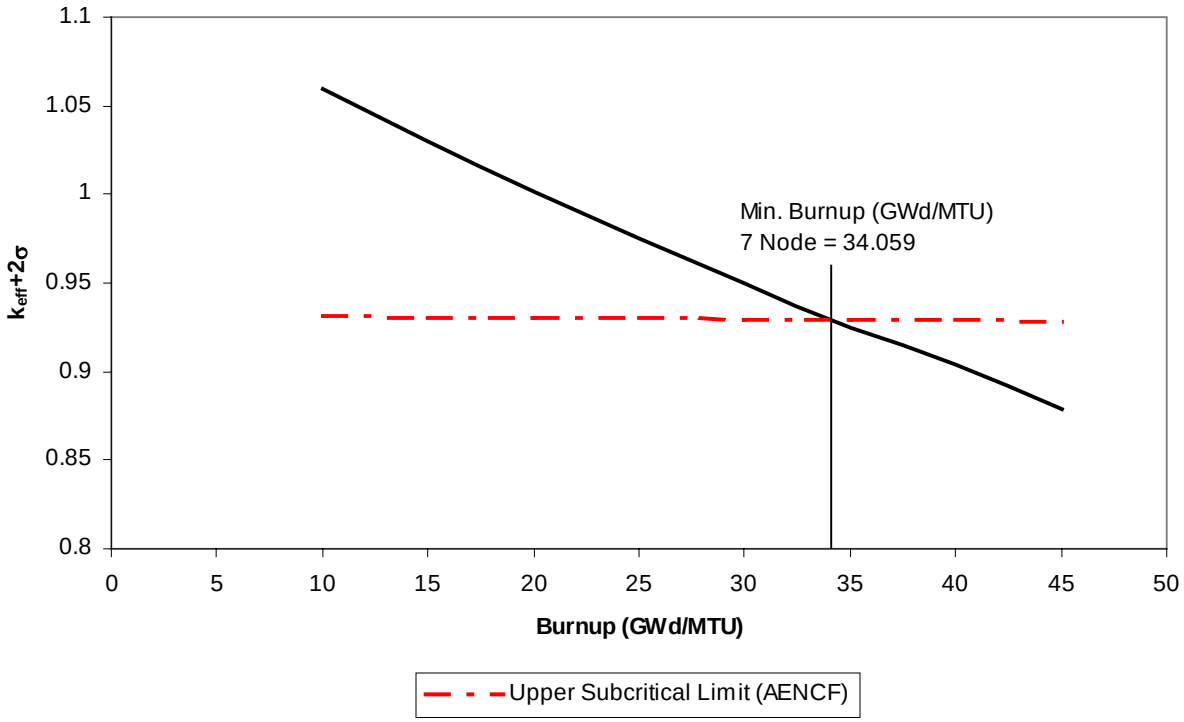

Figure 14. Preclosure 7 Node Spent Nuclear Fuel k_{eff} Results for 4.5 Wt% U-235 Initial Enrichment

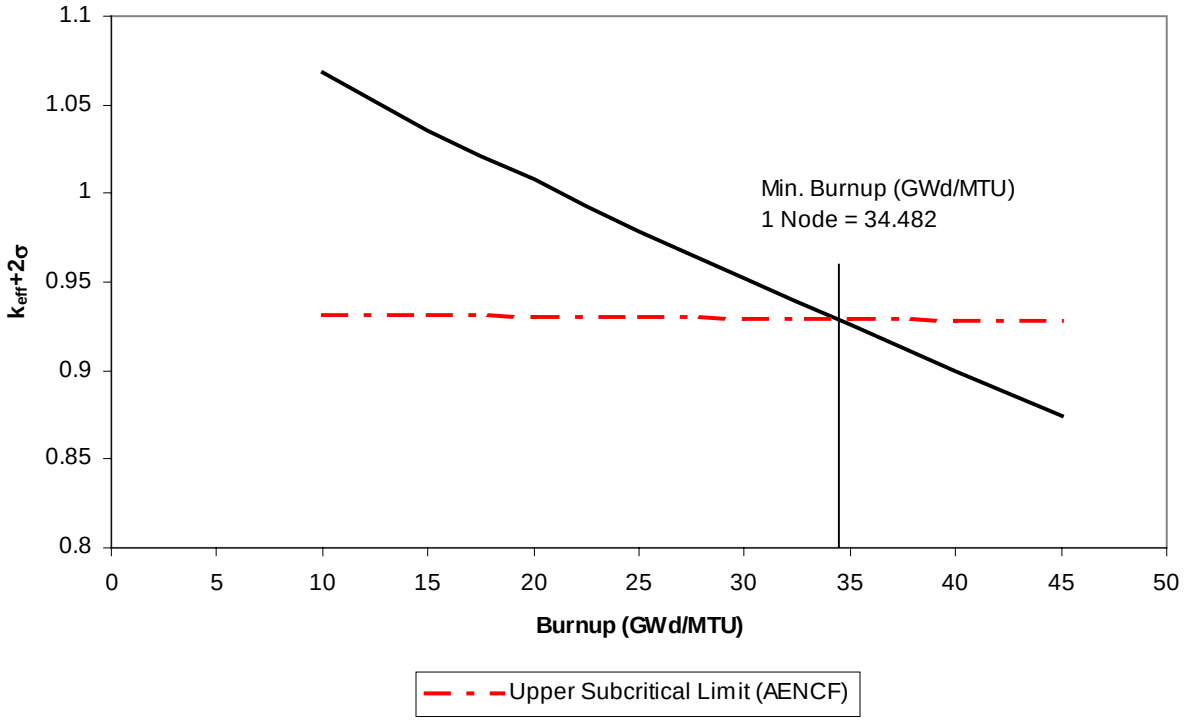

Figure 15. Preclosure 1 Node Spent Nuclear Fuel k_{eff} Results for 4.5 Wt% U-235 Initial Enrichment

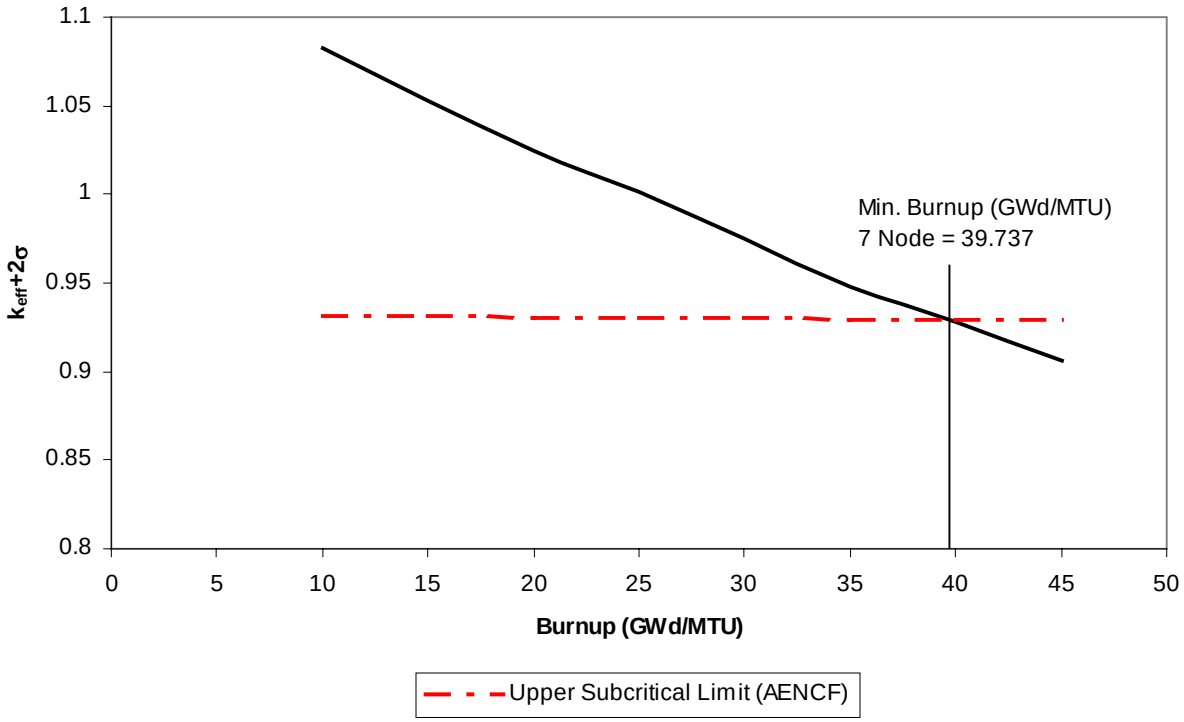

Figure 16. Preclosure 7 Node Spent Nuclear Fuel k_{eff} Results for 5.0 Wt% U-235 Initial Enrichment

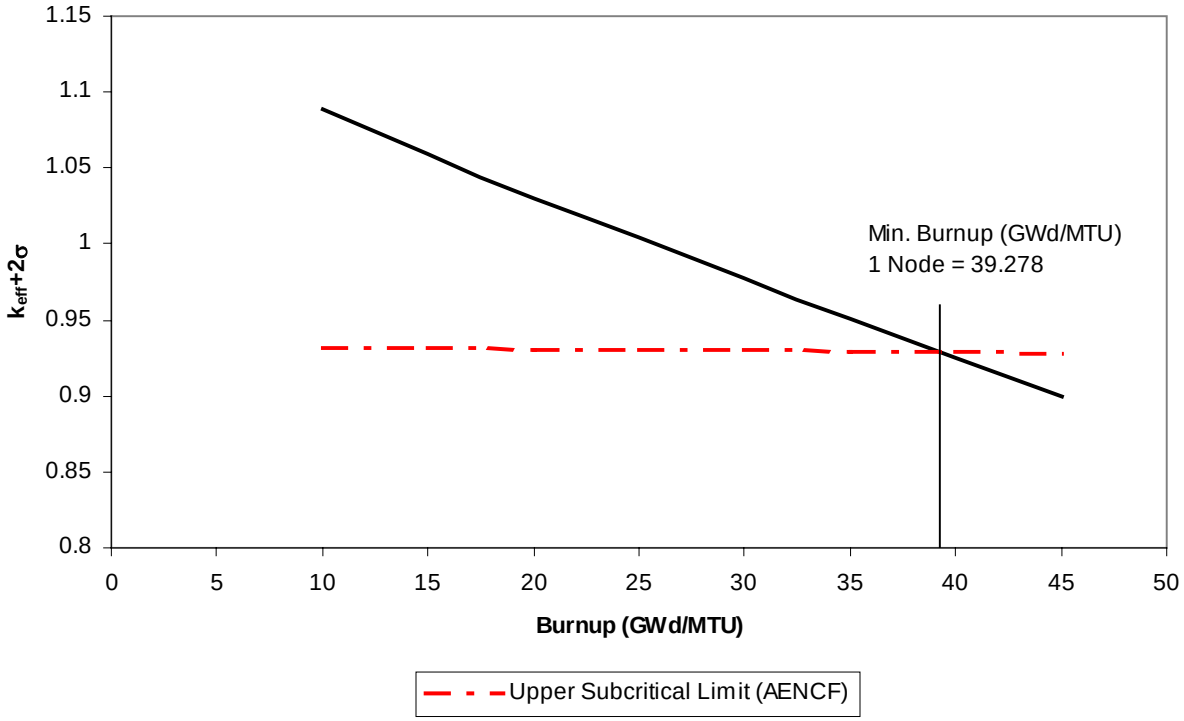

Figure 17. Preclosure 1 Node Spent Nuclear Fuel k_{eff} Results for 5.0 Wt% U-235 Initial Enrichment

Table 21. Minimum Required Burnups for Intercept of Upper Subcritical Limit

Initial Enrichment (Wt% U-235)	7 Node Fuel Zone		1 Node Fuel Zone	
	Burnup (GWd/MTU)	5% BU Unc.[a]	Burnup (GWd/MTU)	5% BU Unc.[a]
1.974	0	0	0	0
2.5	10.315	10.831	11.472	12.046
3	16.941	17.788	17.710	18.596
3.5	23.100	24.255	23.655	24.838
4	29.028	30.479	29.062	30.515
4.5	34.059	35.762	34.482	36.206
5	39.737	41.724	39.278	41.242

NOTE: [a] Required minimum burnup including 5% uncertainty associated with assembly burnup records

BSC (2003b, Section 6.2.2) states that the SNF isotopics (BSC 2003b, Section 6) in a single axial zone representation bound commercial PWR fuel assemblies at the same initial enrichment and burnup. Therefore, using a limiting axial profile in conjunction with the bounding isotopics would be adding additional conservatism that has already been bounded and is unnecessary. The seven axial zone representation results were provided for comparison purposes only, and to illustrate that for the selected bounding configurations, axial profile effects are negligible.

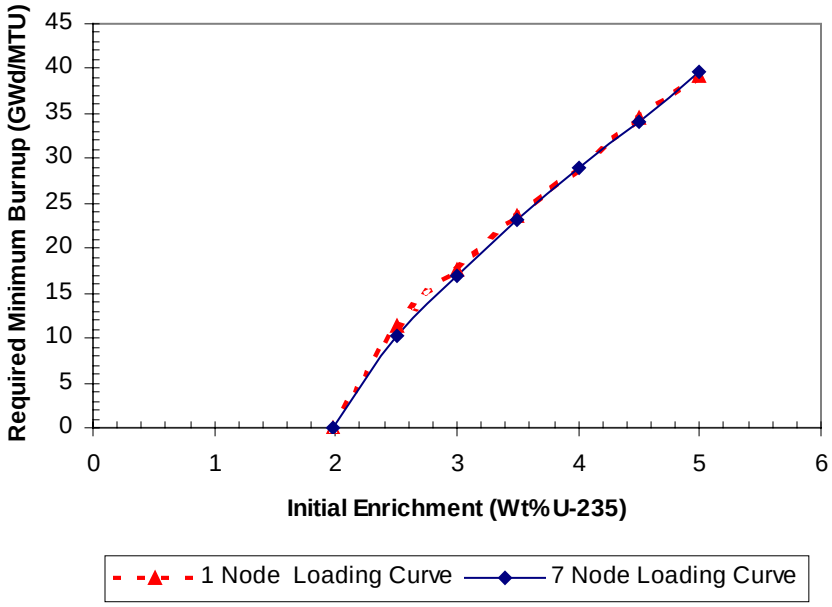

Figure 18. Required Minimum Burnups for Intercept of Upper Subcritical Limit

6.2.2 Postclosure

The results for spent fuel with five-year decay time (the five-year decay time is based on the minimum cooling time required for the fuel assemblies to be classified as standard fuel [10 CFR 961.11]) isotopic compositions are presented in Table 23. The five-year decay time isotopics are used because they bound fuel that is cooled longer with respect to reactivity. The minimum burnup required for each initial enrichment is determined by plotting the calculated k_{eff} versus the burnup. The burnup value of the intersection of the plotted curve with the CL is the required minimum burnup and are illustrated in Figures 19 through 32 and summarized in Table 24 and Figure 33. The k_{eff} values plotted include a two-σ allowance for computational uncertainty. Any burnup value greater than this will result in a k_{eff} less than the CL, and is acceptable to be loaded into the waste package. In Figures 19 through 32, the CL is presented as a function of AENCF. The reported CL intercept values correspond to those for the CL as a function of the most conservative trend parameter as prescribed by YMP 2003 (Section 3.5.3.2.6). The CL equation is provided in Table 22.

Table 22. Spent Nuclear Fuel Critical Limit Function

Trend Parameter	CL Equation
AENCF	CL (AENCF) = -0.06262*AENCF + 0.9920

Source: Framatome ANP (2003, Table 11)

Table 23. Postclosure Spent Nuclear Fuel k_{eff} Results

Initial Enrichment(Wt% U-235)	Burnup (GWd/ MTU)	7 Node Fuel Zone			1 Node Fuel Zone			$\Delta k_{eff} + 2\sigma$[a]
		k_{eff}	σ	AENCF (MeV)	k_{eff}	σ	AENCF (MeV)	
2.0	10	0.88261	0.0005	0.2106	0.88941	0.00044	0.2091	-0.0067
	15	0.85428	0.0005	0.2215	0.85981	0.00051	0.2224	-0.0055
	20	0.82789	0.00044	0.2326	0.83066	0.00052	0.2340	-0.0029
	25	0.80912	0.00054	0.2395	0.80823	0.00048	0.2446	0.0010
2.5	10	0.92833	0.00051	0.1974	0.93462	0.00049	0.1968	-0.0062
	15	0.89825	0.00057	0.2091	0.90268	0.00049	0.2095	-0.0043
	20	0.87083	0.00057	0.2173	0.87386	0.00054	0.2198	-0.0030
	25	0.84687	0.00049	0.2261	0.84572	0.00044	0.2300	0.0012
	30	0.82326	0.00053	0.2331	0.82157	0.00049	0.2405	0.0018
3.0	10	0.96898	0.00053	0.1885	0.97382	0.00053	0.1880	-0.0048
	15	0.93858	0.00058	0.1983	0.9431	0.00052	0.1981	-0.0044
	20	0.90847	0.00051	0.2067	0.91238	0.00054	0.2080	-0.0040
	25	0.88502	0.00053	0.2136	0.88339	0.00048	0.2182	0.0017
	30	0.86038	0.00054	0.2215	0.85625	0.00051	0.2288	0.0042
	35	0.83389	0.00052	0.2310	0.83187	0.00048	0.2384	0.0021
	40	0.81595	0.00048	0.2379	0.80985	0.00047	0.2469	0.0061
3.5	10	1.00293	0.00053	0.1811	1.00762	0.00051	0.1809	-0.0046
	15	0.97181	0.00055	0.1898	0.97687	0.00049	0.1902	-0.0049
	20	0.94191	0.00055	0.1978	0.94679	0.00054	0.2003	-0.0049
	25	0.9176	0.00058	0.2056	0.91784	0.00056	0.2086	-0.0002
	30	0.89178	0.00051	0.2126	0.8896	0.00053	0.2178	0.0021
	35	0.86684	0.00051	0.2205	0.86361	0.00048	0.2271	0.0033
	40	0.84817	0.00054	0.2259	0.84012	0.00051	0.2360	0.0081
	45	0.82228	0.00053	0.2366	0.81709	0.00049	0.2447	0.0053
4.0	10	1.03059	0.00054	0.1763	1.03738	0.00052	0.1760	-0.0068
	15	1.00061	0.00056	0.1841	1.00734	0.00054	0.1843	-0.0067
	20	0.97152	0.00058	0.1915	0.97721	0.00054	0.1922	-0.0056
	25	0.94649	0.00051	0.1979	0.94867	0.00053	0.2009	-0.0022
	30	0.92166	0.00055	0.2044	0.92043	0.00045	0.2091	0.0014
	35	0.89509	0.00052	0.2126	0.89356	0.00053	0.2180	0.0015
	40	0.87697	0.00053	0.2180	0.86873	0.0005	0.2262	0.0083
	45	0.85105	0.00055	0.2257	0.8449	0.00048	0.2337	0.0063
4.5	10	1.05776	0.00051	0.1727	1.06256	0.00061	0.1722	-0.0050
	15	1.02722	0.00055	0.1793	1.03281	0.00053	0.1798	-0.0055
	20	0.99887	0.00052	0.1863	1.00513	0.0006	0.1867	-0.0064
	25	0.97387	0.00054	0.1918	0.97668	0.00052	0.1945	-0.0028
	30	0.94795	0.00054	0.1982	0.94905	0.00055	0.2018	-0.0011
	35	0.92133	0.00055	0.2067	0.92157	0.00047	0.2093	-0.0001
	40	0.9022	0.00054	0.2107	0.89641	0.00055	0.2177	0.0058

Table 23. Postclosure Spent Nuclear Fuel k_{eff} Results

Initial Enrichment(Wt% U-235)	Burnup (GWd/ MTU)	7 Node Fuel Zone			1 Node Fuel Zone			$\Delta k_{eff} + 2\sigma$[a]
		k_{eff}	σ	AENCF (MeV)	k_{eff}	σ	AENCF (MeV)	
	45	0.87778	0.00059	0.2187	0.87247	0.00051	0.2259	0.0055
5.0	10	1.07938	0.00058	0.1689	1.08386	0.00055	0.1689	-0.0044
	15	1.05009	0.00058	0.1755	1.05647	0.00053	0.1755	-0.0063
	20	1.01987	0.00054	0.1824	1.02724	0.00053	0.1829	-0.0073
	25	0.99812	0.00058	0.1874	1.00018	0.00054	0.1890	-0.0020
	30	0.97272	0.00063	0.1936	0.97296	0.00055	0.1964	-0.0001
	35	0.94438	0.00056	0.2004	0.94592	0.00049	0.2041	-0.0014
	40	0.9287	0.0006	0.2047	0.92162	0.00051	0.2106	0.0073
	45	0.90086	0.00053	0.2125	0.89623	0.00046	0.2178	0.0048

NOTE: [a] $\Delta k_{eff} + 2\sigma = (k_{eff} + 2\sigma)_{7\ Node} - (k_{eff} + 2\sigma)_{1\ Node}$

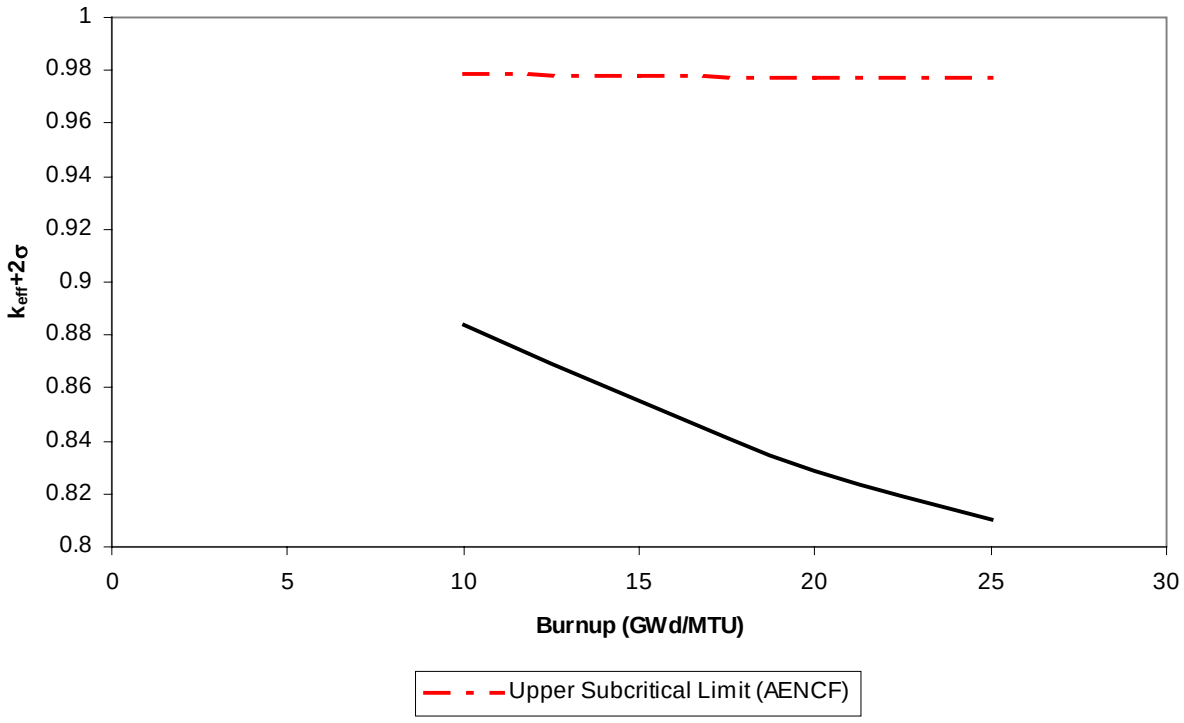

Figure 19. Postclosure 7 Node Spent Nuclear Fuel k_{eff} Results for 2.0 Wt% U-235 Initial Enrichment

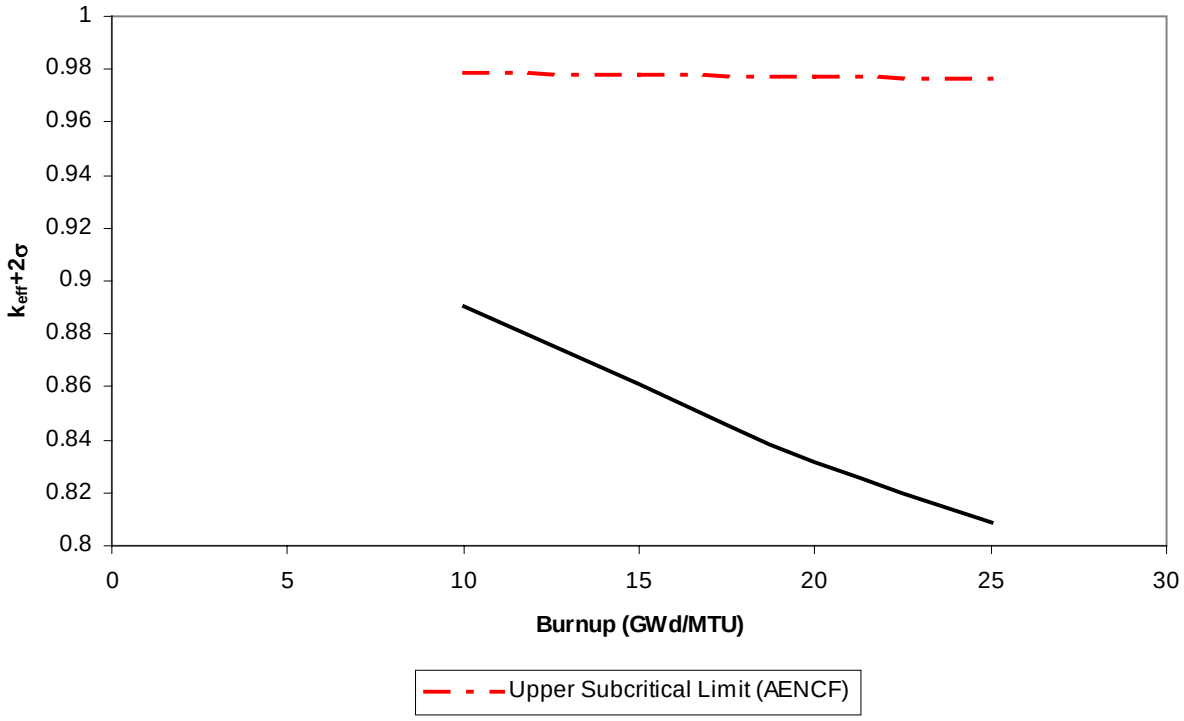

Figure 20. Postclosure 1 Node Spent Nuclear Fuel k_{eff} Results for 2.0 Wt% U-235 Initial Enrichment

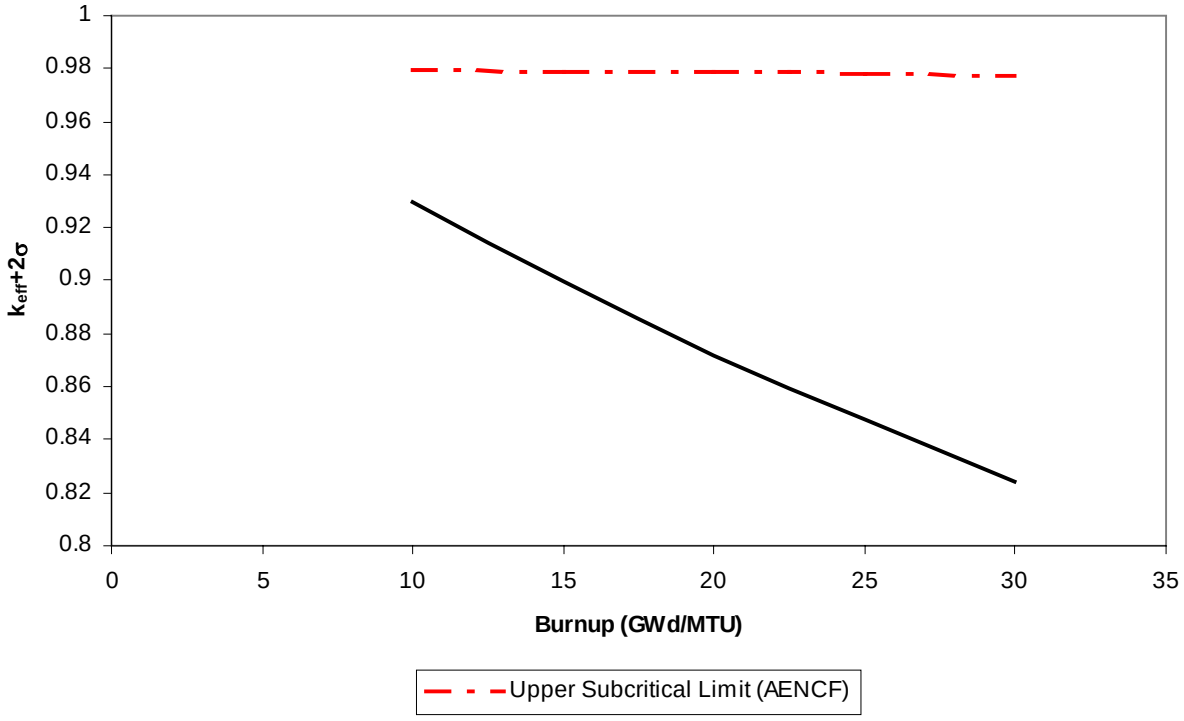

Figure 21. Postclosure 7 Node Spent Nuclear Fuel k_{eff} Results for 2.5 Wt% U-235 Initial Enrichment

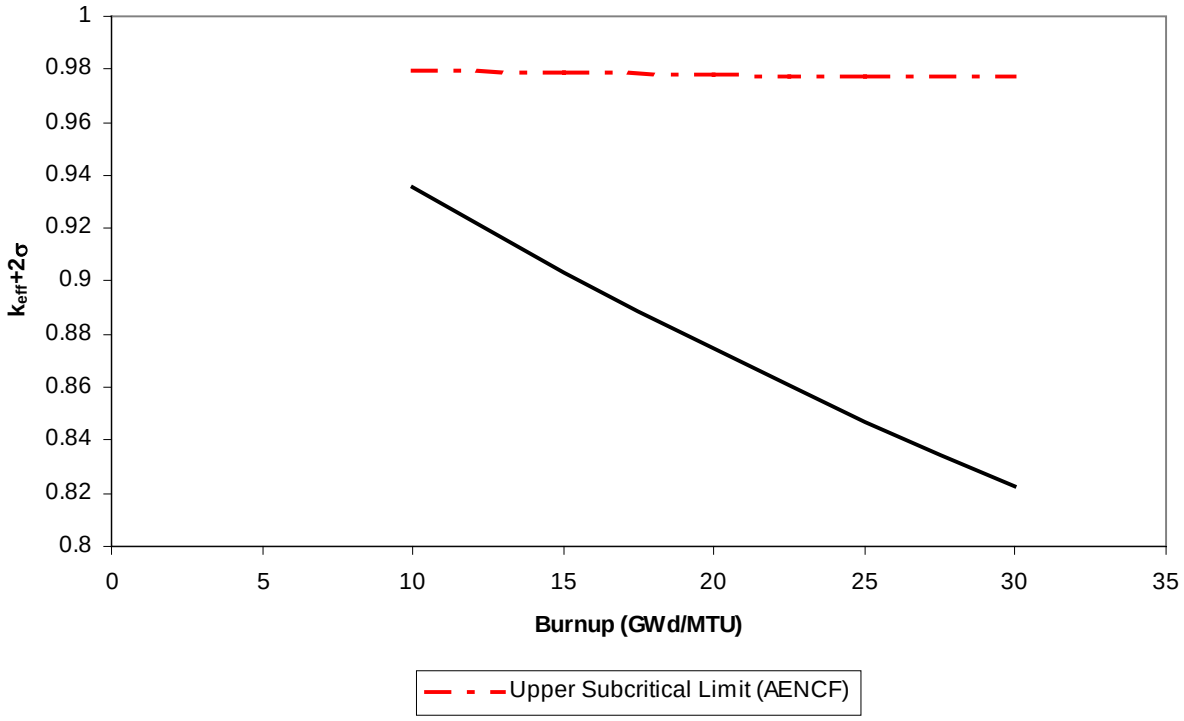

Figure 22. Postclosure 1 Node Spent Nuclear Fuel k_{eff} Results for 2.5 Wt% U-235 Initial Enrichment

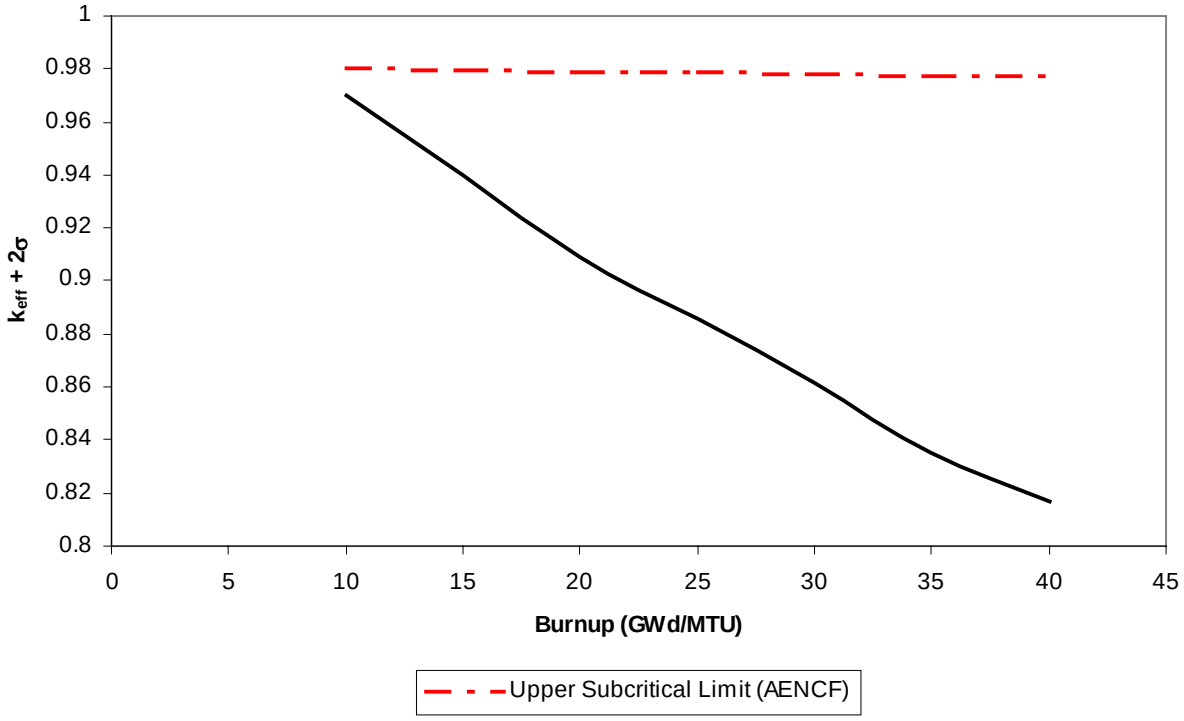

Figure 23. Postclosure 7 Node Spent Nuclear Fuel k_{eff} Results for 3.0 Wt% U-235 Initial Enrichment

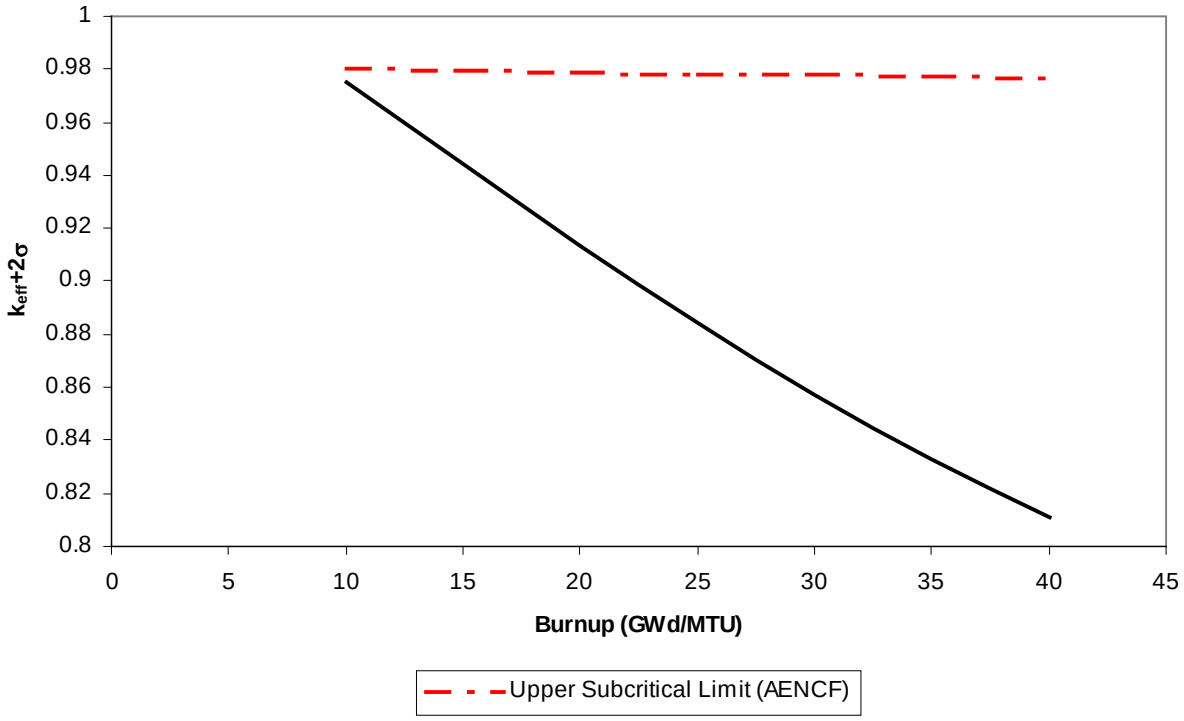

Figure 24. Postclosure 1 Node Spent Nuclear Fuel k_{eff} Results for 3.0 Wt% U-235 Initial Enrichment

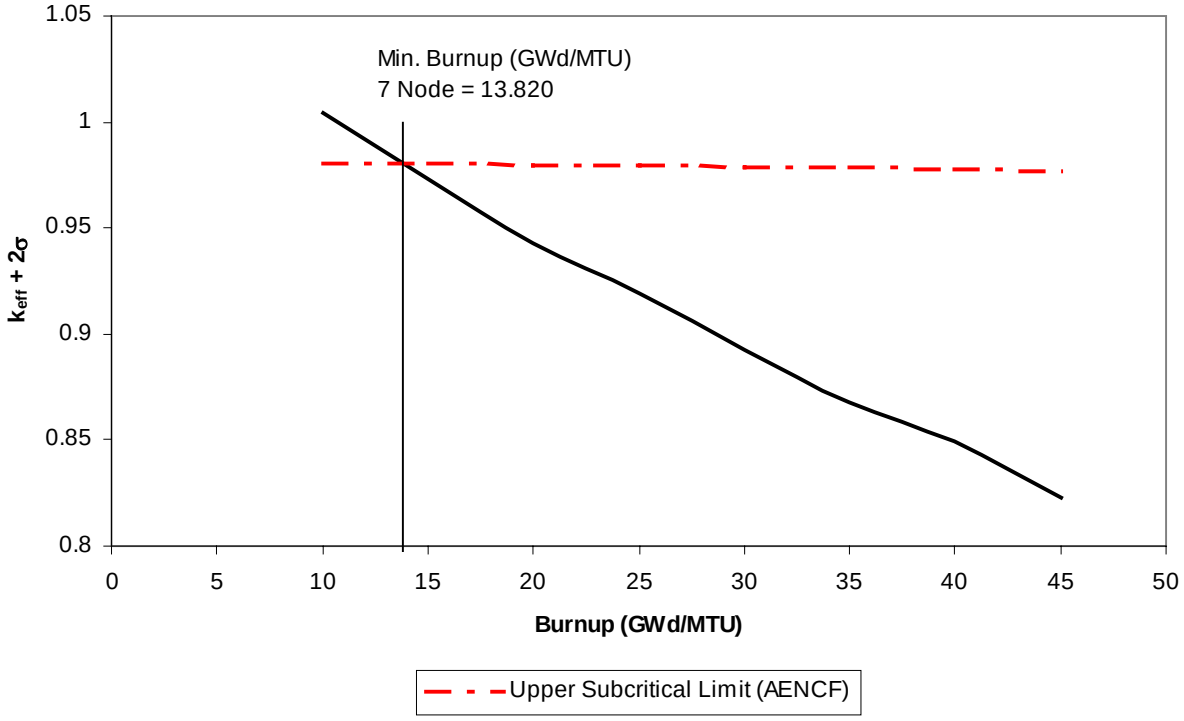

Figure 25. Postclosure 7 Node Spent Nuclear Fuel k_{eff} Results for 3.5 Wt% U-235 Initial Enrichment

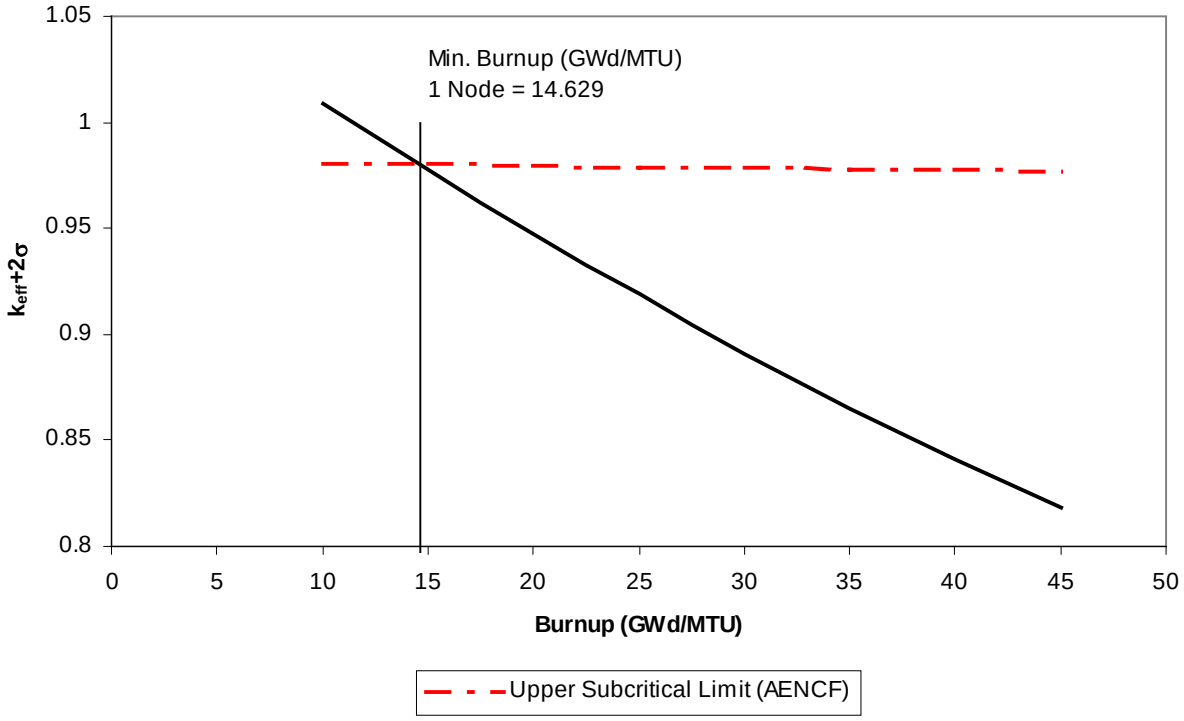

Figure 26. Postclosure 1 Node Spent Nuclear Fuel k_{eff} Results for 3.5 Wt% U-235 Initial Enrichment

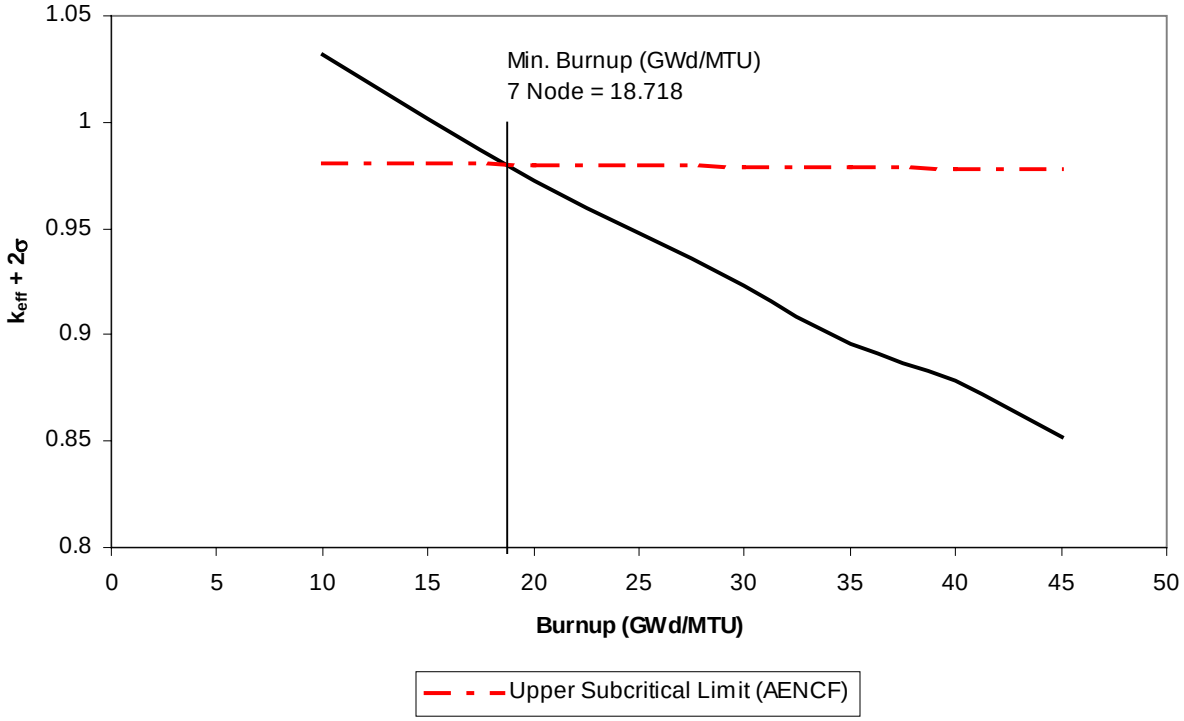

Figure 27. Postclosure 7 Node Spent Nuclear Fuel k_{eff} Results for 4.0 Wt% U-235 Initial Enrichment

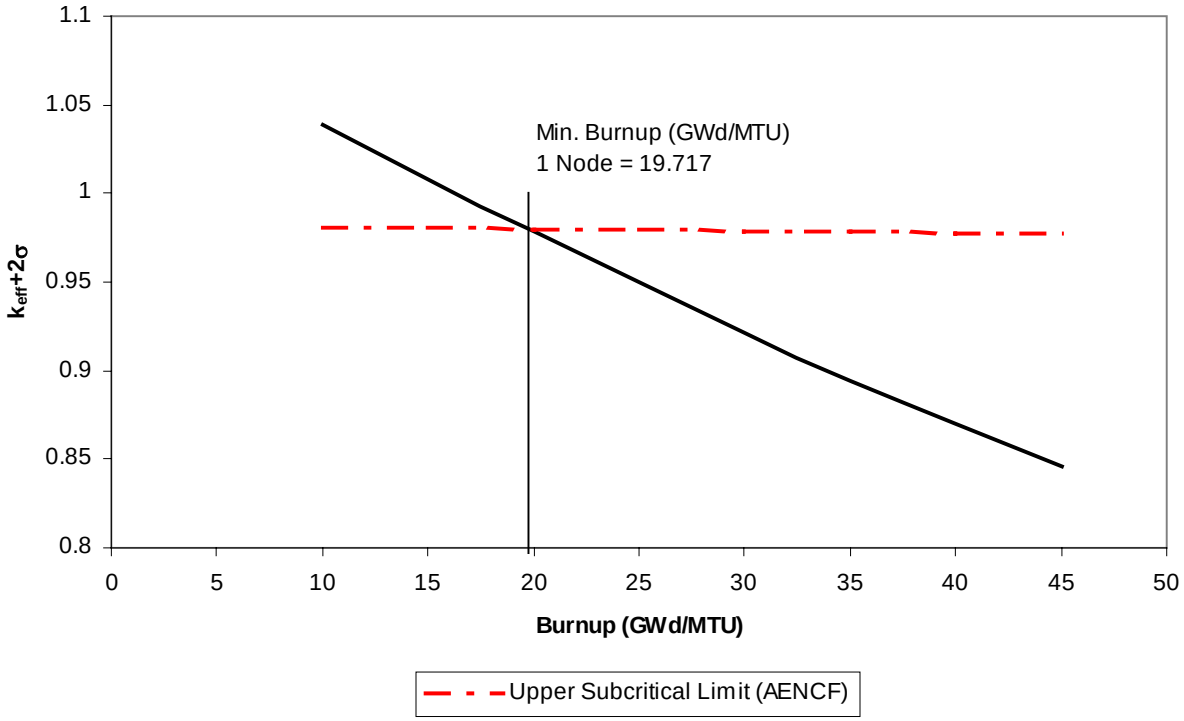

Figure 28. Postclosure 1 Node Spent Nuclear Fuel k_{eff} Results for 4.0 Wt% U-235 Initial Enrichment

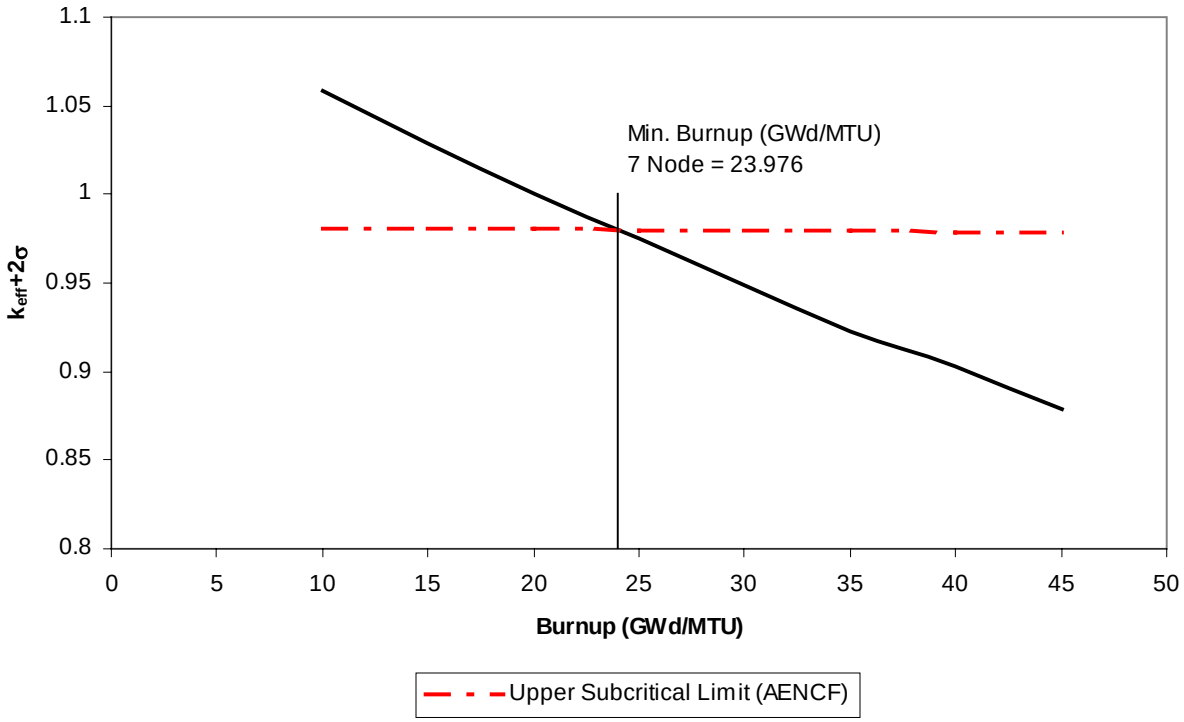

Figure 29. Postclosure 7 Node Spent Nuclear Fuel k_{eff} Results for 4.5 Wt% U-235 Initial Enrichment

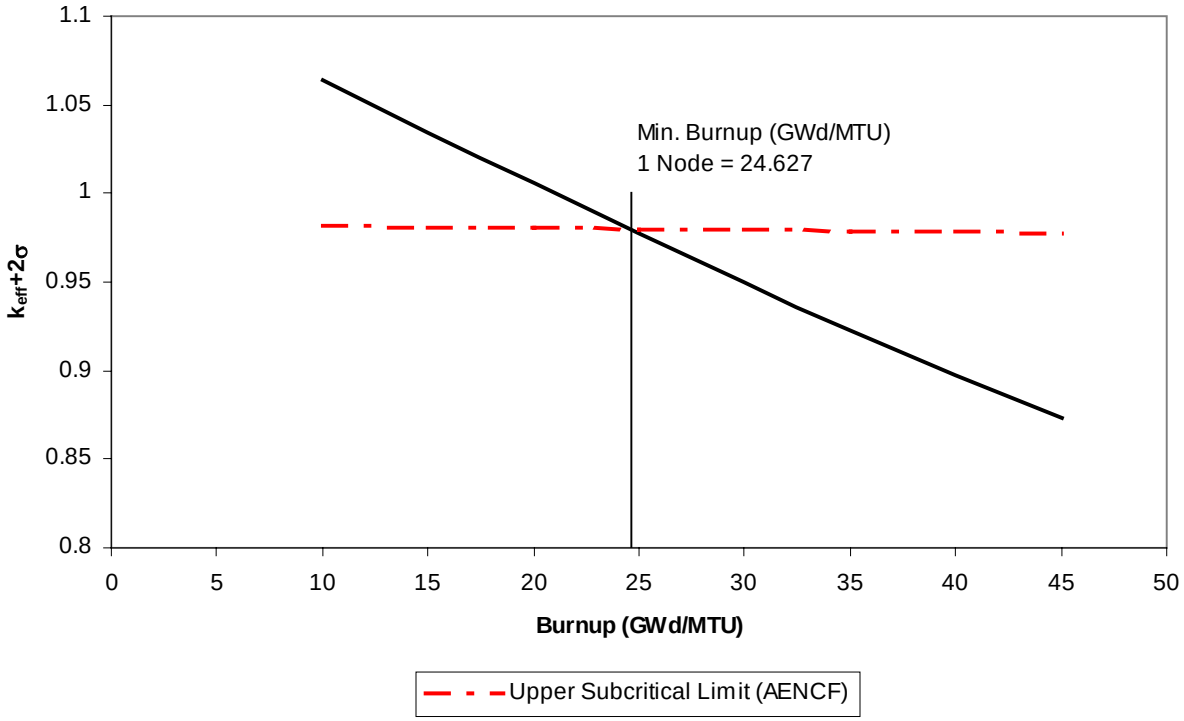

Figure 30. Postclosure 1 Node Spent Nuclear Fuel k_{eff} Results for 4.5 Wt% U-235 Initial Enrichment

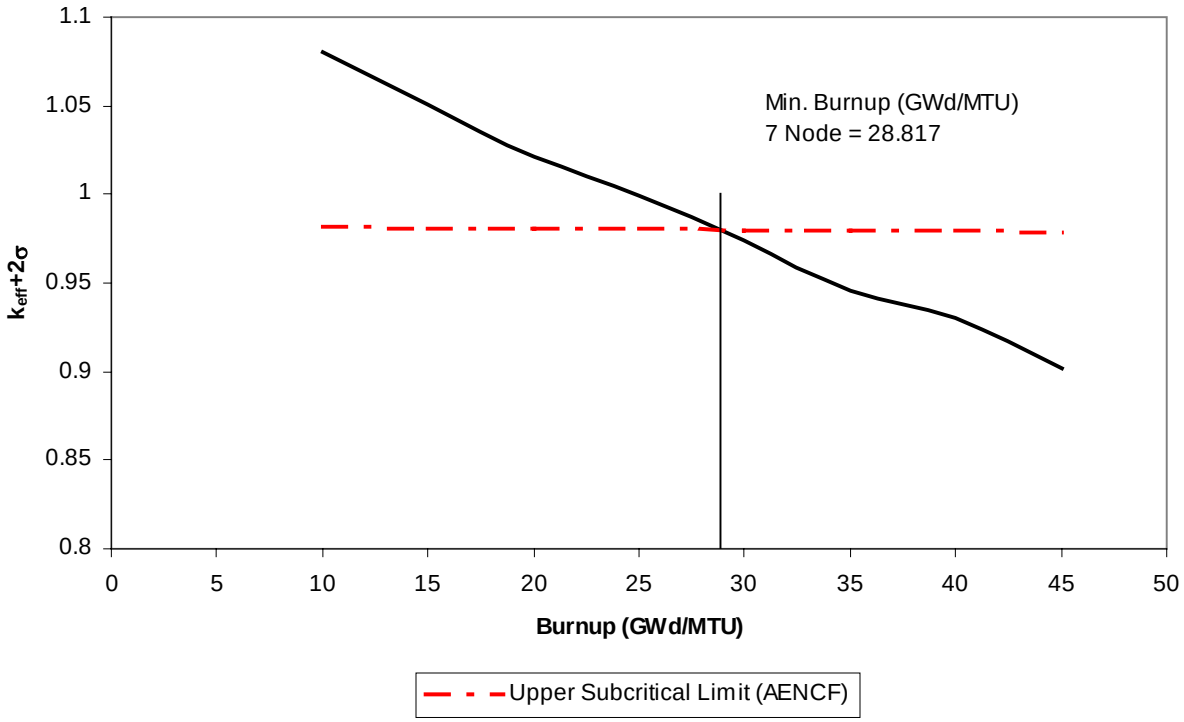

Figure 31. Postclosure 7 Node Spent Nuclear Fuel k_{eff} Results for 5.0 Wt% U-235 Initial Enrichment

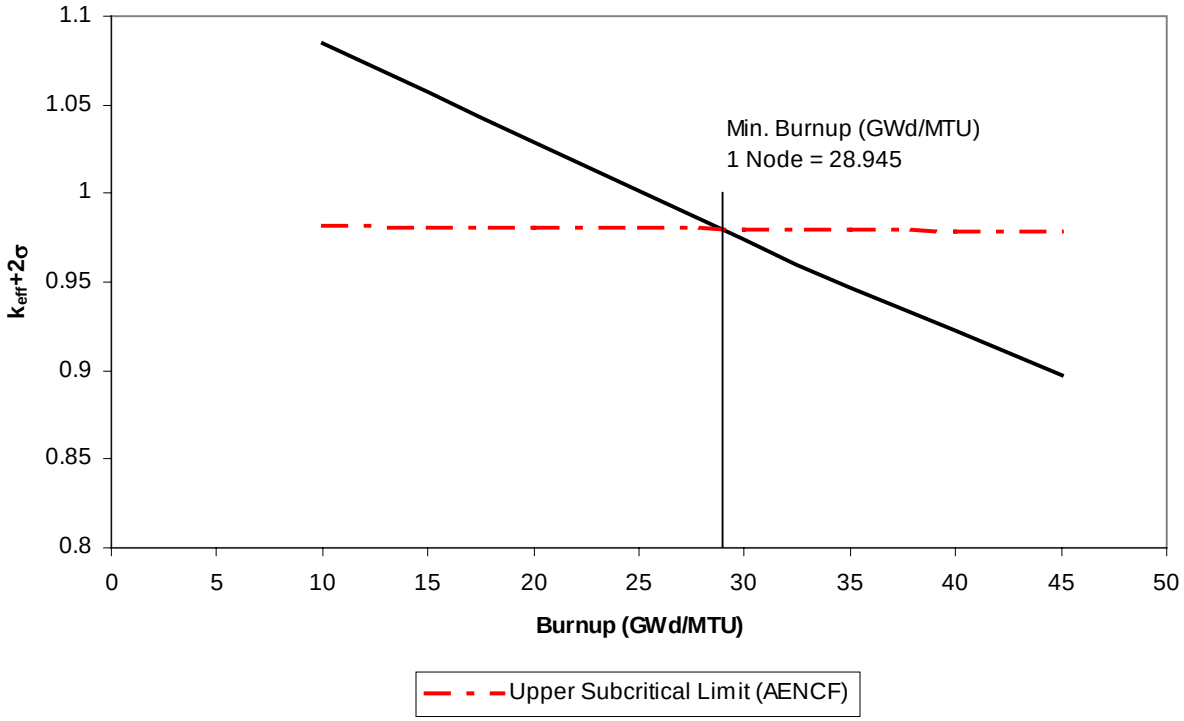

Figure 32. Postclosure 1 Node Spent Nuclear Fuel k_{eff} Results for 5.0 Wt% U-235 Initial Enrichment

Table 24. Minimum Required Burnups for Intercept of Critical Limit

Initial Enrichment (Wt% U-235)	7 Node Fuel Zone		1 Node Fuel Zone	
	Burnup (GWd/MTU)	5% BU Unc.[a]	Burnup (GWd/MTU)	5% BU Unc.[a]
2.393	0.000	0.000	0.000	0.000
2.5[b]	1.398	1.468	2.924	3.070
3.0[b]	8.290	8.705	9.112	9.568
3.5	13.820	14.511	14.629	15.360
4.0	18.718	19.654	19.717	20.703
4.5	23.976	25.175	24.627	25.858
5.0	28.817	30.258	28.945	30.392

NOTES: [a] Required minimum burnup including 5% uncertainty associated with assembly burnup records
[b] Where the intercept was below 10 GW/MTU the values were extrapolated

BSC (2003b) states that the SNF isotopics (BSC 2003b, Section 6) in a single axial zone representation bound commercial PWR fuel assemblies at the same initial enrichment and burnup. Therefore, using a limiting axial profile in conjunction with the bounding isotopics would be adding additional conservatism that has already been bounded and is unnecessary. The seven axial zone representation results were provided for comparison purposes only, and to illustrate that for the selected bounding configurations, axial profile effects are negligible.

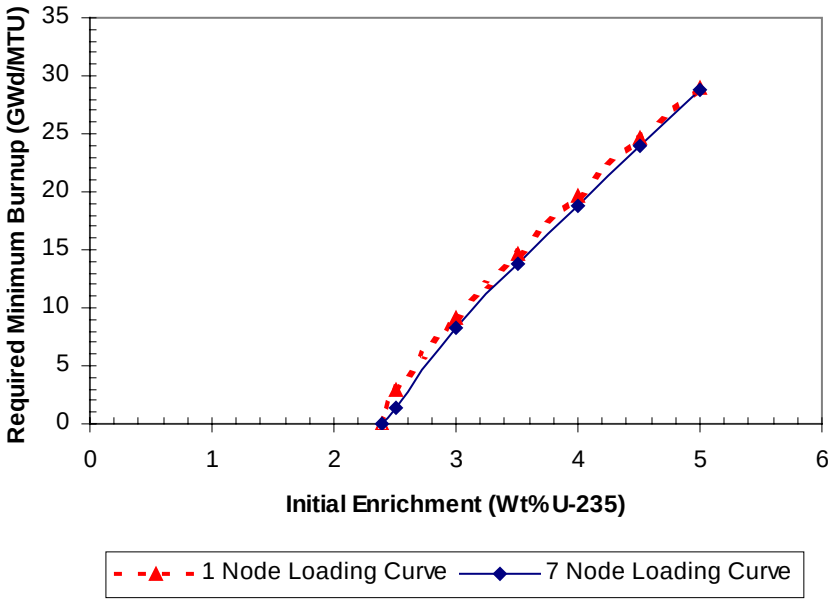

Figure 33. Required Minimum Burnups for Intercept of Critical Limit

6.2.3 Waste Stream Comparison

The waste stream inventory in terms of number of fuel assemblies at given burnups and enrichments was taken from *Waste Packages and Source Terms for the Commercial 1999 Design Basis Waste Streams* (CRWMS M&O 2000, Attachment III) using the "Case A" arrival forecast. "Case A" refers to 10-year-old youngest fuel first for 63,000 MTU. This arrival forecast was selected based on Licensing Position LP-009, *Waste Stream Parameters* (Williams 2003, Section 3.4). The results of the loading curve compared against the waste stream inventory are presented in Figure 34. This curve is based on the selection of the minimum required burnups using a single axial zone representation including a 5% burnup uncertainty associated with assembly burnup records. The squares in the legend indicate number groupings of assemblies at a particular burnup and enrichment (e.g., 100-199 indicates that there are 100 to 199 assemblies at a listed burnup and enrichment); *Base LC* is the loading curve based on the nominal required minimum burnup; and *Fitted Polynomial* is the quintic polynomial fitted to the loading curve adjusted for a five percent uncertainty associated with the reported assembly burnups. The waste stream information that was extracted and sorted is provided in Attachment IV as the workbook *wstreamplot.xls*.

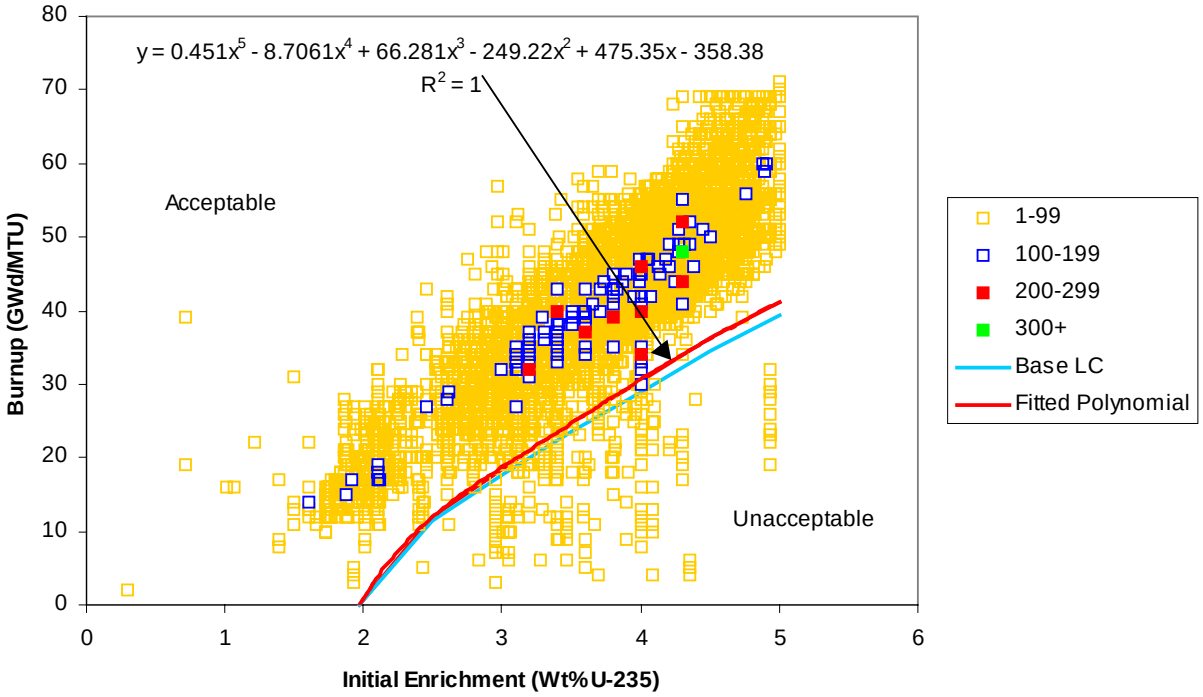

NOTE: The fitted polynomial represents the loading curve based on a five percent burnup uncertainty of the bounding curve (Base LC)

Figure 34. Loading Curve and Projected Waste Stream

Waste stream population comparisons are provided in Table 25 for the 21-PWR waste package with absorber plates. Assemblies that are considered "unacceptable" do not meet the requirements for loading into the 21-PWR waste package with absorber plates, and will need to be disposed of in a different waste package design.

Table 25. Loading Curve Waste Stream Acceptability Comparison

Loading Curve Configuration	# Assemblies Below Minimum Required Burnup	Acceptable (%)	Unacceptable (%)
Base LC	1194	98.73	1.27
Fitted Polynomial	1524	98.37	1.63

6.2.4 Misloaded Assembly

Since there is a possibility of inserting a single SNF assembly into a waste package during loading that does not meet the requirements of the design basis loading curve (*Commercial Spent Nuclear Fuel Waste Package Misload Analysis* [BSC 2003c, p. 26]), the impact of a misloaded assembly was evaluated. A comparison for the burnup/enrichment pairs that make up the loading curve was made against configurations involving a misloaded assembly. For the comparisons, the misloaded assembly used was an assembly that was 10 GWd/MTU and 20 GWd/MTU below the design basis required burnup for a given enrichment. The isotopic material compositions were interpolated from BSC (2003b, Section 6). For conservative purposes with respect to criticality, the misloaded assembly was placed in the most reactive position within the waste package (center position). The

results of the comparisons are provided in Tables 26 and 27 and illustrated in Figure 35, with the nominal cases using the design basis required burnup based on the equation presented in Figure 34.

Table 26. Misloaded Assembly Results for 10 GWd/MTU Underburned Assembly

Enrichment (Wt% U-235)/ Design Basis Required Burnup (GWd/MTU)	Misloaded Waste Package			Nominally Loaded Waste Package			
	k_{eff}	σ	AENCF (MeV)	k_{eff}	σ	AENCF (MeV)	$\Delta k_{eff} + 2\sigma$
2.5 / 11.472	0.93871	0.00050	0.1951	0.92799	0.00054	0.2000	0.01064
3.0 / 17.710	0.93884	0.00049	0.1999	0.92807	0.00046	0.2033	0.01083
3.5 / 23.655	0.93769	0.00049	0.2021	0.92808	0.00052	0.2047	0.00955
4.0 / 29.062	0.93760	0.00052	0.2041	0.92839	0.00050	0.2062	0.00925
4.5 / 34.482	0.93517	0.00051	0.2061	0.92663	0.00055	0.2079	0.00846
5.0 / 39.278	0.93673	0.00058	0.2065	0.92796	0.00054	0.2087	0.00885

Table 27. Misloaded Assembly Results for 20 GWd/MTU Underburned Assembly

Enrichment (Wt% U-235)/ Design Basis Required Burnup (GWd/MTU)	Misloaded Waste Package			Nominally Loaded Waste Package			
	k_{eff}	σ	AENCF (MeV)	k_{eff}	σ	AENCF (MeV)	$\Delta k_{eff} + 2\sigma$
3.5 / 23.953	0.95487	0.00053	0.1983	0.92808	0.00052	0.2047	0.02681
4.0 / 29.511	0.95327	0.00050	0.2005	0.92839	0.00050	0.2062	0.02488
4.5 / 34.645	0.94999	0.00053	0.2022	0.92663	0.00055	0.2079	0.02332
5.0 / 39.567	0.94812	0.00057	0.2037	0.92796	0.00054	0.2087	0.02022

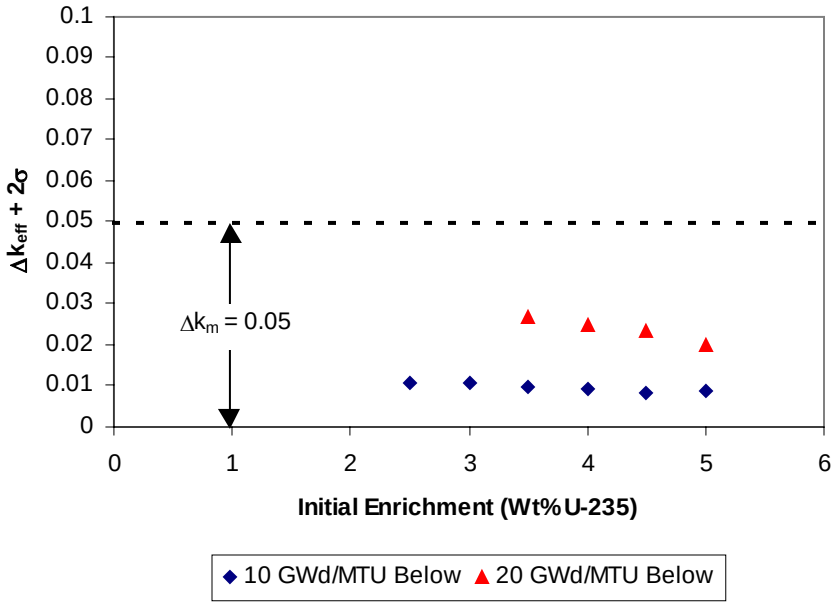

Figure 35. Misloaded Assembly Results

Figure 35 shows that the preclosure reactivity effect of misloading underburned commercial SNF into an intact, flooded 21-PWR waste package, with absorber plates, is about one percent for fuel underburned by 10 GWd/MTU, and two to three percent for SNF underburned by 20 GWd/MTU. Since the arbitrary margin imposed to ensure subcriticality (Δk_m) is five percent, the misloading of even grossly underburned SNF will not actually result in a critical configuration. Note that no credit is being taken for the fact that not all SNF will be at the design basis required minimum burnup value - most SNF will actually be at higher burnups that will reduce the reactivity of the waste package and compensate for the positive reactivity caused by a misloaded, underburned SNF assembly.

6.3 SUMMARY OF RESULTS

Results presented in Attachment I (Table 32) illustrate that the 21-PWR waste package with absorber plates will not go critical with commercial SNF if there is no moderator present within the waste package (i.e., dry criticality is not possible). A misloaded, underburned assembly is considered probable (BSC 2003c, p. 26), but since the preclosure administrative margin is large enough to subsume the increase in reactivity associated with a substantially underburned assembly, the waste package will not go critical during the preclosure time period. Note that these calculations are conservatively based on a fully flooded waste package, although the waste packages are expected to exclude water moderation. It is expected that loaded waste packages will have enough assemblies sufficiently above the design basis minimum required burnup to compensate for a misloaded assembly during the preclosure or postclosure time period.

This report recommends that the 21-PWR waste package with Ni-Gd Alloy absorber plates be loaded using the loading curve with the five percent uncertainty assessed to the burnup values. The loading curve is described by the quintic polynomial presented in Equation 11.

$$y(x) = 0.451x^5 - 8.7061x^4 + 66.281x^3 - 249.22x^2 + 475.35x - 358.38 \qquad \text{(Eq. 11)}$$

where

x = the initial enrichment of the fuel assembly in wt% U-235
y(x) = the required minimum burnup (GWd/MTU) for an assembly with enrichment x

This recommendation is made based on the expectation that the probability of selecting enough assemblies with sufficient burnups above the design basis value to compensate for a single misloaded assembly is adequate for keeping the waste package criticality probability below the threshold criterion. Using this loading curve allows 98.28 percent of the current PWR projected waste stream to be disposed of in the 21-PWR waste package with Ni-Gd Alloy absorber plates waste package. A different waste package design could be used for disposing of the remaining 1.72 percent of the projected PWR waste stream or predetermined loading patterns could be used to blend assemblies that are below the design basis minimum burnup with assemblies that have high enough burnups to compensate.

All outputs are reasonable compared to the inputs and the results of this calculation are suitable for their intended use.

7. REFERENCES

7.1 DOCUMENTS CITED

ASM International. 1987. *Corrosion.* Volume 13 of *Metals Handbook.* 9th Edition. Metals Park, Ohio: ASM International. TIC: 209807.

ASM International 1990a. *Properties and Selection: Nonferrous Alloys and Special-Purpose Materials.* Volume 2 of *ASM Handbook.* Formerly 10th Edition, Metals Handbook. 5th Printing 1998. [Materials Park, Ohio]: ASM International. TIC: 241059.

ASM International 1990b. *Properties and Selection: Irons, Steels, and High-Performance Alloys.* Volume 1 of *Metals Handbook.* 10th Edition. Materials Park, Ohio: ASM International. TIC: 245666.

Audi, G. and Wapstra, A.H. 1995. *Atomic Mass Adjustment, Mass List for Analysis.* [Upton, New York: Brookhaven National Laboratory, National Nuclear Data Center]. TIC: 242718.

B&W Fuel Company 1991. *Final Design Package Babcock & Wilcox BR-100 100 Ton Rail/Barge Spent Fuel Shipping Cask.* Volume 2. 51-1203400-01. DBABE0000-00272-1000-00014 REV 00. Lynchburg, Virginia: B&W Fuel Company. ACC: MOV.19960802.0083.

Bowman, S.M.; Hermann, O.W.; and Brady, M.C. 1995. *Sequoyah Unit 2 Cycle 3.* Volume 2 of *Scale-4 Analysis of Pressurized Water Reactor Critical Configurations.* ORNL/TM-12294/V2. Oak Ridge, Tennessee: Oak Ridge National Laboratory. TIC: 244397.

Briesmeister, J.F., ed. 1997. *MCNP-A General Monte Carlo N-Particle Transport Code.* LA-12625-M, Version 4B. Los Alamos, New Mexico: Los Alamos National Laboratory. ACC: MOL.19980624.0328.

BSC (Bechtel SAIC Company) 2003a. *PWR Axial Burnup Profile Analysis.* CAL-DSU-NU-000012 REV 00A. Las Vegas, Nevada: Bechtel SAIC Company. ACC: DOC.20031002.0002.

BSC (Bechtel SAIC Company) 2003b. *Isotopic Generation and Confirmation of the PWR Application Model.* CAL-DSU-NU-000004 REV 00A. Las Vegas, Nevada: Bechtel SAIC Company. ACC: DOC.20031110.0003.

BSC (Bechtel SAIC Company) 2003c. *Commercial Spent Nuclear Fuel Waste Package Misload Analysis.* CAL-WHS-MD-000003 REV 00A. Las Vegas, Nevada: Bechtel SAIC Company. ACC: DOC.20031002.0005.

BSC (Bechtel SAIC Company) 2004a. *21 PWR A, B, D & E Fuel Plates.* 000-MW0-DSU0-01201-000-00B. Las Vegas, Nevada: Bechtel SAIC Company. ACC: ENG.20040803.0004.

BSC (Bechtel SAIC Company) 2004b. *21 PWR C Fuel Plate.* 000-MW0-DSU0-01301-000-00B. Las Vegas, Nevada: M&O. ACC: ENG.20040804.0001.

BSC (Bechtel SAIC Company) 2004c. *Design and Engineering, 21 PWR Corner Guide.* 000-MW0-DSU0-01001-000-00A. Las Vegas, Nevada: Bechtel SAIC Company. ACC: ENG.20040305.0005.

BSC (Bechtel SAIC Company) 2004d. *Design and Engineering, 21 PWR End Side Guide.* 000-MW0-DSU0-00901-000-00A. Las Vegas, Nevada: Bechtel SAIC Company. ACC: ENG.20040305.0010.

BSC (Bechtel SAIC Company) 2004e. *Design and Engineering, 21 PWR Side Guide.* 000-MW0-DSU0-00801-000-00A. Las Vegas, Nevada: Bechtel SAIC Company. ACC: ENG.20040305.0002.

BSC (Bechtel SAIC Company) 2004f. *Design and Engineering, 21-PWR Waste Package Configuration.* 000-MW0-DSU0-00402-000-00B. Las Vegas, Nevada: Bechtel SAIC Company. ACC: ENG.20040119.0004.

BSC (Bechtel SAIC Company) 2004g. *21-PWR Waste Package Configuration.* 000-MW0-DSU0-00403-000-00D. Las Vegas, Nevada: Bechtel SAIC Company. ACC: ENG.20040708.0005.

BSC (Bechtel SAIC Company) 2004h. *Design and Engineering, Fuel Tube.* 000-MW0-DSU0-02001-000-00A. Las Vegas, Nevada: Bechtel SAIC Company. ACC: ENG.20040305.0012.

BSC (Bechtel SAIC Company) 2004i. *Geochemistry Model Abstraction and Sensitivity Studies for the 21 PWR CSNF Waste Packages.* MDL-DSU-MD-000001 REV 00 [Errata 001]. Las Vegas, Nevada: Bechtel SAIC Company. ACC: MOL.20021107.0154; DOC.20040225.0005.

BSC (Bechtel SAIC Company) 2004j. *Seismic Consequence Abstraction.* MDL-WIS-PA-000003 REV 0 Errata 1. Las Vegas, Nevada: Bechtel SAIC Company. ACC: DOC.20030818.0006; DOC.20040218.0002.

BSC (Bechtel SAIC Company) 2004k. *Q-List.* 000-30R-MGR0-00500-000-000 REV 00. Las Vegas, Nevada: Bechtel SAIC Company. ACC: ENG.20040721.0007.

BSC (Bechtel SAIC Company) 2004l. *Total Dust Settling on Naval Long Waste Packages in 100 Years.* 800-M0C-VU00-00900-000-00A. Las Vegas, Nevada: Bechtel SAIC Company. ACC: ENG.20040913.0001.

BSC (Bechtel SAIC Company) 2004m. *Waste Package Masses.* 000-00C-MGR0-01100-000-00B. Las Vegas, Nevada: Bechtel SAIC Company. ACC: ENG.20040603.0008.

Cacciapouti, R.J. and Van Volkinburg, S. 1997. *Axial Burnup Profile Database for Pressurized Water Reactors*. YAEC-1937. Bolton, Massachusetts: Yankee Atomic Electric Company. ACC: MOL.19980209.0184.

Canori, G.F. and Leitner, M.M. 2003. *Project Requirements Document.* TER-MGR-MD-000001 REV 02. Las Vegas, Nevada: Bechtel SAIC Company. ACC: DOC.20031222.0006.

CRWMS M&O 1998a. *Software Qualification Report for MCNP Version 4B2, A General Monte Carlo N-Particle Transport Code.* CSCI: 30033 V4B2LV. DI: 30033-2003, Rev. 01. Las Vegas, Nevada: CRWMS M&O. ACC: MOL.19980622.0637.

CRWMS M&O 1998b. *Selection of MCNP Cross Section Libraries*. B00000000-01717-5705-00099 REV 00. Las Vegas, Nevada: CRWMS M&O. ACC: MOL.19980722.0042.

CRWMS M&O 1998c. *Summary Report of Commercial Reactor Criticality Data for Sequoyah Unit 2.* B00000000-01717-5705-00064 REV 01. Las Vegas, Nevada: CRWMS M&O. ACC: MOL.19980716.0015.

CRWMS M&O 1998d. *Summary Report of Commercial Reactor Criticality Data for McGuire Unit 1.* B00000000-01717-5705-00063 REV 01. Las Vegas, Nevada: CRWMS M&O. ACC: MOL.19980622.0079.

CRWMS M&O 2000. *Waste Packages and Source Terms for the Commercial 1999 Design Basis Waste Streams.* CAL-MGR-MD-000001 REV 00. Las Vegas, Nevada: CRWMS M&O. ACC: MOL.20000214.0479.

DOE (U.S. Department of Energy) 1987. *Appendix 2A. Physical Descriptions of LWR Fuel Assemblies.* Volume 3 of *Characteristics of Spent Fuel, High-Level Waste, and Other Radioactive Wastes Which May Require Long-Term Isolation.* DOE/RW-0184. Washington, D.C.: U.S. Department of Energy, Office of Civilian Radioactive Waste Management. ACC: HQX.19880405.0024.

DOE (U.S. Department of Energy) 2004. *Quality Assurance Requirements and Description.* DOE/RW-0333P, Rev. 16. Washington, D.C.: U.S. Department of Energy, Office of Civilian Radioactive Waste Management. ACC: DOC.20040907.0002.

Doraswamy, N. 2004. *Project Design Criteria Document.* 000-3DR-MGR0-00100-000-002. Las Vegas, Nevada: Bechtel SAIC Company. ACC: ENG.20040721.0003.

Einziger, R.E. 1991. "Effects of an Oxidizing Atmosphere in a Spent Fuel Packaging Facility." *Proceedings of the Topical Meeting on Nuclear Waste Packaging, FOCUS '91, September 29–October 2, 1991, Las Vegas, Nevada.* Pages 88-99. La Grange Park, Illinois: American Nuclear Society. TIC: 231173.

Framatome ANP 2003. *Critical Limit Development for 21 PWR Waste Package.* 32-5029773-00. [Lynchburg, Virginia]: Framatome ANP. ACC: DOC.20031212.0004.

Gelest, Inc. 2004. *Gelest Silicone Fluids: Stable, Inert Media.* Morrisville, Pennsylvania: Gelest, Inc. TIC: 256122.

Inco Alloys International. 1998. *INCONEL Alloy 625*. Huntington, West Virginia: Inco Alloys International. TIC: 240361.

Lide, D.R., ed. 2002. *CRC Handbook of Chemistry and Physics.* 83rd Edition. Boca Raton, Florida: CRC Press. TIC: 253582

Lynch, C.T., ed. 1989. *Practical Handbook of Materials Science.* Boca Raton, Florida: CRC Press. TIC: 240577.

Parrington, J.R.; Knox, H.D.; Breneman, S.L.; Baum, E.M.; and Feiner, F. 1996. *Nuclides and Isotopes, Chart of the Nuclides.* 15th Edition. San Jose, California: General Electric Company and KAPL, Inc. TIC: 233705.

Punatar, M.K. 2001. *Summary Report of Commercial Reactor Criticality Data for Crystal River Unit 3.* TDR-UDC-NU-000001 REV 02. Las Vegas, Nevada: Bechtel SAIC Company. ACC: MOL.20010702.0087.

Roberts, W.L.; Campbell, T.J.; and Rapp, G.R., Jr. 1990. *Encyclopedia of Minerals.* 2nd Edition. New York, New York: Van Nostrand Reinhold. TIC: 242976.

Stout, R.B. and Leider, H.R., eds. 1997. *Waste Form Characteristics Report Revision 1.* UCRL-ID-108314. Version 1.2. Livermore, California: Lawrence Livermore National Laboratory. ACC: MOL.19980512.0133.

Todreas, N.E. and Kazimi, M.S. 1990. *Nuclear Systems I, Thermal Hydraulic Fundamentals.* New York, New York: Hemisphere Publishing. TIC: 226511.

Williams, N.H. 2003. "Contract No. DE-AC28-01RW12101 - Licensing Position-009, Waste Stream Parameters." Letter from N.H. Williams (BSC) to J.D. Ziegler (DOE/ORD), November 13, 2003, 1105039412, with enclosure. ACC: MOL.20031215.0076.

Williams, N.H. 2004. *Decision Proposal, Technical Decision, Statement for Consideration: Change the Current Neutron Absorber Material in the CSNF Waste Packages from Borated Stainless Steel to a Nickel-Gadolinium Alloy.* Tracking No. TMRB-2004-009. [Las Vegas, Nevada: Bechtel SAIC Company]. ACC: MOL.20040622.0307.

YMP (Yucca Mountain Site Characterization Project) 2003. *Disposal Criticality Analysis Methodology Topical Report.* YMP/TR-004Q, Rev. 02. Las Vegas, Nevada: Yucca Mountain Site Characterization Office. ACC: DOC.20031110.0005.

7.2 CODES, REGULATIONS, STANDARDS , AND PROCEDURES

10 CFR (Code of Federal Regulations) 63. Energy: Disposal of High-Level Radioactive Wastes in a Geologic Repository at Yucca Mountain, Nevada. Readily available.

10 CFR (Code of Federal Regulations) 961. Energy: Standard Contract for Disposal of Spent Nuclear Fuel and/or High-Level Radioactive Waste. Readily Available.

ASME (American Society of Mechanical Engineers) 2001. *2001 ASME Boiler and Pressure Vessel Code (includes 2002 addenda).* New York, New York: American Society of Mechanical Engineers. TIC: 251425.

ASTM A 516/A 516M-90. 1991. *Standard Specification for Pressure Vessel Plates, Carbon Steel, for Moderate-and Lower-Temperature Service.* West Conshohocken, Pennsylvania: American Society for Testing and Materials. TIC: 240032.

ASTM B 811-97. 2000. *Standard Specification for Wrought Zirconium Alloy Seamless Tubes for Nuclear Reactor Fuel Cladding.* West Conshohocken, Pennsylvania: American Society for Testing and Materials. TIC: 247245.

ASTM B 932-04. 2004. *Standard Specification for Low-Carbon Nickel-Chromium-Molybdenum-Gadolinium Alloy Plate, Sheet, and Strip.* West Conshohocken, Pennsylvania: American Society for Testing and Materials. TIC: 255846.

ASTM G 1-90 (Reapproved 1999). 1999. *Standard Practice for Preparing, Cleaning, and Evaluating Corrosion Test Specimens*. West Conshohocken, Pennsylvania: American Society for Testing and Materials. TIC: 238771.

LP-SI.11Q-BSC, Rev. 0, ICN 0. *Software Management.* Washington, D.C.: U.S. Department of Energy, Office of Civilian Radioactive Waste Management. ACC: DOC.20040225.0007.

NRC (U.S. Nuclear Regulatory Commission) 2000. *Standard Review Plan for Spent Fuel Dry Storage Facilities.* NUREG-1567. Washington, D.C.: U.S. Nuclear Regulatory Commission. TIC: 247929.

7.3 SOURCE DATA LISTED BY DATA TRACKING NUMBER

GS000308313211.001. Geochemistry of Repository Block. Submittal date: 03/27/2000.

MO0003RIB00071.000. Physical and Chemical Characteristics of Alloy 22. Submittal date: 03/13/2000.

MO0109HYMXPROP.001. Matrix Hydrologic Properties Data. Submittal date: 09/17/2001.

LB990501233129.001. Fracture Properties for the UZ Model Grids and Uncalibrated Fracture and Matrix Properties for the UZ Model Layers for AMR U0090, "Analysis of Hydrologic Properties Data". Submittal date: 08/25/1999.

7.4 SOFTWARE CODES

CRWMS M&O 1998e. *Software Code: MCNP.* V4B2LV. HP, HPUX 9.07 and 10.20; PC, Windows 95; Sun, Solaris 2.6. 30033 V4B2LV.

8. ATTACHMENTS

Table 28 presents the attachment specifications for this calculation file.

Table 28. Attachment Listing

Attachment #	# of Pages	Date Created	Description
I	12	N/A	Sensitivity Studies
II	6	N/A	PWR Assembly Lattice Design Sensitivity
III	2	N/A	Listing of contents on Attachment IV
IV	N/A	09/20/2004	Compact Disc attachment containing information listed in Attachment III

Attachment I: Sensitivity Studies

I. DESCRIPTION AND RESULTS

Sensitivity studies were performed to observe the waste package as it behaves over time in the repository and to determine which material characteristics result in the highest k_{eff} values. A brief description of the sensitivity studies performed and their results is provided in the following sections.

In each of the sensitivity cases, the waste package dimensions correspond to those provided in Attachment IV (*21PWRWP.zip*) with any irradiated fuel compositions taken from BSC (2003b, Section 6). Each configuration is represented with dry tuff surrounding the waste package. The dry tuff composition for each of the sensitivity cases is represented as listed in Table 29.

Table 29. Tuff Composition for Sensitivity Cases

Compound	Wt%
SiO_2	76.29
Al_2O_3	12.55
FeO	0.14
Fe_2O_3	0.97
MgO	0.13
CaO	0.5
Na_2O	3.52
K_2O	4.83
TiO_2	0.11
P_2O_5	0.05
MnO	0.07

Source: DTN:GS000308313211.001, mean values from file zz_sep_249138.txt.

NOTE: Derived elemental/isotopic number densities for MCNP inputs are provided in Attachment IV, workbook *Tuff composition.xls*, sheet *Latest_Tuff*

I.1 FUEL DENSITY EFFECTS

Variations in fuel density were evaluated. This set of cases was performed in order to assess the fuel density that would result in the highest k_{eff} values given the fixed lattice dimensions of the B&W 15x15 fuel assembly. Fuel density values were varied from 9.8 g/cm^3 through 10.8 g/cm^3 for a representative assembly with 3.0 wt% U-235 fresh fuel and 3.0 wt% U-235 initial enriched fuel with a burnup of 30 GWd/MTU. The results of this set of cases are presented in Table 30.

Table 30. Spent Nuclear Fuel Density k_{eff} Results[a]

Fuel Density (g/cm^3)	Fresh			Burned		
	k_{eff}	σ	Filename[b]	k_{eff}	σ	Filename[b]
9.8	1.03949	0.0005	case1	0.852	0.00053	case1
10	1.0411	0.00053	case2	0.85357	0.00057	case2
10.2	1.04304	0.00059	case3	0.85398	0.00051	case3
10.4	1.04491	0.00051	case4	0.8568	0.00048	case4
10.6	1.04783	0.00053	case5	0.85785	0.00049	case5
10.8	1.04955	0.00052	case6	0.85906	0.00048	case6

NOTES: [a] Homogenized end-fitting regions used a water density of 0.1 g/cm^3 in the homogenization. Since these cases only evaluate the trend of k_{eff} with different fuel densities, and the end-fitting regions are outside the active fuel region and constant in all the cases, there is no impact on the trend.
[b] Filenames are the same but are contained in a unique directory structure in Attachment IV as explained in Attachment III.

The results show that an increase in fuel density, which effectively increases the fissile mass in a fixed geometry, causes k_{eff} to increase.

I.2 WASTE PACKAGE FUEL ASSEMBLY GEOMETRY

Variations in fuel assembly geometries were evaluated. This set of cases investigated the effects of different positioning of the fuel assemblies within the waste package. Three configurations where evaluated. One where the assembly was centered within the waste package basket cell as could occur when the waste package is in a vertical position during loading operations, and two where the fuel assemblies are resting against the basket plates which occurs when the waste package is in a horizontal position. The three different geometric representations are provided in Figures 36 through 38 and the results presented in Table 31. Base case compositions correspond to a fuel assembly with 3.0 wt% U-235 fresh fuel and density of 10.741 g/cm^3.

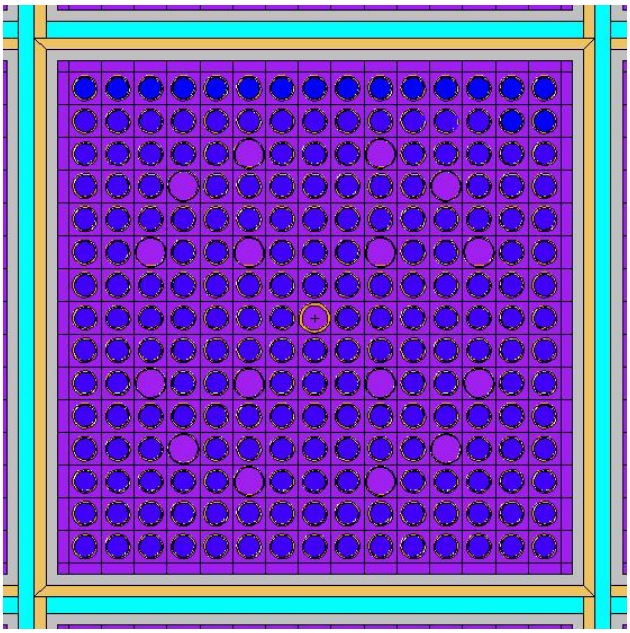

Figure 36. Standard Vertical Position Waste Package Geometry

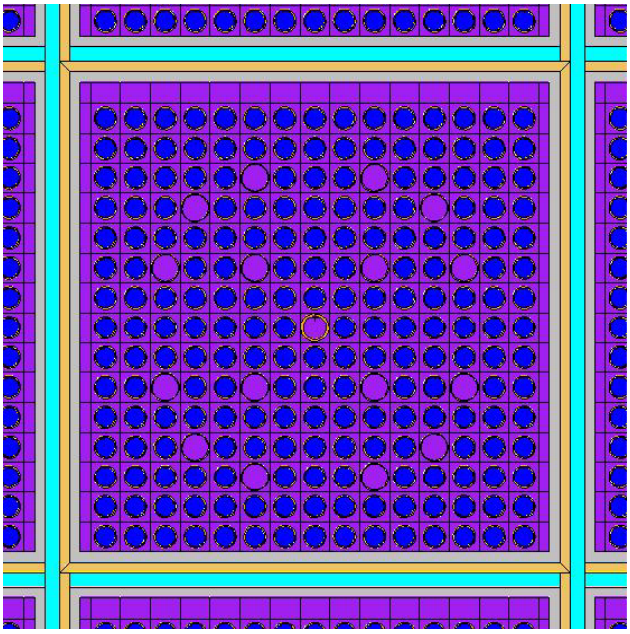

Figure 37. Standard Horizontal Position Waste Package Geometry

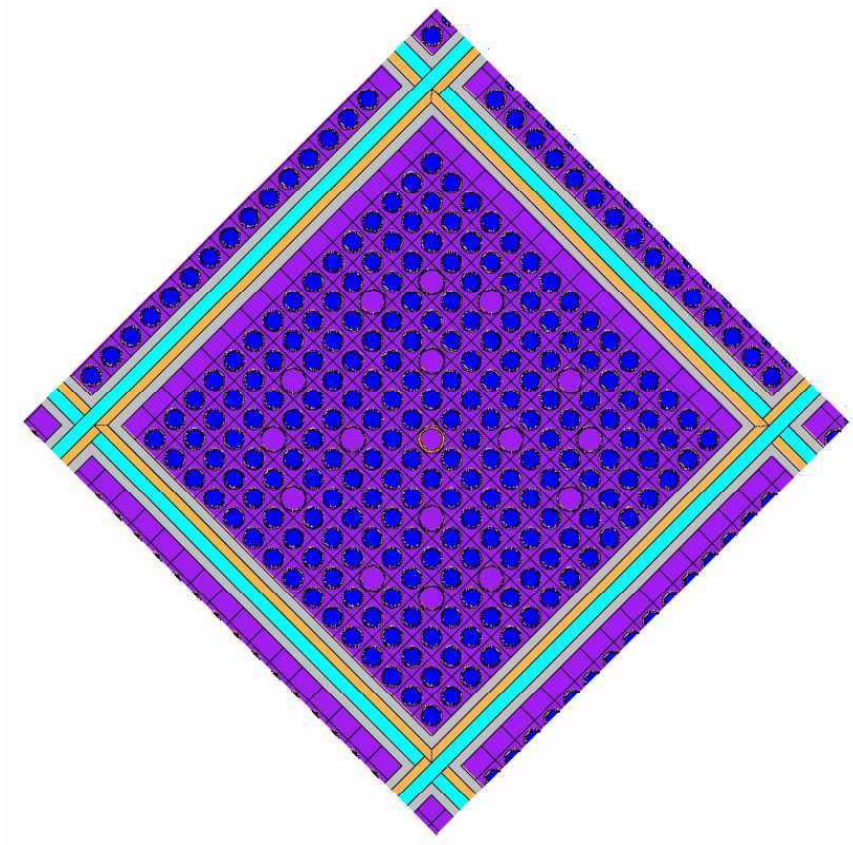

Figure 38. Rotated Horizontal Position Waste Package Geometry

Table 31. Fuel Assembly Geometry k_{eff} Results

Configuration	k_{eff}	σ	Base Filename
Standard Vertical	1.04892	0.00051	vert
Standard Horizontal	1.04100	0.00053	horiz1
Rotated Horizontal	1.03346	0.00049	horiz2

The results show that a standard vertical geometry representation produces the highest k_{eff}.

I.3 OPTIMUM MODERATOR DENSITY

A search for optimum moderator density was performed. This set of cases was used to show that the fuel assemblies placed into a waste package configuration is an under-moderated system. Moderator density values were varied from 0.0 g/cm^3 through 1.0 g/cm^3. Base case values correspond to a fresh fuel assembly with 3.0 wt% U-235 initial enrichment. The results of this set of cases are presented in Table 32 and are illustrated in Figure 39.

Table 32. Moderator Density Sensitivity Results

Moderator Density (g/cm^3)	k_{eff}	σ	Filename
0.0[a]	0.45169	0.00021	Case0a
0.0	0.34835	0.00020	Case0
0.1	0.56110	0.00039	Case1
0.2	0.68843	0.00045	Case2
0.3	0.77881	0.00051	Case3
0.4	0.85103	0.00054	Case4
0.5	0.90441	0.00053	Case5
0.6	0.94797	0.00054	Case6
0.7	0.98167	0.00050	Case7
0.8	1.00983	0.00053	Case8
0.9	1.03076	0.00061	Case9
1.0	1.04892	0.00051	vert

NOTE: [a] Case used 5.0 wt% U-235 enriched fuel to evaluate maximum dry fuel reactivity

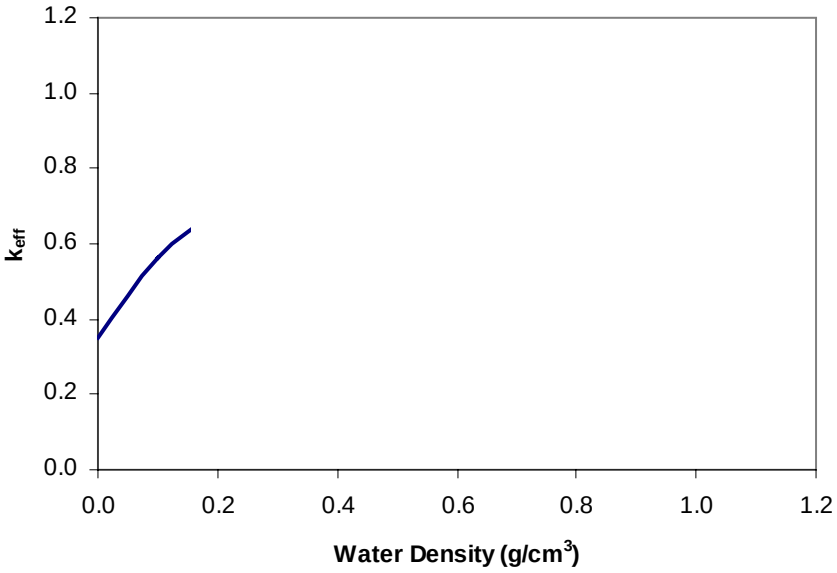

Figure 39. Moderator Density Sensitivity Results

Another moderator material instead of water was also evaluated. Hydraulic fluid/oil that may leak from a handling crane. Estimates indicate that a 100 ton or 200 ton crane, which could be utilized by the handling facility, would contain approximately 100 to 135 gallons of fluid/oil. The representative hydraulic fluid follows the description provided in Gelest, inc. (2004) and the material safety data sheet contained in Attachment IV (*0130223.pdf*) and has a chemical form as follows:

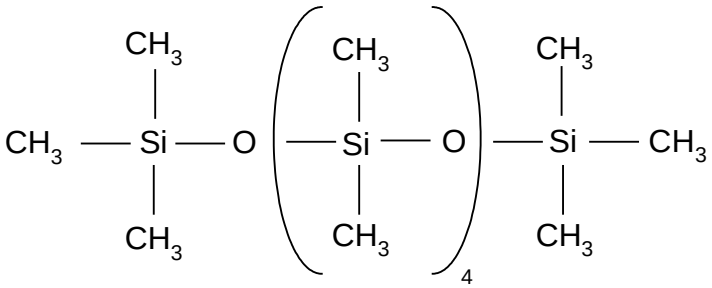

Source: Gelest Inc. 2004, p. 11

For the event of this fluid/oil getting into the waste package several cases were evaluated to observe the effects on system reactivity. The cases were as follows:

Case1 - the entire waste package is filled with fluid/oil at a density of 0.9 g/cm^3 (quantity indicates this is non-mechanistic, but will bound all other configurations (k_{eff} = 0.97892, σ = 0.00053)

In order to assess whether the hydraulic fluid results in an over- or under-moderation of the system, the density of the material was lowered in these cases to observe the effects on k_{eff}:

Case2 - used a density of 0.85 g/cm^3 (k_{eff} = 0.96779, σ = 0.00051)

Case3 - used a density of 0.8 g/cm^3 (k_{eff} = 0.95510, σ = 0.00054)

Since the resulting k_{eff} values decreased with decreased density, the system is under-moderated and no further evaluations are warranted. Water is a better moderator than the representative hydraulic fluid.

I.4 SIMPLIFIED GEOMETRY

Several geometric simplifications were evaluated in order to determine the impact on system reactivity. An external trunion region and basket stiffeners are present on the drawings presented in Attachment IV (*21PWRWP.zip*). A comparison was made between cases with and without the trunion region with or without the stiffeners being represented, as well as with the trunions, stiffeners, and representative hardware material on the axial ends (accounts for various for barrier lids). The configurations were evaluated with 3.0 wt% U-235 fresh fuel. The results of this set of cases are presented in Table 33.

Table 33. Simplified Geometry Results

Case Description	k_{eff}	σ	Filename
Base case with no trunion region and basket stiffeners present	1.04892	0.00051	vert
Base case with trunion region, basket stiffeners present, and axial hardware outside inner region represented	1.04892	0.00051	wtsends
Base case with no trunion region and no stiffeners present	1.04921	0.00055	wostif
Base case with trunion region and stiffeners present	1.04892	0.00051	wtands

These results indicate that the presence of trunions, stiffeners, or both in the representation have an insignificant impact on system reactivity.

I.5 TUFF EVALUATIONS

Variations for tuff present in and around the waste package were evaluated. This set of cases was performed in order to assess the impact tuff could have on system reactivity. Various levels of saturation were evaluated, as well as geometric arrangements. Configurations were evaluated using the 15x15 assembly design with 3.0 wt% U-235 fresh fuel. The results for the external reflector tuff cases are presented in Table 34. Cases where the tuff material was uniformly dispersed within the waste package are presented in Table 35. This set of cases is very unlikely since the basket plates would serve as a barrier to prevent tuff from getting into the internal regions of the basket geometry. Cases where the tuff would most likely be able to enter the waste package and be mobile would be in solution, and were evaluated with the results presented in Table 36. Two solution sets were evaluated, one where the solution is in all void regions, and one where it accumulates external to the fuel basket tubes over the active fuel region. Derivations of the tuff material compositions were performed in Attachment IV (spreadsheet *Tuff composition.xls*).

Table 34. External Waste Package Reflector Evaluation Results

Case Description	k_{eff}	σ	Filename
Dry tuff outside waste package	1.04892	0.00051	vert
100% saturated tuff outside waste package	1.04895	0.00055	tuffsat
Water outside waste package	1.04962	0.00055	water
Void outside waste package	1.04882	0.00055	void

Table 35. Waste Package Tuff Internal Configuration Solid Results

Case Description	k_{eff}	σ	Filename
Dry tuff in all void regions	0.39419	0.00021	t0all
100% saturated tuff in all void regions	0.59427	0.00039	t100all

Table 36. Waste Package Tuff Internal Configuration Solution Results

Case Description	Solution in All Void		Solution in Void Outside FBT[a]		Filename[b]
	k_{eff}	σ	k_{eff}	σ	
10 volume percent of available saturated tuff in solution	1.04873	0.00053	1.04914	0.00052	t10
20 volume percent of available saturated tuff in solution	1.04896	0.00058	1.04956	0.00047	t20
30 volume percent of available saturated tuff in solution	1.04863	0.00056	1.04808	0.00048	t30
40 volume percent of available saturated tuff in solution	1.04897	0.00051	1.04902	0.00053	t40
50 volume percent of available saturated tuff in solution	1.05047	0.00052	1.04972	0.00057	t50
100 volume percent of available saturated tuff in solution	1.04880	0.00053	1.04882	0.00048	t100

NOTES: [a] FBT = fuel basket tube
[b] Filenames are the same but are contained in a unique directory structure in Attachment IV as explained in Attachment III.

These results indicate that the 50 volume percent case distributing the tuff mixture over all void regions produces the highest k_{eff} value. This is based on having 50% of the original assumed 20 kg of tuff (see Assumption 3.6) that could get into the waste package entering and being in solution. Since this is an assumed amount of tuff that can get inside the waste package, and the results (varied from 10% though 100%) are statistically equivalent k_{eff} values at the 95 percent confidence level as using pure water for moderator and reflector, having 20 kg of tuff or less in the waste package is considered to produce equivalent reactivity levels as pure water.

I.6 INTERNAL COMPONENT DEGRADATION

A set of sensitivity cases was performed to evaluate effects of changing conditions as waste package internal components degrade. These cases are based on the waste package internal structures degrading before the waste form and is representative of configuration class IP-3 from YMP (2003,

Figure 3-2). The cases used a 3.0 wt% U-235 fresh fuel composition for each of the runs. Variations were made to the amount of corrosion product retained within the basket cells to observe the sensitivity of neutron spectrum. The corrosion product mixture composition was derived in Attachment IV (spreadsheet *misc.xls*, sheet *degraded_sens*) based on the amounts of iron and aluminum contained within the basket cells. Iron was assumed to form the mineral Hematite (Fe_2O_3) or Goethite (FeOOH), and aluminum was assumed to form into the mineral Gibbsite ($Al[OH]_3$). The results and a brief description of the cases are provided in Table 37.

Table 37. k_{eff} Results for Degraded Internal Component Cases

Filename	Case Description	k_{eff}	σ
case1	Nominal with carbon steel as Hematite and Al as Gibbsite in original locations, fully flooded	1.03613	0.00046
case2	Nominal with carbon steel as Goethite and Al as Gibbsite in original locations, fully flooded	1.02445	0.00053
case3	Same as case1 but oxidized plates in expanded volume	1.04614	0.00055
case4	Same as case2 but oxidized plates in expanded volume	1.02547	0.00051
case5	Al and steel removed from system, fully flooded	1.03121	0.00056
case6g	All corrosion product (CP) distributed uniformly throughout package (all Fe represented as goethite), fully flooded	0.9156	0.0005
case6h	All CP distributed uniformly throughout package (all Fe represented as hematite), fully flooded	0.90662	0.00053
case7g	Same as case6g but at 33% CP retention level	0.99090	0.00051
case7h	Same as case6h but at 33% CP retention level	0.98819	0.00048
case8g	Same as case6g but at 66% CP retention level	0.95247	0.00051
case8h	Same as case6h but at 66% CP retention level	0.94640	0.00053
case9	Same as case3 but absorber plates at 5mm thickness	1.04351	0.00053

The results indicate that a fully flooded system with the oxidized aluminum and iron remaining in place (case3) produces the highest system reactivity. The iron mineral hematite produces higher k_{eff} values for this configuration. Corrosion products mixed in solution displace moderator, which reduces neutron thermalization within the assemblies and thus results in lower k_{eff} values.

I.7 ABSORBER PLATE DEGRADATION

A series of cases were evaluated in order to determine the effects of the absorber plate as it degrades over time. Variations were made to the amount of corrosion product retained within the basket cells to observe the sensitivity of neutron spectrum. The corrosion product mixture composition was derived in Attachment IV (spreadsheet *misc.xls*, sheet *degraded_sens*) based on the amounts of iron and aluminum contained within the basket cells. Iron was assumed to form the mineral Hematite (Fe_2O_3), and aluminum was assumed to form into the mineral Gibbsite ($Al[OH]_3$).

Current degradation rate information (Williams 2004) for the Ni-Gd alloy indicate that the maximum amount of degradation will be less than 1 mm per side, resulting in a minimum of 5 mm of Ni-Gd absorber. Since geochemistry calculations for this material and waste package configuration are not available, varied amounts of estimated corrosion product composition were evaluated. The amounts varied from 0% to 100%. The results for this set of cases are presented in Table 38.

Table 38. k_{eff} Results for 5mm Thick Absorber Plate Cases

Corrosion Product Retained	k_{eff}	σ	Filename
0%	1.03421	0.00057	5m0cp
33%	0.99101	0.00053	5m33cp
66%	0.95058	0.00046	5m66cp
100%	0.91264	0.00053	5m100cp

These results indicate that the configuration is more reactive without corrosion product composition represented in the basket cells, as was also indicated in Table 37.

Table 39 illustrates results as a function of absorber plate (Ni-Gd Alloy) thickness, with 0% and 100% corrosion product retention.

Table 39. k_{eff} Results as a function of Absorber Plate Thickness

% Absorber Plate Removed	Remaining Plate Thickness (mm)	100% Corrosion Product Retention		0% Corrosion Product Retention		Filename[a]
		k_{eff}	σ	k_{eff}	σ	
0	7.25	0.90687	0.0005	1.03130	0.00061	0d
10	6.525	0.90669	0.00052	1.03043	0.00057	10d
20	5.8	0.90855	0.00051	1.03248	0.00057	20d
30	5.075	0.9117	0.00055	1.03382	0.00051	30d
40	4.35	0.91411	0.00053	1.03451	0.00055	40d

NOTE: [a] Filenames are the same but are contained in a unique directory structure in Attachment IV as explained in Attachment III

These results indicate that the 0% corrosion product retention cases produce higher k_{eff} values than the 100% corrosion product retention cases, and the system k_{eff} increases for a fully flooded system as the absorber plates become thinner.

I.8 COMPROMISED FUEL RODS

This configuration class is based on the waste form degrading before or at the same rate as the waste package internal structures and is representative of configuration classes IP-1 and IP-2 from YMP (2003, Figure 3-2). Seismic studies have determined that a peak ground velocity of 1.067 m/s or greater results in fuel cladding failure (BSC 2004j, Table 30) which results in exposure of the spent nuclear fuel to an oxidizing atmosphere. Once the fuel cladding is breached, oxidation of the fuel material can occur and cause clad breach propagation (unzipping). Therefore, a set of cases was evaluated that involved oxidized fuel. The thermodynamically stable state for oxidized uranium is UO_3 (Einziger 1991, p. 88). If moisture is present in the atmosphere hydration may also occur (Einziger 1991, p. 88) and form the compound $UO_3(H_2O)_2$ (Einziger 1991, Figure 1) otherwise known as the mineral schoepite (BSC 2004i, Attachment I, file *data0 files.zip*, file *data0.ymf*).

A set of sensitivity studies was performed in order to evaluate various configurations. The cases used a 3.0 wt% U-235 fresh fuel schoepite composition for each of the runs except case0 and case0nw which are provided for fresh fuel base case k_∞ values to compare against. The compositions were derived in Attachment IV (spreadsheet *misc.xls,* sheet *schoepite*) for the fuel material. The results and a brief description of the cases are provided in Table 40. It should be noted that the sensitivity runs were for an infinite two-dimensional lattice configuration in a representative waste package basket geometry, which is the reason for the high eigenvalues.

Table 40. Compromised Fuel Assembly Sensitivity Cases

Filename	Case Description	k_∞	σ
case0	Fresh fuel base case for comparison, fully flooded in nominal geometry.	1.08436	0.00093
case0nw	Same as case0 but dry conditions.	0.46317	0.00037
case1	Schoepite expanded around clad; nominal standard vertical geometry; dry conditions; Schoepite block at theoretical density.	1.02388	0.00095
case2	Schoepite expanded around clad; aluminum shunts and fuel basket tube have corroded into gibbsite and goethite, respectively, occupying original volumes; nominal standard vertical geometry, dry conditions, Schoepite block at theoretical density.	0.95172	0.00111
case3	Same as Case2 but the gibbsite and goethite volume is expanded and applied to the thickness along the active fuel length.	0.92806	0.00104
case4	Same as Case1 but the system is compressed to the point where the basket plates are in contact with the fuel basket tubes.	1.02551	0.00099
case5	Same configuration as Case4 but the basket plate materials and fuel basket tube have oxidized into gibbsite and goethite.	0.95743	0.00098
case6	Same as Case5 but the waste package compression is in the vertical direction with expansion in the x direction.	0.95389	0.00105
case7	Like Case2 but fuel basket tube is represented as hematite instead of goethite.	0.96238	0.00099
case8	Same as Case5 but the fuel basket tube is hematite instead of goethite.	0.96785	0.00107

Table 40. Compromised Fuel Assembly Sensitivity Cases

Filename	Case Description	k_∞	σ
case9	Same conditions as Case1 but system is fully collapsed so there is no spacing between fuel basket tube, schoepite, and basket. Nominal pin pitch used.	1.02997	0.00096
case9a	Same conditions as Case1 but system is fully collapsed so there is no spacing between fuel basket tube and schoepite. Pin pitch adjusted so schoepite has no spaces around it in unit cell. Also, surrounds guide tubes and instrument tubes.	1.03559	0.00094
case9b	Same as case9a with schoepite at theoretical density with all clad, guide tubes, and instrument tubes removed from system. Basket materials collapsed around schoepite block.	1.0776	0.00092
case10	Same as Case1 but water fills all void space.	1.02817	0.00097
case11 g and h	Same as Case3 but the fuel basket tube corrosion product composition has settled within the basket cell and assembly is in standard horizontal position geometry (See Figure 37); g designates goethite as the primary iron mineral and h denotes hematite as the primary iron mineral, CP in solution.	0.94719	0.00102
		0.95350	0.00099
case12 g and h	Same as Case11 but CP oxide is uniformly distributed throughout basket cell; g designates goethite as the primary iron mineral and h denotes hematite as the primary iron mineral.	0.94269	0.00097
		0.94577	0.00103
case13	Same as Case12 but only water in basket cell.	0.98394	0.001
case14	Same as Case10 but the water and schoepite are homogenized throughout FBT region.	1.08035	0.00097
case15 g and h	Like case12 but CP and schoepite are uniformly mixed as dry CP occupying space throughout basket cell; g designates goethite as the primary iron mineral and h denotes hematite as the primary iron mineral, CP in solution.	1.00210	0.00080
		0.98491	0.00086

The results indicate that a nominal configuration with schoepite uniformly dispersed in solution in a fully flooded system that can result from a seismic event produces the highest reactivity (case14) for ruptured fuel rods. The case0 configuration resulted in a higher reactivity, and is representative of the preclosure intact fuel rod nominal configuration.

I.9 WASTE PACKAGE INTERACTION

A set of cases was evaluated to assess the impact of package-to-package interaction during preclosure operations. Variations were made in the spacing and interstitial material between packages to observe the sensitivity to such parameters. The interstitial material was represented as void and water, and the spacing was varied from 0 to 1 cm. A brief description of each case and the results are presented in Table 41.

Table 41. Waste Package Interaction Results

Case Description	k_{eff}	σ	Filename
Single WP with no others, filled with water and void outside	1.04882	0.00055	c0
Infinite array of WP touching water inside and void outside	1.04947	0.00052	c1
Infinite array of WP touching void inside and water outside	0.33384	0.00022	c2
Infinite array of WP touching water inside and water outside	1.04808	0.00051	c3
Infinite array of WP 1 cm spacing water inside and void outside	1.04930	0.00054	c4
Infinite array of WP 1 cm spacing void inside and water outside	0.33111	0.00022	c5
Infinite array of WP 1 cm spacing water inside and water outside	1.04779	0.00051	c6

These results indicate that waste packages have a negligible neutronic influence on other waste packages. Without water, the waste packages have no criticality concern, and with water represented in different areas, the eigenvalues are within two sigma of the single waste package.

Attachment II: PWR Assembly Lattice Design Sensitivity

Variations in fuel assembly lattice design were evaluated. This set of cases was performed in order to assess which fuel assembly lattice design would result in the highest k_{eff} values when loaded in a waste package configuration and confirm Assumption 3.1. Fuel assembly lattices were varied using Babcock & Wilcox (B&W), Westinghouse (W), and Combustion Engineering (CE) geometric arrangements in pure water. These cases were evaluated using a fresh fuel enrichment of 5.0 wt% U-235 in a nominal waste package configuration and 5.0 wt% U-235 initial fresh fuel enrichment at 30 GWd/MTU burnup isotopic compositions. Pertinent assembly design parameters for the representations are provided in Table 42. Although spacer grid information is presented in Table 42, the MCNP representations did not represent them in order to maximize system reactivity. Throughout this section STD refers to standard, and OFA refers to optimized fuel assembly designs.

Table 42. Fuel Assembly Parameters

Assembly Design / Parameter[a]	B&W 15x15[b]	W 17x17 (STD)[c]	W 17x17 (OFA)[d]	CE 14x14[e]	CE 15x15[e]	CE 16x16[e]	W 15x15[e]	W 15x15 (OFA)[e]
Rod pitch (cm [in.])	1.44272	1.25984	1.25984	1.4732 (0.580)	1.397 (0.550)	1.28524 (0.506)	1.43002 (0.563)	1.43002 (0.563)
Assembly pitch (cm [in.])	21.81098	21.50364	21.50364	20.574 (8.1)	20.828 (8.2)	20.574 (8.1)	21.42236 (8.434)	21.39696 (8.424)
Rod outer diameter (OD) (cm [in.])	1.0922	0.94996	0.91440	1.1176 (0.44)	1.06172 (0.418)	0.97028 (0.382)	1.07188 (0.422)	1.07188 (0.422)
Cladding thickness (cm [in.])	0.06731	0.05715	0.05715	0.07112 (0.028)	0.06604 (0.026)	0.0635 (0.025)	0.061468 (0.0242)	0.061468 (0.0242)
Rod length (cm [in.])	390.366	385.1534	384.704	373.38 (147)	355.6 (140)	408.94 (161)	385.7752 (151.88)	385.699 (151.85)
Active fuel length (cm [in.])	360.172	365.76	365.76	347.98 (137)	335.28 (132)	381 (150)	363.22 (143)	365.76 (144)
U mass per assembly	463.63 kg	458.88 kg	423.12 kg	386 kg (0.386 MT)	412.769 kg (910 lbs)	426 kg (0.426 MT)	469 kg (0.469 MT)	462.7 kg (0.4627 MT)
Plenum spring material	SS304	SS302[f]	SS302[f]	SS302	SS302	SS302	SS302	SS302
Plenum spring mass per assembly (g [lb])	N/A	N/A	N/A	45.359 (0.10)	22.6796 (0.050)	45.359 (0.10)	18.5973 (0.041)	11.3398 (0.025)
Plenum length (cm [in.])	28.766	17.9654	17.516	21.2725 (8.375)	N/A	24.19858 (9.527)	20.828 (8.2)	20.828 (8.2)
Upper end-fiting length (cm [in.])	8.731	15.506	15.506	16.8402 (6.63)	7.9756 (3.140)	24.69642 (9.723)	8.8773 (3.495)	9.017 (3.550)
Lower end-fitting length (cm [in.])	16.723	11.951	11.951	7.9375 (3.125)	8.2296 (3.24)	9.68248 (3.812)	6.95452 (2.738)	6.95452 (2.738)
Intermediate spacer grid material	Inconel-718	Inconel[g]	Zircaloy	Zircaloy-4	Zircaloy-4	Zircaloy-4	Inconel-718	Zircaloy-4
Upper spacer grid material	Inconel-718	Inconel[g]	Inconel[g]	Zircaloy-4	Zircaloy-4	Zircaloy-4	Inconel-718	Inconel-718
Bottom spacer grid	Inconel-	Inconel[g]	Inconel[g]	Inconel-	Inconel-	Inconel-	N/A	Inconel-

Table 42. Fuel Assembly Parameters

Assembly Design / Parameter[a]	B&W 15x15[b]	W 17x17 (STD)[c]	W 17x17 (OFA)[d]	CE 14x14[e]	CE 15x15[e]	CE 16x16[e]	W 15x15[e]	W 15x15 (OFA)[e]
material	718			625	625	625		718
Intermediate grid length (cm)	3.81	3.35788	5.71500	4.284[h]	2.946[h]	5.432[h]	3.81	5.715
Upper grid length (cm)	8.573	14.656	14.656	4.284[h]	2.946[h]	5.432[h]	3.81	3.81
Bottom grid length (cm)	N/A	3.35788	3.35788	9.044[h]	6.63[h]	10.3188	N/A	3.81
Total number of spacer grids	7	8	8	9	10	11	7	7
Number of guide tubes	16	24	24	5	8[k]	5	20	20
Guide tube OD (cm)	1.3462	1.22428 1.08966	1.20396 1.08966	2.832[i]	1.1978	2.832[i]	1.382[i]	1.382[i]
Guide tube wall thickness (cm [in.])	0.04064	0.04064	0.04064	0.091[i]	N/A	0.091[i]	0.043[i]	0.043[i]
Instrument tube OD (cm)	1.38193	1.22428	1.20396	2.832[i]	1.059[j]	1.059[i]	1.382[i]	1.382[i]
Instrument tube wall thickness (cm)	0.130895	0.04064	0.04064	0.091[i]	0.069[j]	0.069[i]	0.043[i]	0.043[i]

NOTES:
[a] Referenced dimensions in inches provided in parentheses and converted to cm where applicable.
[b] Parameters from Punatar (2001, Section 2 and Table 3-1).
[c] Parameters from CRWMS-M&O (1998c, Section 2 and Table 3-1).
[d] Parameters from CRWMS-M&O (1998d, Section 2 and Table 3-1).
[e] Parameters from DOE (1987, pp. 2A-55 to 2A-58 and Figure 1-4 for the CE 14x14 design; pp. 2A-67 to 2A-70 and Figure 1-1 for the CE 15x15 design; pp. 2A-73 to 2A-76 and Figure 1-9 for the CE 16x16 design; pp. 2A-319 to 2A-322 and drawing 1598E32 for the W 15x15 design; and pp. 2A-325 to 2A-328 and drawing 1607E93 for the W 15x15 OFA design.
[f] Material from DOE (1987, pp. 2A-352 and 2A-346)
[g] References did not specify type, therefore Inconel-718 was used in the representations.
[h] Values based on Assumption 3.9
[i] Parameters from Stout and Leider (1997, pp. 2.1.2.2-2 and 2.1.2.2-3); not used in representation due to lack of information regarding location.
[j] Based on Assumption 3.10
[k] There are eight Zircaloy-4 guide bars (DOE 1987, p. 2A-68) in this design which were not represented in order to maximize reactivity

The assembly materials listed here refer to the upper and lower end-fitting materials and the spacer grid materials. The primary material components in the upper and lower end-fitting regions are SS304 (see Table 9), Inconel (represented as Inconel-718 as shown in Table 10 or Inconel-625 as shown in Table 43), Zircaloy-4 as represented in Table 8, and moderator (represented as water at 1.0 g/cm^3 density). Both the upper and lower end-fitting regions are represented with material compositions that represent the homogenization of the components in the regions for each assembly design. The homogenization of the base components into single homogenized material compositions is performed using Equations 4 through 6. Table 43 presents the material composition for Inconel-625 spacer grids constituent natural isotopic weight percents for use in MCNP using Equations 2 and 3. Each of the homogenized material compositions is derived in Attachment IV (Workbook *homog_mats.xls*).

Table 43. Inconel 625 Material Composition

Element/ Isotope	ZAID[a]	Wt%	Element/ Isotope	ZAID[a]	Wt%
C-nat	6000.50c	0.1000	Fe-58[b]	26058.60c	0.0145
Si-nat	14000.50c	0.5000	Ni-58[b]	28058.60c	39.0889
P-31	15031.50c	0.0150	Ni-60[b]	28060.60c	15.4562
S-32	16032.50c	0.0150	Ni-61[b]	28061.60c	0.6835
Cr-50[b]	24050.60c	0.8973	Ni-62[b]	28062.60c	2.1946
Cr-52[b]	24052.60c	17.9955	Ni-64[b]	28064.60c	0.5769
Cr-53[b]	24053.60c	2.0798	Ti-nat	22000.50c	0.4000
Cr-54[b]	24054.60c	0.5273	Al-27	13027.50c	0.4000
Mn-55	25055.50c	0.5000	Co-59	27059.50c	1.0000
Fe-54[b]	26054.60c	0.2850	Mo-nat	42000.50c	9.0000
Fe-56[b]	26056.60c	4.5934	Nb[c]	73181.50c	3.6500
Fe-57[b]	26057.60c	0.1071	Density = 8.44 g/cm^3		

Source: Inco Alloys International 1998, pp. 1 and 2

NOTE: [a] ZAID = MCNP material identifier.
[b] Expanded constituent natural isotopic weight percents derived using Equations 2 and 3.
[c] Reference identifies this material as "columbium," which is actually the element niobium.

Table 44 presents the assembly hardware component masses and Tables 45 and 46 present the component material volume fractions for the upper and lower end-fitting regions. Since the spacer grids are not being represented in the spacer grid homogenization parameters are not being listed. Each of the homogenized material compositions is derived in Attachment IV (Workbook *homog_mats.xls*) along with the volume fractions for components that were not available.

Table 44. Assembly End-Fitting Hardware Component Masses

	Upper End-Fitting				
Hardware Part Name	**CE 14x14**	**CE 15x15**	**CE 16x16**	**W 15x15**	**W 15x15 OFA**
Locking posts (kg/assembly)	2.63 (SS304)	N/A	7.3 (SS304)	N/A	N/A
Hold-down spring (kg/assembly)	1.1 (Inconel 718)[a]	N/A	4.5 (Inconel 718)[a]	1.14 (Inconel 718)[a]	0.96 (Inconel 718)[a]
Flow plate (kg/assembly)	1.45 (SS304)	N/A	3.2 (SS304)	N/A	N/A
Hold-down plate (kg/assembly)	1.0 (SS304)	N/A	1.8 (SS304)	N/A	N/A
Top nozzle (kg/assembly)	N/A	4.5 (SS304)	N/A	10.7 (SS304)	6.89 (SS304)
	Lower End-Fitting				
Bottom nozzle (kg/assembly)	5.0 (SS304)	5.4 (SS304)	5.4 (SS304)	5.44 (SS304)	5.44 (SS304)

Source: DOE 1987, pp. 2A-56, 2A-68, 2A-74, 2A-320, and 2A-326

NOTE: [a] DOE 1987 lists this material as CE nickel alloy. No information is available for this material so it was represented as Inconel 718 (See Assumption 3.11).

Table 45. Upper End-Fitting Component Material Volume Fractions

Assembly Design	Volume Fractions in Upper End-Fitting Region			
	SS304	Inconel	Zircaloy-4	Moderator
B&W 15x15[a]	0.2756	0.0441	0.0081	0.6722
W 17x17 STD[b]	0.1243	0.0168	0.0	0.8589
W 17x17 OFA[c]	0.1303	0.0178	0.0051	0.8469
CE 14x14[d]	9.0209E-02	1.884E-02	N/A	0.8910
CE 15x15[d]	0.1646	N/A	N/A	0.8354
CE 16x16[d]	0.1489	0.0526	N/A	0.7985
W 15x15[d]	0.3325	0.0342	N/A	0.6333
W 15x15 OFA[d]	0.2113	0.0284	N/A	0.7603

NOTES: [a] Values from Punatar (2001, Table 2-6)
[b] Values from CRWMS M&O (1998c, p. 9)
[C] Values from CRWMS M&O (1998d, p. 15)
[d] Values derived from information provided in Tables 42 and 44 based on conservation of mass and volume

Table 46. Lower End-Fitting Component Material Volume Fractions

Assembly Design	Volume Fractions in Lower End-Fitting Region			
	SS304	Inconel	Zircaloy-4	Moderator
B&W 15x15[a]	0.1656	0.0306	0.0125	0.7913
W 17x17 STD[b]	0.1625	0.0	0.0	0.8375
W 17x17 OFA[c]	0.1439	0.0	0.0137	0.8424
CE 14x14[d]	0.1884	0.0	0.0	0.8116
CE 15x15[d]	0.1915	0.0	0.0	0.8085
CE 16x16[d]	0.1668	0.0	0.0	0.8332
W 15x15[d]	0.2158	0.0	0.0	0.7842
W 15x15 OFA[d]	0.2194	0.0	0.0	0.7806

NOTES: [a] Values from Punatar (2001, Table 2-3)
[b] Values from CRWMS-M&O (1998c, p. 9)
[C] Values from CRWMS-M&O (1998d, p. 15)
[d] Values derived from information provided in Tables 42 and 44 based on conservation of mass and volume

Table 47 presents the upper and lower fuel rod plenum material volume fractions.

Table 47. Fuel Rod Plenum Material Volume Fractions

Assembly Design	Plenum Location	Stainless Steel	Gas (represented as void)	Zircaloy-4
B&W 15x15[a]	Upper	0.0811	0.7793	0.1396
	Lower	0.1569	0.5973	0.2458
W 17x17 STD[a]	Upper	0.0976	0.8368	0.0655
	Lower	0.1532	0.6389	0.2080
W 17x17 OFA[a]	Upper	0.1753	0.8247	0.0000
	Lower	0.0000	0.0000	1.0000
CE 14x14[b]	Upper	0.0162	0.9838	0.0000
	Lower[c]	0.0000	0.0000	0.0000
CE 15x15[b]	Upper	0.0012	0.9988	0.0000
	Lower	0.0000	0.0000	0.0000
CE 16x16[b]	Upper	0.0142	0.9858	0.0000
	Lower	0.0000	0.0000	0.0000
W 15x15[b]	Upper	0.0006	0.9994	0.0000
	Lower	0.0000	0.0000	1.0000
W 15x15 OFA[b]	Upper	0.0003	0.9997	0.0000
	Lower	0.0000	0.0000	1.0000

NOTES: [a] Values derived in Attachment IV, workbook *homog_mats.xls*
[b] Upper plenum region represented as spring and void based on conservation of mass and volume from dimensions listed in Table 42
[c] Represented as solid Al_2O_3 spacer at density of 3.97 g/cm^3 (Lide, p. 4-39)

Each of the fuel assembly designs were represented in MCNP using a fuel density of 10.741 g/cm^3 in order to minimize on linear mass loading differences, which are inherent based on the design differences. Based on this density and the referenced active fuel lengths, the total mass per assembly is greater than its nominal loading, and is based on the design parameters. Therefore trying to keep the total mass per assembly constant is not appropriate here. The results for the PWR assembly lattice design sensitivity cases are presented in Table 48 and indicate that the B&W 15x15 assembly design is the most reactive, but is statistically equivalent at the 95% confidence limit to the W 17x17 OFA.

Table 48. Fuel Assembly Lattice Design k_{eff} Results

Assembly	Filename	k_{eff}	σ
B&W 15x15	BW15	1.16167	0.00055
W 17x17 OFA	W17OFA	1.16147	0.00055
W 17x17 STD	W17STD	1.15613	0.00058
W 15x15 OFA	W15OFA	1.1593	0.00064
W 15x15	W15	1.16082	0.00057
CE 14x14	CE14	1.11257	0.00058
CE 15x15	CE15	1.11695	0.00059
CE 16x16	CE16	1.11273	0.00056

INTENTIONALLY LEFT BLANK

Attachment III: Attachment CD Listing

This attachment contains a listing and description of the files contained on the attachment CD of this report (Attachment IV). The CD was written using ROXIO Easy CD Creator 5 Basic installed on CRWMS M&O tag number 150527 central processing unit, and can be viewed on most standard CD-ROM drives. The zip archive was created using WINZIP 8.1. The file attributes on the CD are as follows:

Filename	File Size (bytes)	File Date	File Time	Description
21PWRWP.zip	1,204,743	8/24/2004	08:24a	21-PWR Waste Package Configuration Design Drawings
0130223.pdf	68,126	6/10/2004	10:03a	MSDS for representative hydraulic fluid
cases.zip	51,010,067	9/20/2004	10:58a	Archive containing MCNP files
misc.xls	1,114,112	9/10/2004	08:24a	Excel spreadsheet containing various geometry and material derivations
Tuff composition.xls	59,904	9/09/2004	01:02p	Excel spreadsheet containing tuff composition derivations
homog_mats.xls	438,784	9/01/2004	11:17a	Excel spreadsheet containing fuel assembly hardware component derivations
wstreamplot.xls	710,656	9/20/2004	12:59p	Excel spreadsheet containing sorted waste stream information
IDBinputs.xls	265,728	9/10/2004	03:43p	Excel spreadsheet containing irradiated fuel isotopic compositions

There are 8 total files for the archive file *21PWRWP.zip* with no particular naming system. The files contain the dimensions for the 21-PWR waste package configuration.

There are 672 total files (not including folders) contained in a unique directory structure for the archive file *cases.zip*. Files without on "o" at the end are input files, and files with an "o" at the end are output files. The following extracted directory structure corresponds as follows:

/*temp3*/*PWRLC01CD/temp/**:

where * corresponds as follows:

/I.1/ - Contains files listed in Attachment I, Section I.1 with subdirectories *burned* and *fresh* corresponding to burned fuel isotopic composition and fresh fuel isotopic composition cases, respectively.
/I.2/ - Contains files listed in Attachment I, Section I.2
/I.3/ - Contains files listed in Attachment I, Section I.3 with subdirectories *Hyd_Fluid* and *Water_density* corresponding to hydraulic fluid and water density cases, respectively.
/I.4/ - Contains files listed in Attachment I, Section I.4
/I.5/ - Contains files listed in Attachment I, Section I.5 with subdirectories *Tuff_External*, *InWPVoid*, *ExtFBT*, and *Tsol* corresponding to the tabulated results in Attachment I, Tables 34, 35, and 36, respectively.
/I.6/ - Contains files listed in Attachment I, Section I.6

/I.7/ - Contains files listed in Attachment I, Section I.7 with subdirectories *5mm*, *100cp*, and *Water* corresponding to the tabulated results in Attachment I, Tables 38 and 39, respectively.
/I.8/ - Contains files listed in Attachment I, Section I.8
/I.9/ - Contains files listed in Attachment I, Section I.9

/Fresh_Fuel/ - Contains files used for the determination of the maximum fresh fuel enrichment that can be loaded into the waste package with two lower level directories denoted */Post_config/* and */Pre_config/* for postclosure and preclosure bounding configurations, respectively. The file naming system is as follows: *X.X* that represents the enrichment in wt% U-235 (ranging from 1.5 to 5.0).

/LC/ - Contains files used for developing the loading curve as a function of burnup, with four lower level directories /*7Post*/, /*7Pre*/, /*Post*/, and /*Pre*/ representing the postclosure bounding representation using a seven zone axial burnup profile, the preclosure bounding representation using a seven zone axial burnup profile, the postclosure bounding representation using a single zone axial burnup profile, and the preclosure bounding representation using a single zone axial burnup profile, respectively. The file naming system is as follows: where the *X.X* represents the initial enrichment in wt% U-235 (i.e., 3.5 is 3.5 wt% U-235 [range from 2.0 to 5.0 wt% U-235]), the *YY* represents the burnup in GWd/MTU (range from 10 to 45 GWd/MTU), and the *Z* is either a 1 or a 7 denoting a single zone axial burnup profile or a seven zone axial burnup profile, respectively.

/Misload/ - which contains the subdirectories */Nominal*/, */Sub10/*, and */Sub20*/ representing cases loaded with fuel assemblies at the design basis loading curve value, cases with a 10 GWd/MTU underburned assembly from the design basis required burnup in the central basket location, and cases with a 20 GWd/MTU underburned assembly from the design basis required burnup in the central basket location. The file naming system is as follows: *X.X* for the /*Nominal*/ subdirectory cases representing the initial enrichment in wt% U-235 (i.e., 3.5 is 3.5 wt% U-235 [range from 2.5 to 5.0 wt% U-235]); and *X.XmYY* in /*Sub10*/ and /*Sub20*/ subdirectories with *X.X* representing the initial enrichment in wt% U-235, and the *YY* is either a *10* or a *20* representing a 10 or 20 GWd/MTU underburned assembly.

/*II*/ - Contains files listed in Attachment II.